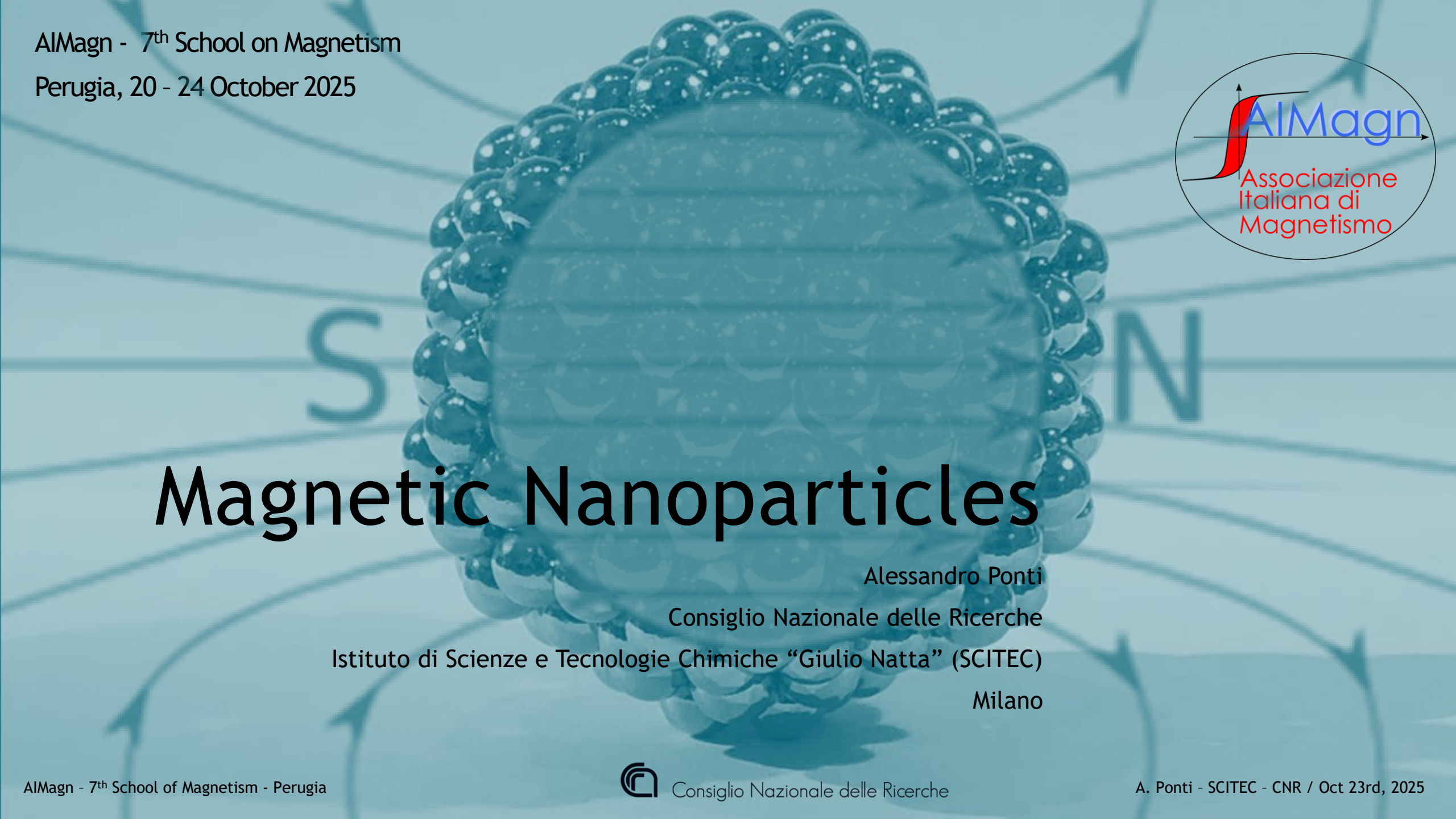
AIMagn - 7th School on Magnetism

Perugia, 20 – 24 October 2025



Magnetic Nanoparticles

Alessandro Ponti

Consiglio Nazionale delle Ricerche

Istituto di Scienze e Tecnologie Chimiche “Giulio Natta” (SCITEC)

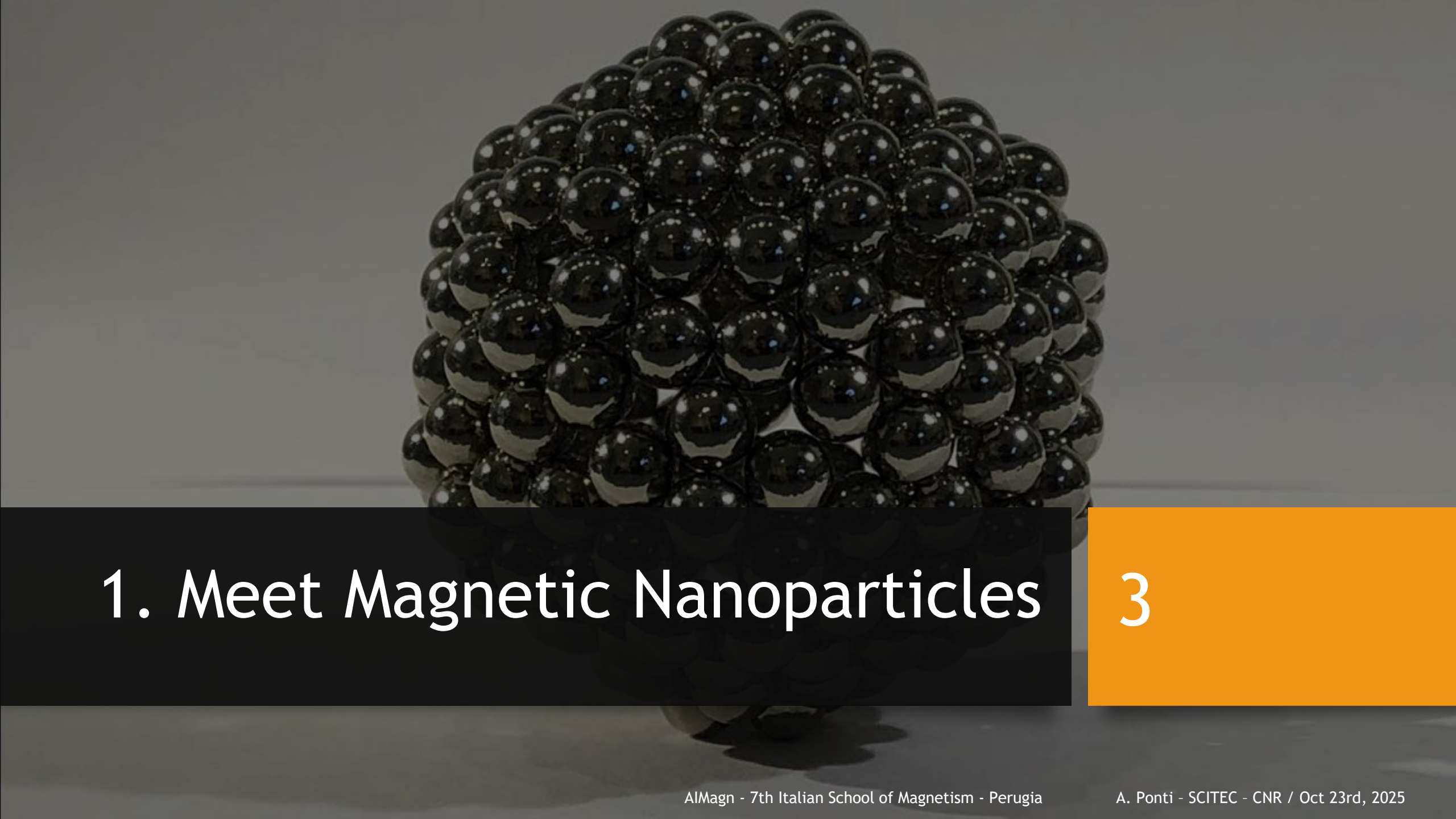
Milano



Outline



1. Meet Magnetic Nanoparticles
2. Magnetic Anisotropy
3. Single Domain NPs
4. The Stoner-Wohlfarth Model
5. Coercivity and Hysteresis
6. Thermal Fluctuations and Superparamagnetism
7. Exchange Bias
8. Interparticle Interactions



1. Meet Magnetic Nanoparticles

3

Big NP : You = You : Earth
Small NP : Cell = Cell : You

What is a nanoparticle?

Any object with at least one dimension **below 100 nm**



Non-manufactured NPs

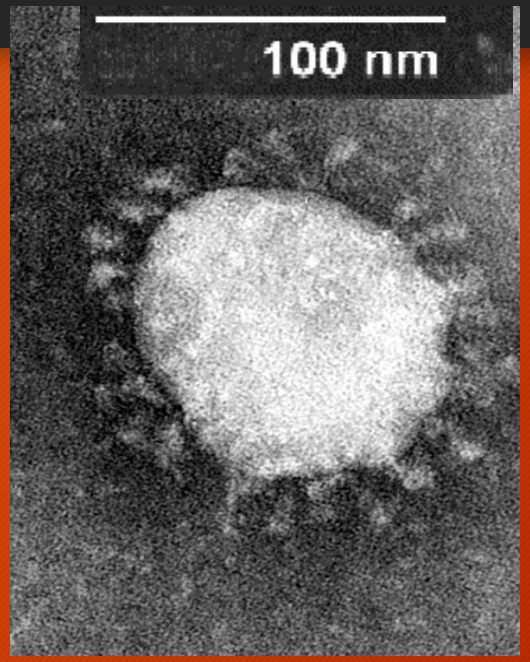
Non-manufactured NPs

have been around for billions of years

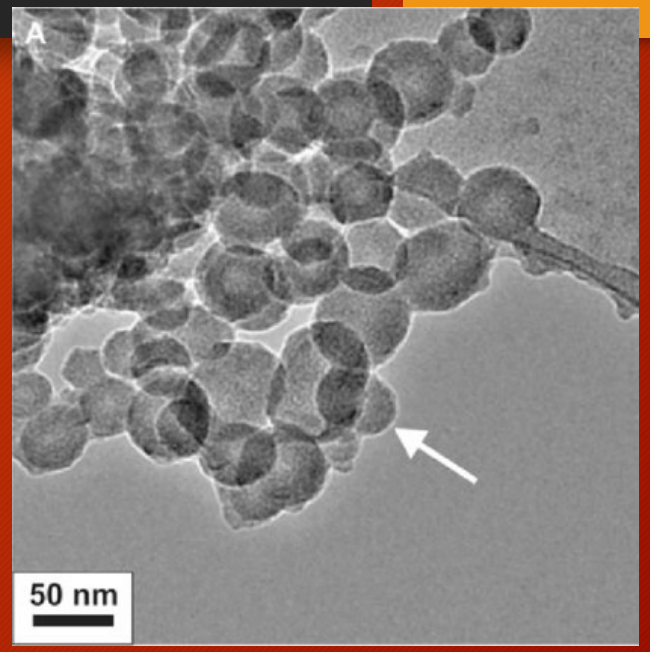
are very complex (morphology, composition, …)

can be natural (*eg*, viruses)

can be anthropogenic (*eg*, from combustion)



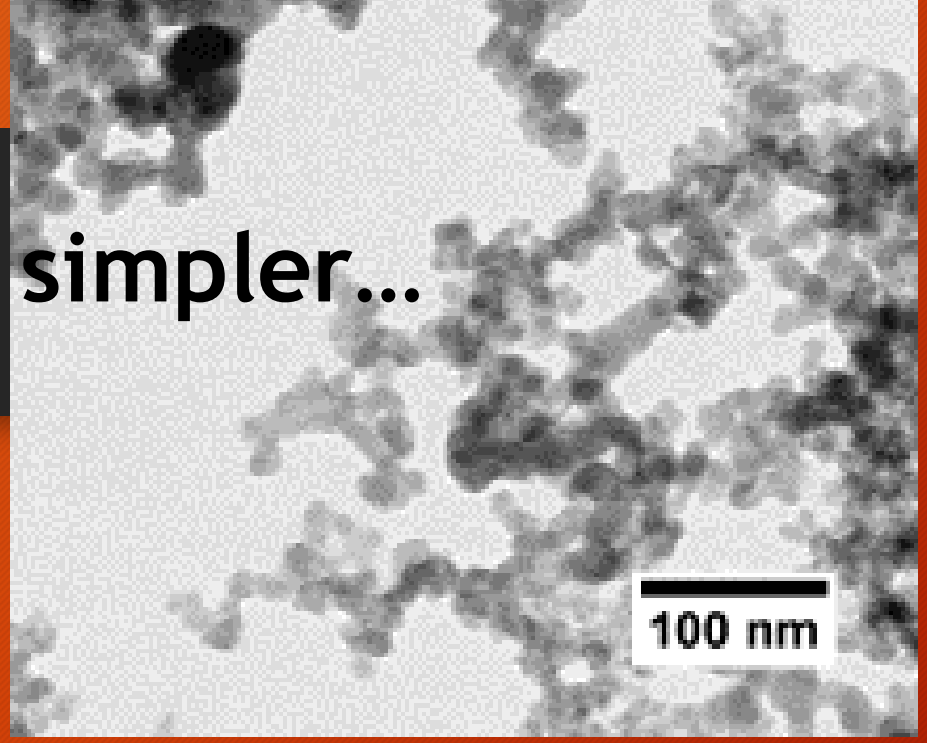
Natural NPs
(2019-nCoV Coronavirus)



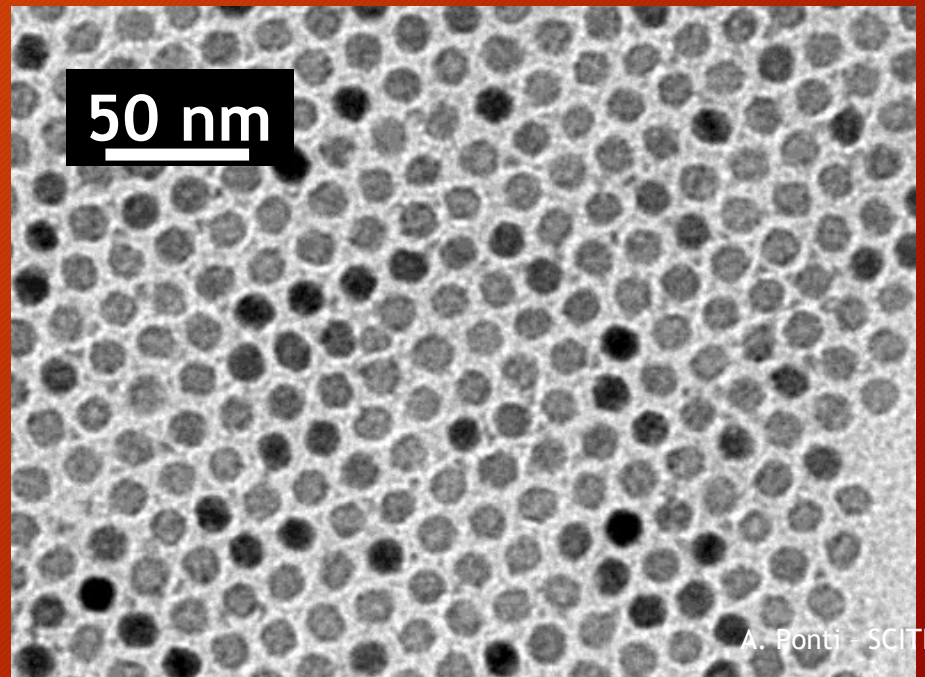
Anthropogenic non-manufactured NPs (diesel soot)

Manufactured NPs are simpler…

Industry-scale manufactured amorphous silica NPs (simple composition, complex morphology)

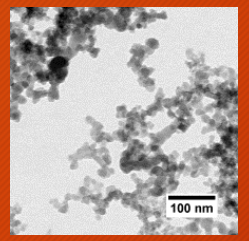


Laboratory-scale manufactured manganese ferrite NPs (simple composition and morphology)



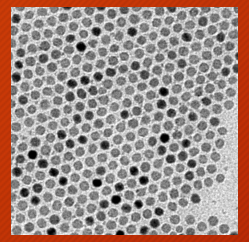
… but recall they form populations!

Industry-scale manufactured
amorphous silica NPs
Penguin colony





Laboratory-scale manufactured
$MnFe_2O_4$ NPs
Fish shoal





NPs never are as simple as chemicals!

Chemical

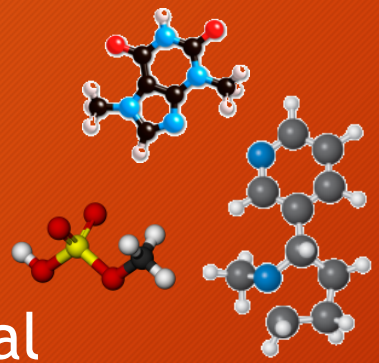
One type of molecule…







…or a few types in a mixture





All molecules are identical

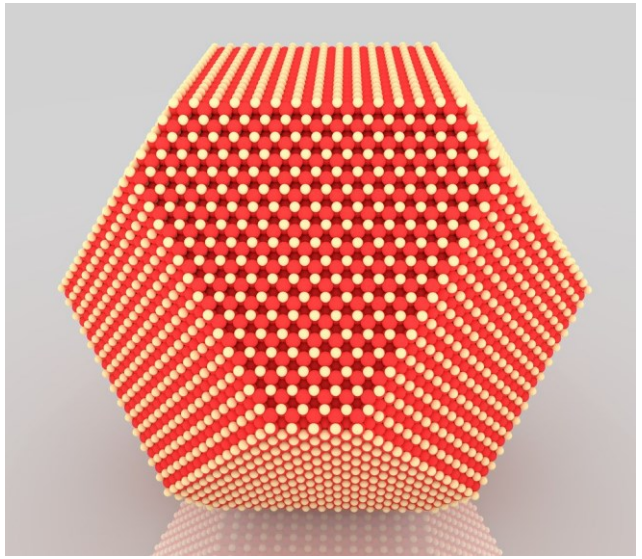
Magnetic NPs (Laboratory-made)

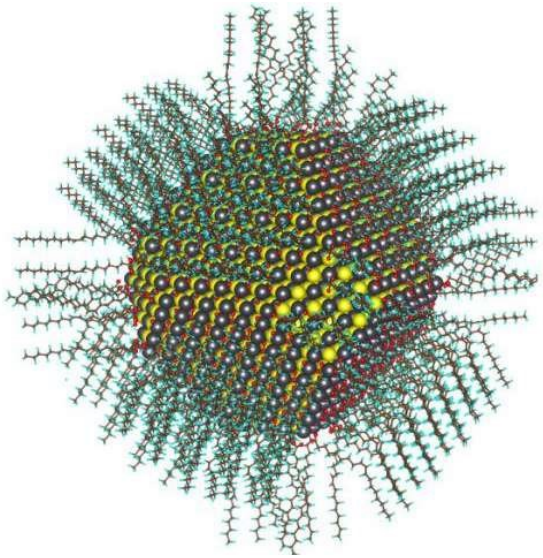
Magnetic NPs are NPs of magnetic materials
(FM, FiM, AFM,…)

Magnetic NPs usually are **nanocrystals**
(single- or poly-)

We aim at controlling

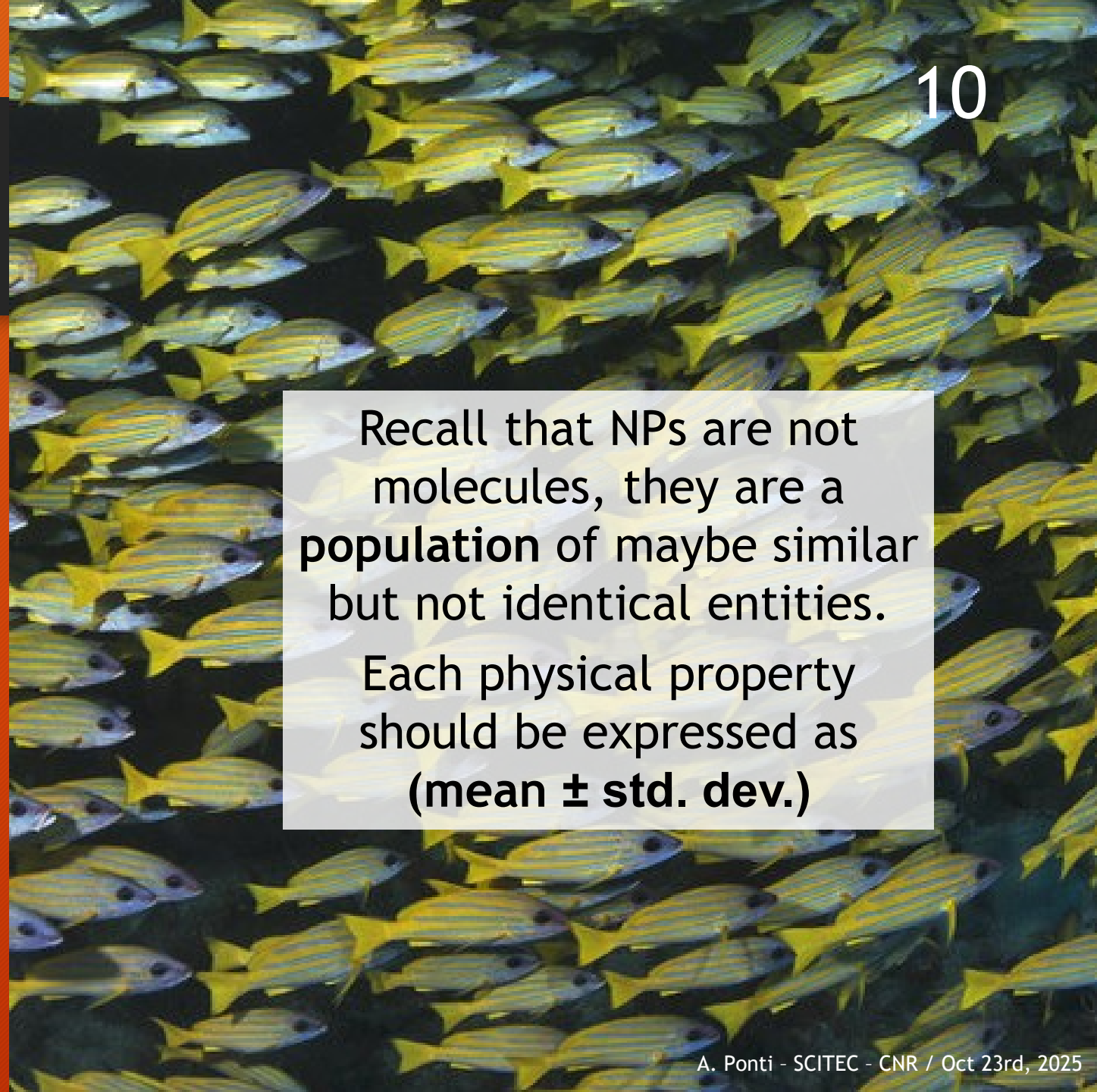
- Composition
- Crystal structure
- Heterostructure
- Size
- Shape
- Coating
- Colloidal stability
- Embedding
- …





What must you know before measuring magnetic properties of NPs?

- **Morphology** (TEM, STEM)
- **Composition**
  - Average, macroscale (ICP-xxx)
  - Local, nanoscale (EF-TEM, STEM-EDX)
  - Coating (FTIR)
- **Crystal structure**
  - Average, macroscale (XRD)
    - Bonus: Rietveld analysis yields crystallite size and microstrain!
  - Local, nanoscale (HR-TEM + GPA)
- **Aggregation state** (DLS)



Recall that NPs are not molecules, they are a **population** of maybe similar but not identical entities.

Each physical property should be expressed as **(mean ± std. dev.)**

Beware of the nanoparticle peddler! They'll sell you NPs and throw in a headache for free.

***My** free advice nobody asked for*

From people asking you to measure magnetic properties of their NPs (maybe it's you yourself) **do require** a full characterization of the NPs, including:

- **Morphology** (size, shape)
- **Heterostructure**
- **Composition** (purity, macroscale, local, coating, ...)
- **Crystal structure** (local, average, phase purity, crystallite size)
- **Aggregation state**



Offelée fa’ el tò mestée



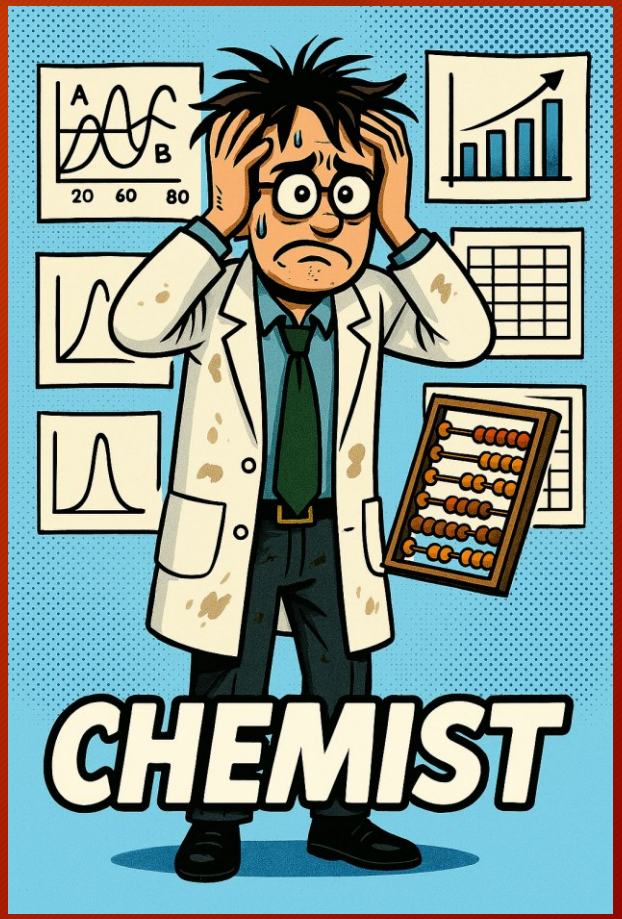
***My second** free advice nobody asked for*

Offelée fa’ el tò mestée

an old proverb from Milan meaning “stick to what you do best and leave the rest to those who do it better”.

Very many techniques are required to synthesize and study magnetic NPs:

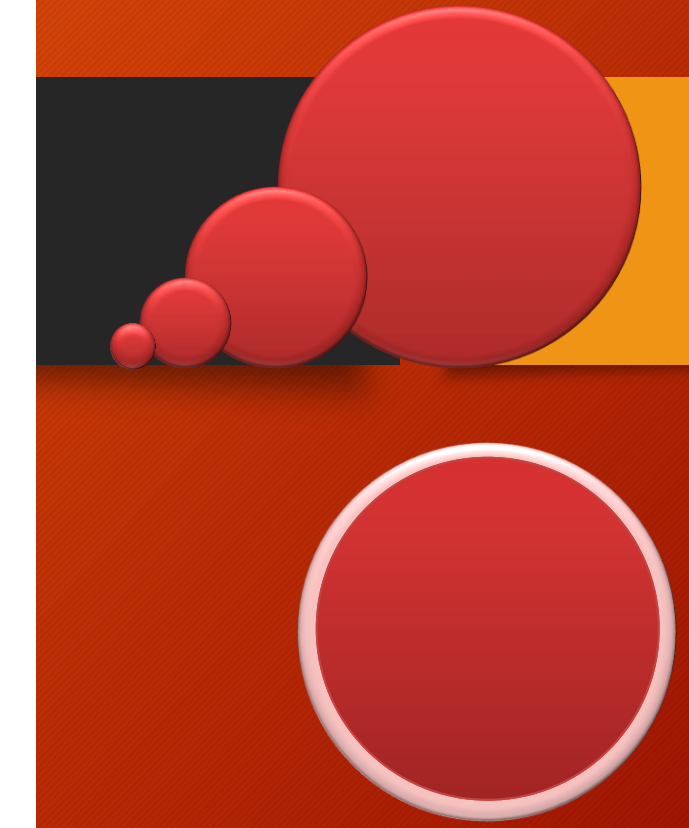
collaborate with experts in fields other than yours.

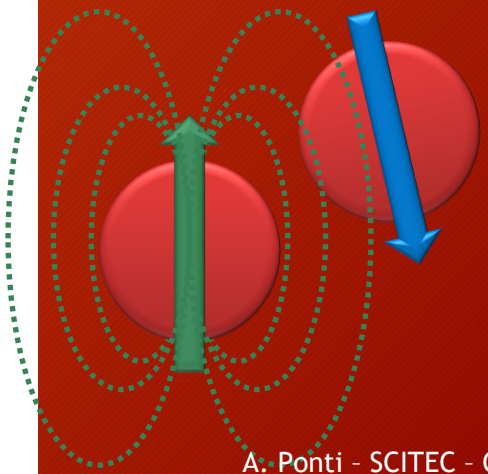


Why should we bother with magnetic NPs?

The behavior of magnetic nanocrystals differs from that shown by the bulk material due to:

- **size** effects
- **surface** effects
- **inter-particle** interactions

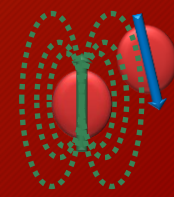




Size effects

- Single domain
- Coherent rotation
- Enhanced remanence
- Enhanced coercivity
- Superparamagnetism

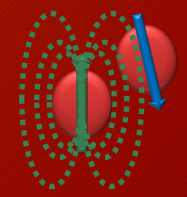




Surface effects

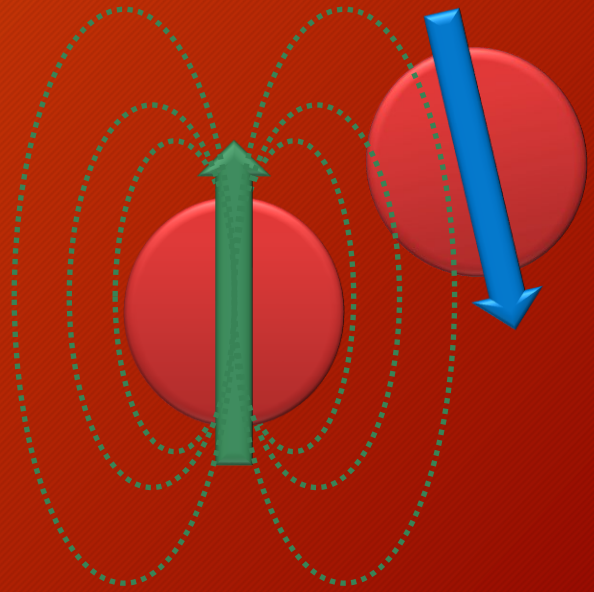
- Surface magnetization different from bulk
- Emerging strong surface anisotropy
- Exchange coupling at interface
- *Difficult to study both experimentally and theoretically*





Interparticle interactions

- **Magnetostatic interactions (dipole-dipole and higher order)**
  - Always present
  - Strongly depend on NP spatial configuration
- **Exchange coupling *via* the matrix**
- **Direct exchange *via* interfacial contact**
- ***Very difficult to study both experimentally and theoretically***



2. Magnetic anisotropy

No magnetism without anisotropy!

What is magnetic anisotropy?

What is magnetic anisotropy?

F. Hellman, in *Encyclopedia of Materials: Science and Technology*, 2001, s. v. Magnetic Films: Anisotropy

- Magnetic anisotropy is the coupling of the magnetization to particular directions
- The magnetic properties depend on the direction in which the magnetic field is applied
- In zero applied field, the magnetization lies along the preferred direction(s)

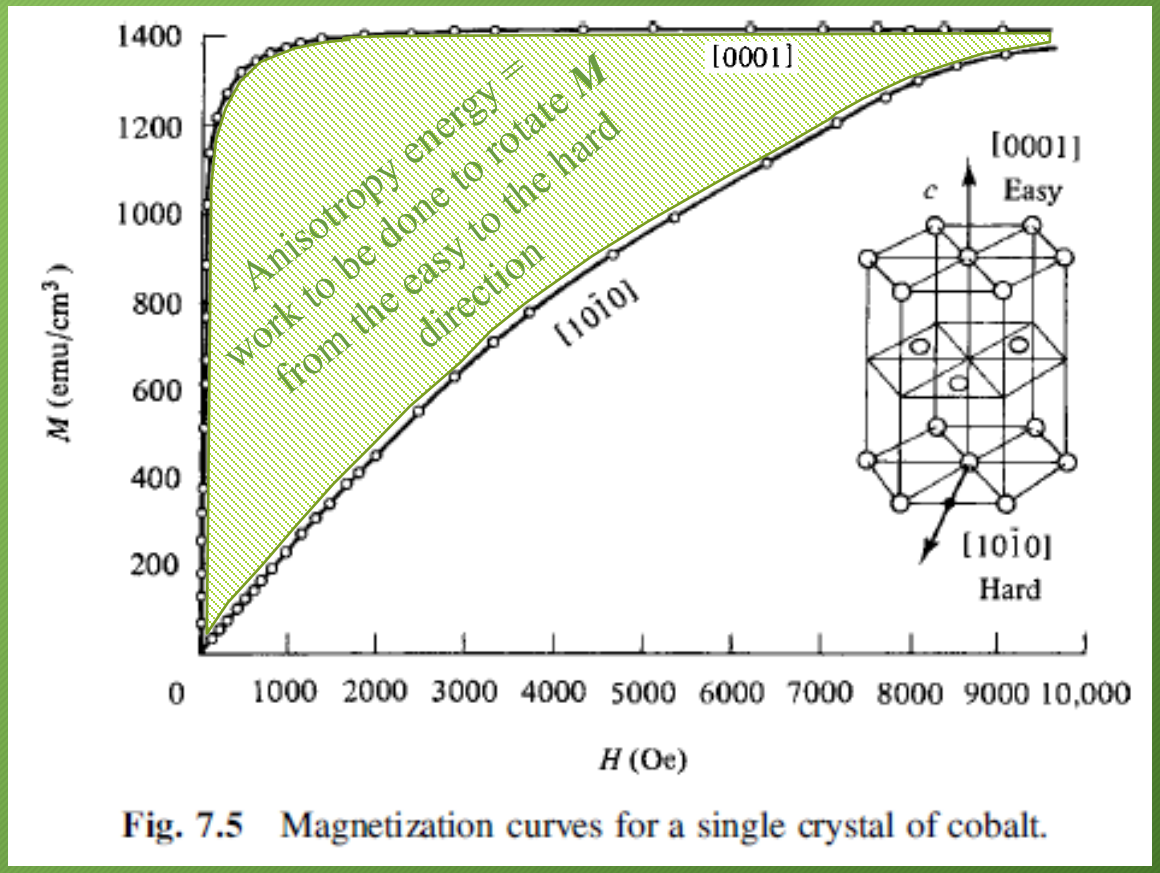


Fig. 7.5 Magnetization curves for a single crystal of cobalt.

What is magnetic anisotropy?

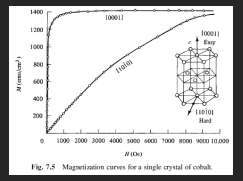


Fig. 7.5 Magnetization curves for a single crystal of cobalt.

F. Hellman, in *Encyclopedia of Materials: Science and Technology*, 2001, s. v. Magnetic Films: Anisotropy

- Magnetic anisotropy is the coupling of the magnetization to particular directions
- The magnetic properties depend on the direction in which the magnetic field is applied
- In zero applied field, the magnetization lies along the preferred direction(s).

Without magnetic anisotropy,

there can be

no coercivity and no remanence

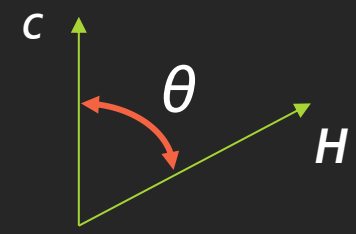
and hence

no permanent magnets

Types of magnetic anisotropy

Magnetocrystalline	direction of M w.r.t. crystal axes, coupling between ***M*** and the lattice via spin-orbit interaction
Magnetostatic (Shape)	direction of M w.r.t. shape axes •coupling between ***M*** and the demagnetizing field via Zeeman int. •energy stored in the sample-generated external field
Magnetoelastic	direction of M w.r.t. lattice, coupling between ***M*** and crystal strain via spin-orbit interaction
Surface	lower symmetry around magnetic atoms/ions at the surface, important in particles with NPs less than ~10 nm (Néel 1954)
Exchange	exchange anisotropy («dipolar») proximity effects such as exchange bias in FM/AFM
Induced	by magnetic annealing (***H***+heat), stress annealing (stress+heat), plastic deformation, etc.

Uniaxial magnetocryst. anisotropy



$$E = K_0 + K_1 \sin^2\theta + K_2 \sin^4\theta + \cdots \qquad (7.3)$$

When K_1 and K_2 are both positive, the energy E is minimum for $\theta = 0$, and the c-axis is an axis of easy magnetization. A crystal with a single easy axis, along which the magnetization can point either up or down, is referred to as a *uniaxial* crystal, as noted above. Its domain structure in the demagnetized state is particularly simple (Fig. 7.6). Elemental cobalt, barium ferrite, and many rare earth transitional metal intermetallic compounds behave in this way.

When K_1 and K_2 are both negative, the minimum value of E occurs at $\theta = 90°$. This creates an *easy plane* of magnetization, which is the basal plane of a hexagonal material, lying perpendicular to the c-axis.

TABLE 7.4 Anisotropy Constants

Structure	Substance	K_1 (10^5 erg/cm^3)	K_2 (10^5 erg/cm^3)
Hexagonal	Co	45	15
	$BaO \cdot 6Fe_2O_3$	33	
	YCo_5	550	
	MnBi	89	27

Co single crystal

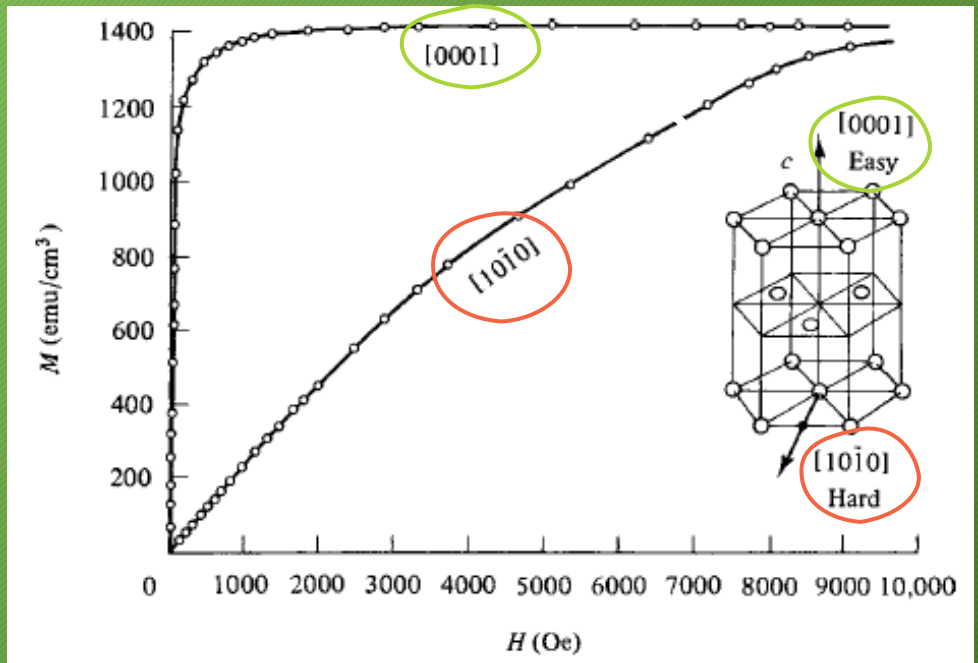


Fig. 7.5 Magnetization curves for a single crystal of cobalt.

Cubic magnetocryst. anisotropy

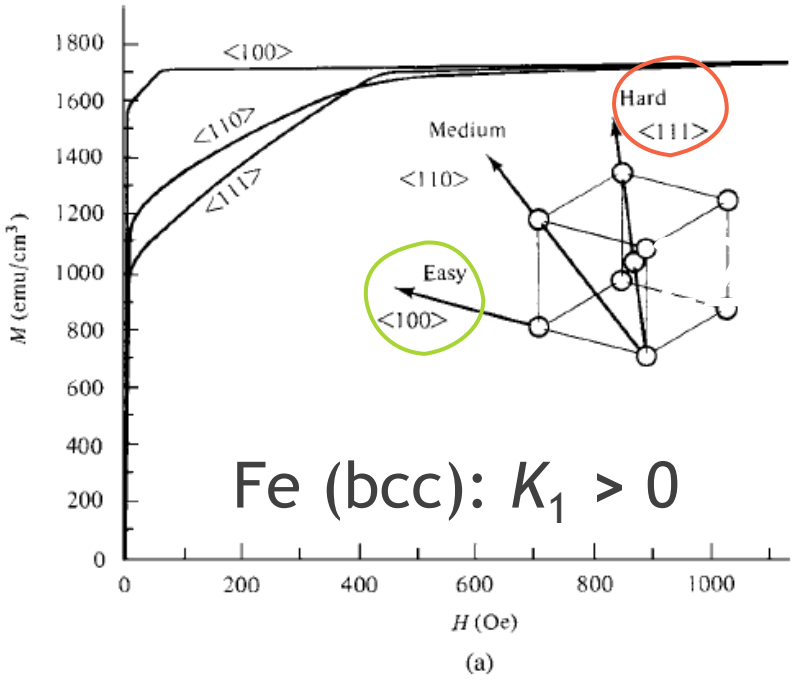
series expansion of the direction cosines of M_s relative to the crystal axes. In a cubic crystal, let M_s make angles a, b, c with the crystal axes, and let α_1, α_2, α_3 be the cosines of these angles, which are called direction cosines. Then

$$E = K_0 + K_1(\alpha_1^2\alpha_2^2 + \alpha_2^2\alpha_3^2 + \alpha_3^2\alpha_1^2) + K_2(\alpha_1^2\alpha_2^2\alpha_3^2) + \cdots \qquad (7.1)$$

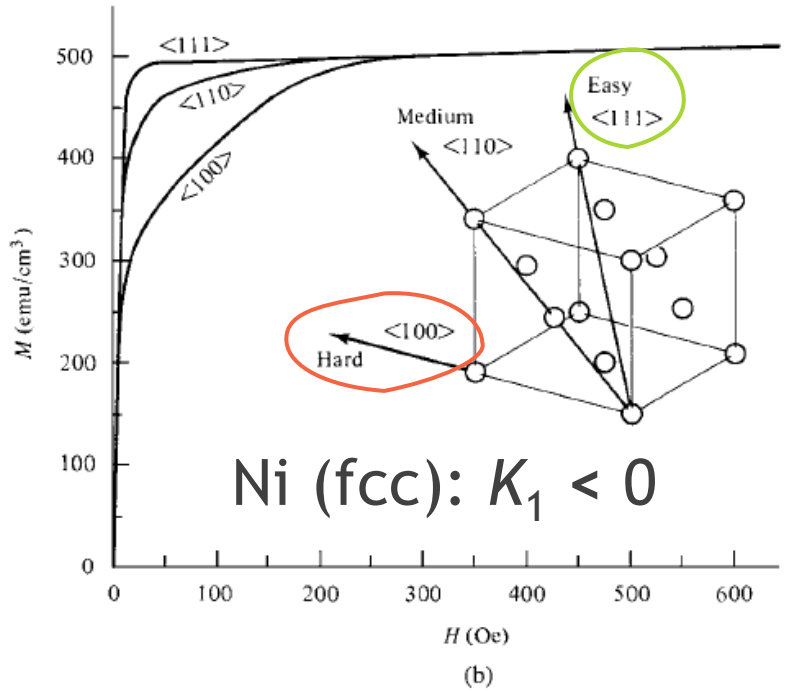
where K_0, K_1, K_2, . . . are constants for a particular material at a particular temperature and

TABLE 7.4 Anisotropy Constants

Structure	Substance	K_1 (10^5 erg/cm^3)	K_2 (10^5 erg/cm^3)
Cubic	Fe	4.8	± 0.5
	Ni	-0.5	-0.2
	$FeO \cdot Fe_2O_3$	-1.1	
	$MnO \cdot Fe_2O_3$	-0.3	
	$NiO \cdot Fe_2O_3$	-0.62	
	$MgO \cdot Fe_2O_3$	-0.25	
	$CoO \cdot Fe_2O_3$	20	



(a)



(b)

Fig. 7.2 Magnetization curves for single crystals of iron (a) and nickel (b).

How magnetocrystalline anisotropy depends on temperature?

One model for the temperature dependence of anisotropy is based on the idea that, as the temperature increases, the local magnetization direction spreads over a range of angles about the mean direction. This raises the energy of the easy direction and lowers the energy of the hard direction, and leads to the prediction that anisotropy will decrease as a power of the reduced magnetization M/M_0, where M_0 is the saturation magnetization at 0K. Specifically, the prediction is that

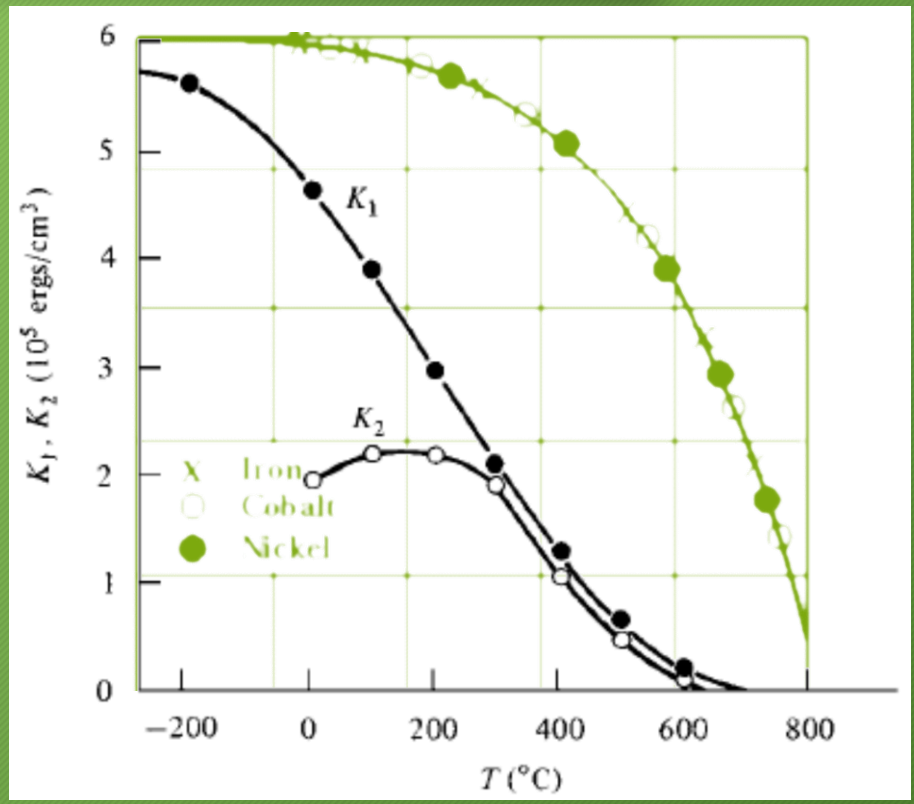
where n is the power of the anisotropy function. So for uniaxial anisotropy ($n = 2$),

$$\frac{K_u}{K_{u,0}} \propto \left(\frac{M_s}{M_{s,0}}\right)^3 \tag{7.53}$$

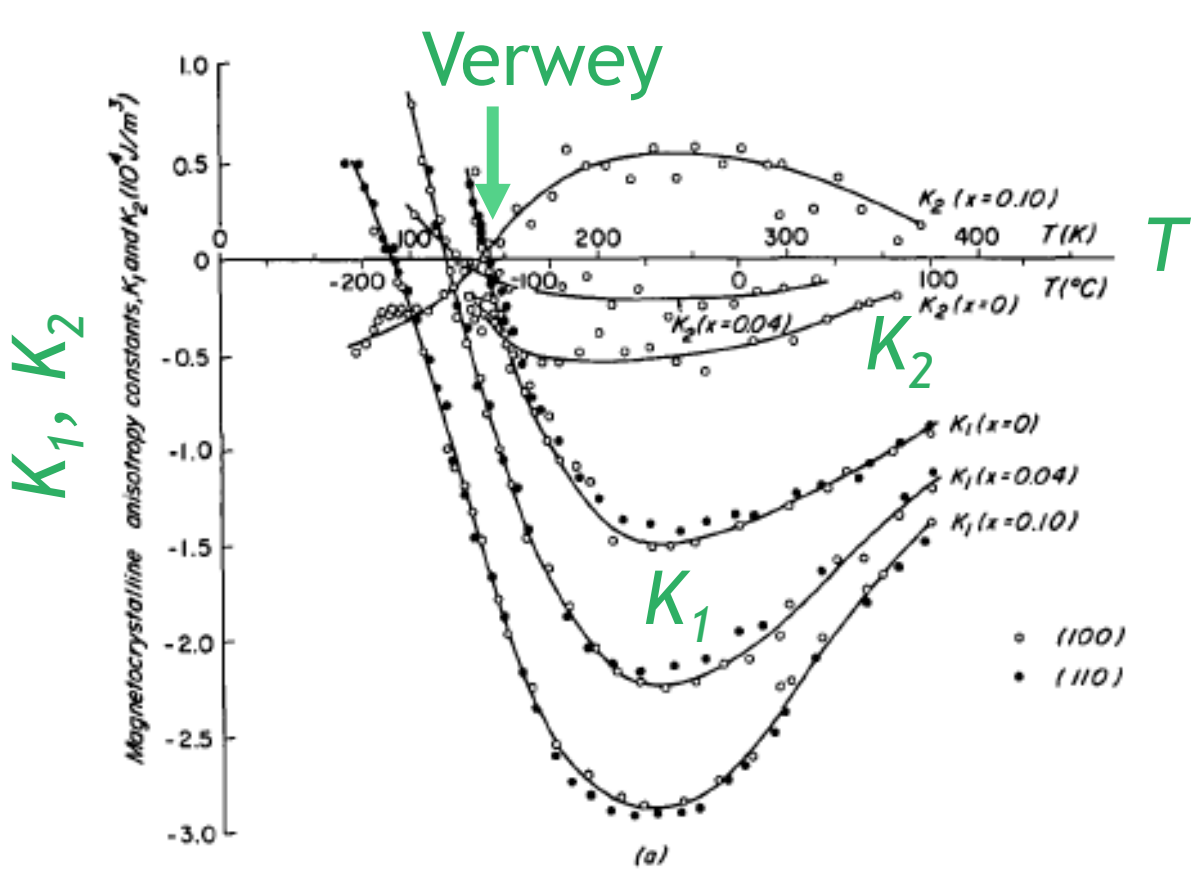
and for cubic anisotropy ($n = 4$)

$$\frac{K_1}{K_{1,0}} \propto \left(\frac{M_s}{M_{s,0}}\right)^{10} \tag{7.54}$$

This model fits the data quite well for iron, but fails badly for some other materials.



Temperature dependence of anisotropy constants. (a) Iron



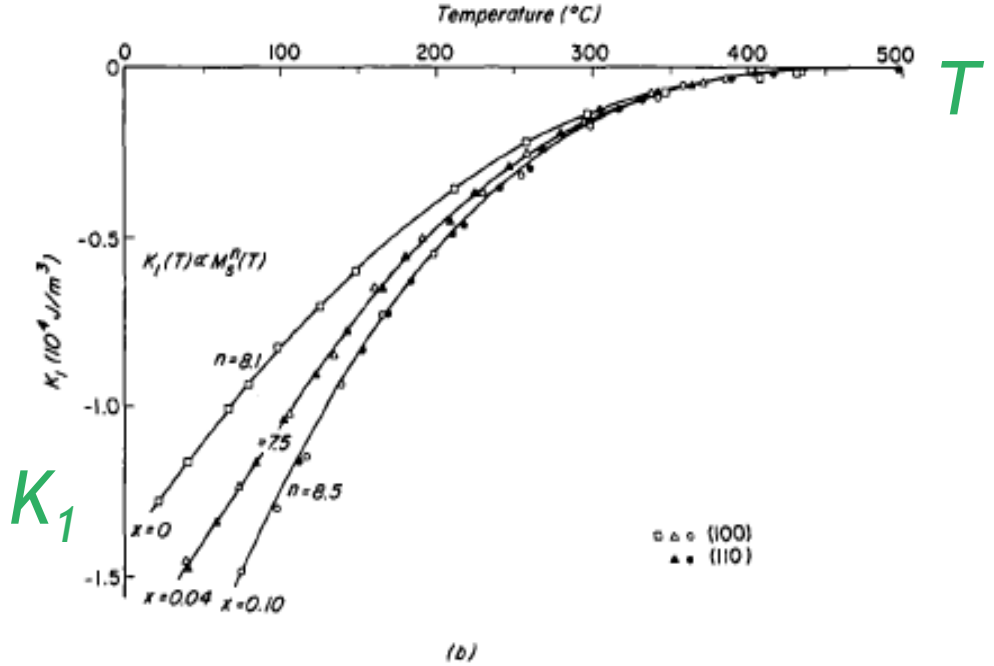


Figure 3.7 Temperature dependence of the magnetocrystalline anisotropy constants K_1 and K_2 in magnetite ($x = 0$) and titanomagnetites near magnetite in composition. Notice the isotropic point at which $K_1 = 0$ at $T_1 = 135$ K ($x = 0$) to 90 K ($x = 0.1$). [After Syono and Ishikawa (1963a) and Fletcher and O'Reilly (1974), with the permission of the authors and the publishers, The Physical Society of Japan, Tokyo, Japan and Institute of Physics Publishing, Bristol, UK.]

The case of magnetite

$$E_{ms} = \frac{1}{2}M^2 N_c + \frac{1}{2}(N_a - N_c)M^2 \sin^2\theta. \quad (7.61)$$

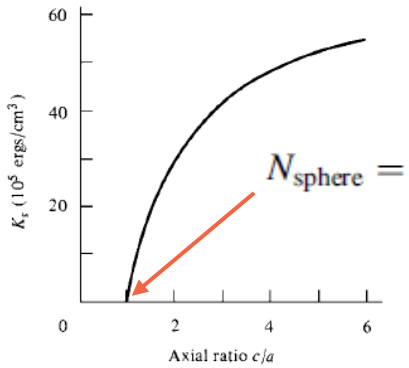
This expression for the magnetostatic energy has an angle-dependent term of exactly the same form as uniaxial crystal anisotropy energy (Equation 7.4). The long axis of the specimen plays the same role as the easy axis of the crystal, and the shape-anisotropy constant K_s is given by

$$K_s = \frac{1}{2}(N_a - N_c)M^2 \text{ erg/cm}^3 \text{ (cgs)} \quad \text{or} \quad K_s = \frac{1}{2}\mu_0(N_a - N_c)M^2 \text{ joule/m}^3 \text{ (SI)}, \quad (7.62)$$

which are often written as

$$K_s = \frac{1}{2}\Delta N M^2 \text{ erg/cm}^3 \text{ (cgs)} \quad \text{or} \quad K_s = \frac{1}{2}\mu_0 \Delta N M^2 \text{ joule/m}^3 \text{ (SI)}. \quad (7.63)$$

Magnetization is easy along the c-axis and equally hard along any axis normal to c. If c shrinks until it equals a, the specimen becomes spherical, $N_a = N_c$, $K_s = 0$, and shape anisotropy disappears. The long axis of the spheroid is labeled $2c$ in Fig. 7.30 to conform with the earlier definition of ellipsoids. It is not to be confused with the c axis of a hexagonal crystal.



$$N_{sphere} = \frac{4\pi}{3}(\text{cgs}) \text{ or } N_{sphere} = \frac{1}{3} \text{ (SI)}.$$

Fig. 7.31 Shape anisotropy constant vs axial ratio of a prolate spheroid. Numerical values calculated for cobalt ($M_s = 1422$ emu cm^{-3}).

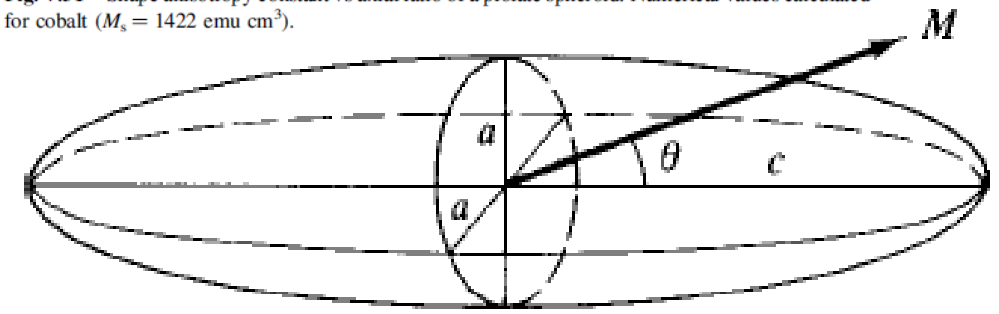


Fig. 7.30 Prolate ellipsoid.

Magnetostatic / Shape anisotropy

Surface anisotropy

Co NPs

M. Respaud et al., Phys. Rev. B 57, 2925, 1998

Enhanced anisotropies are currently observed on fine magnetic particles and have been predicted by theoretical calculations.[36] The volume dependence of K_a can be analyzed on the basis of a simple model in which the total energy barrier is written,

$$\Delta E = K_v' v + K_s' s, \quad (3)$$

where K_v' and K_s' are the volume and the surface uniaxial anisotropy energy constants, respectively, and v and s are the volume and the surface area of the particle. For spherical particles with diameter d, Eq. (3) gives

$$K_a = K_v' + \frac{a_s}{d} K_s', \quad (4)$$

where $a_s = 6$. This dependence has been experimentally

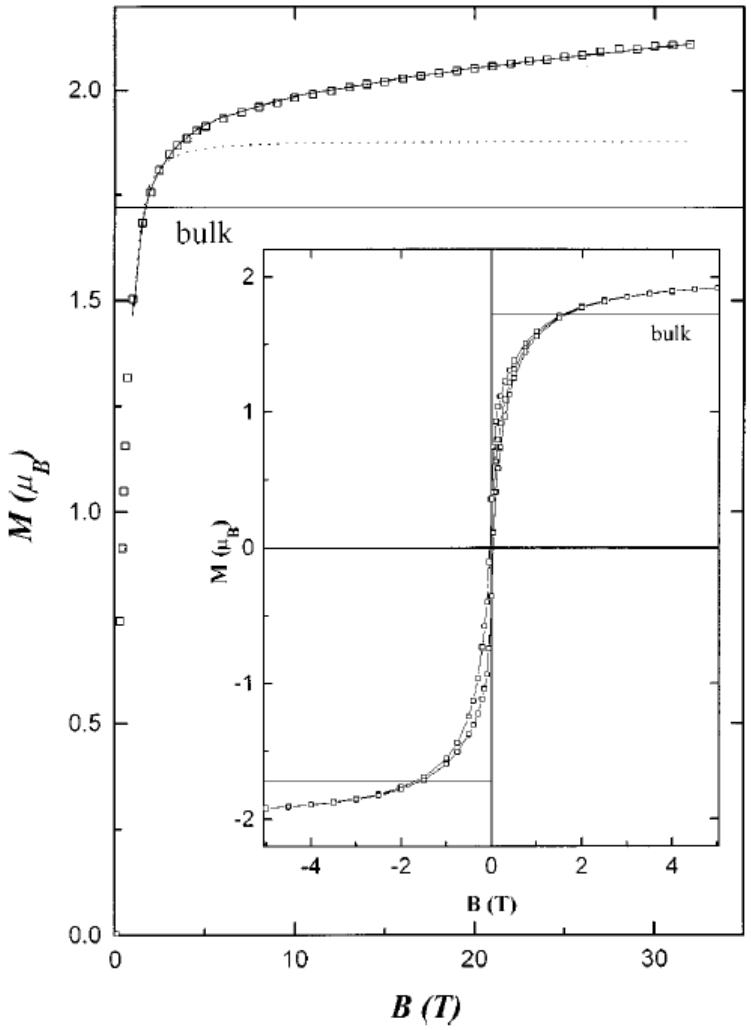


FIG. 9. Experimental initial magnetization up to 35 T for Coll-I (symbols). Inset presents the hysteresis loop at 5 K. The solid line shows the theoretical magnetization using Eq. (2) and $\langle \mu_{Co}(B) \rangle$ presented in Fig. 11. The dashed lines present theoretical magnetization curves for a constant value of $\langle \mu_{Co}(B) \rangle$. The straight line indicates the bulk value magnetic moment per Co atom.

The effective magnetic anisotropies are found to be **larger** than that of the bulk.
The enhanced effective magnetic anisotropy is associated with the large influence of the **surface atoms** and is more significant with decreasing size.

Surface anisotropy

F. Luis et al., Phys. Rev. B 65, 094409, 2002

- Monodisperse spherical **Co NPs** with diameter 0.8 to 5.2 nm (25–7000 atoms).
- The particle size distribution from the susceptibility and magnetization data.
- The distribution of activation energies from a scaling plot of the ac susceptibility.
- Combining these two distributions, it was found that K_{eff} is enhanced with respect to the bulk value and that it is dominated by a strong anisotropy induced at the surface of the clusters.

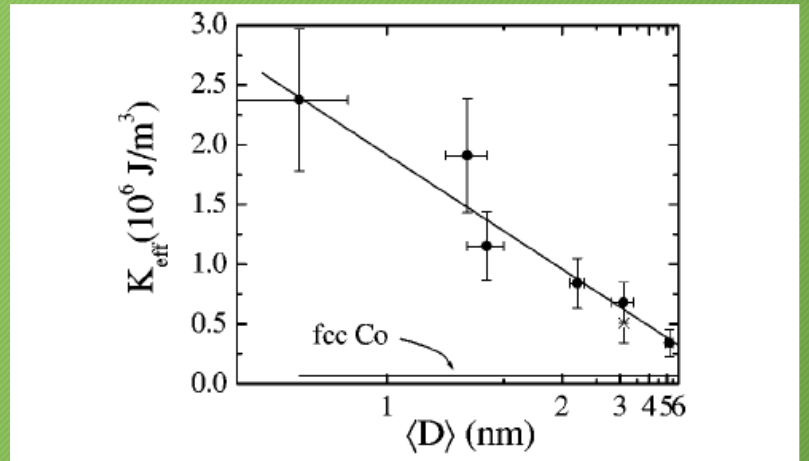
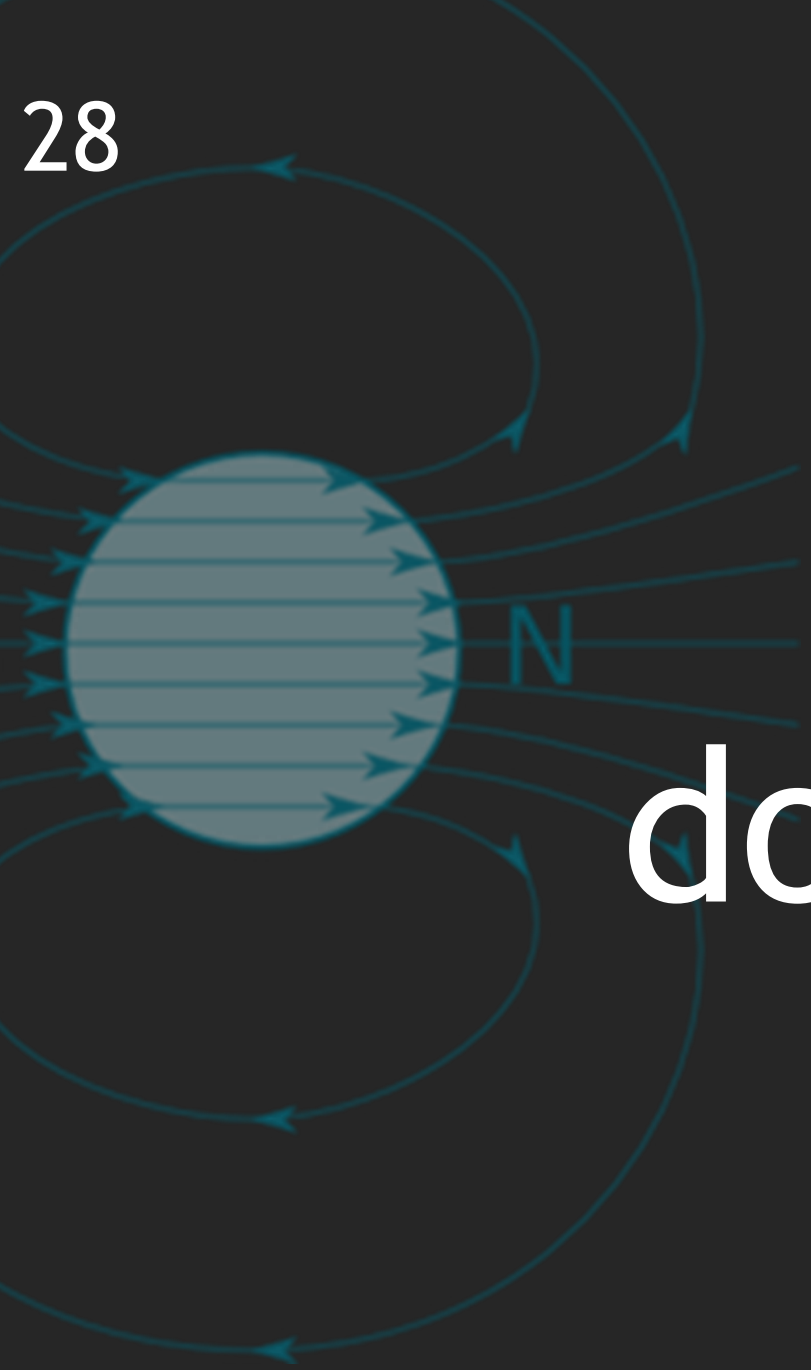


FIG. 7. Size dependence of the effective anisotropy constant for all samples investigated. × gives the value obtained for a single-layer with $t_{Co}=0.7$ nm. The solid line is a best squares fit of the data to Eq. (8).

<D> / nm	E(surf) / J m^{-3}	E(vol) / J m^{-3}	E(surf) / E(vol)
0.83	2.39E+06	5E+04	48
1.4	1.41E+06	5E+04	28
2.2	9.00E+05	5E+04	18
2.9	6.83E+05	5E+04	14
4.2	4.71E+05	5E+04	9
5.2	3.81E+05	5E+04	8

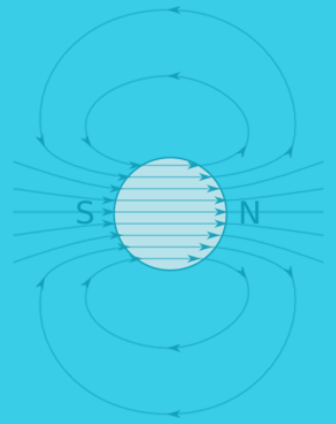
$$K_{eff}=K_{\infty}+\frac{6K_s}{\langle D\rangle}, \qquad (8)$$

with $K_{\infty}=5(\pm 2)\times 10^4$ J/m^3 and $K_s=3.3(\pm 0.5)\times 10^{-1}$ mJ/m^2. This result is robust in the sense that it does



3. Single domain NPs

Below a critical size, magnetic NPs comprise a single domain



Energy terms

The total free energy of a ferromagnetic specimen in an applied magnetic field may be written as the sum of several free energy terms (equation 6-9.1):

$$F_T = F_H + F_D + F_K + F_\sigma + F_e + F_0, \qquad (7\text{-}1.2)$$

F_H = Zeeman ($\boldsymbol{M} \cdot \boldsymbol{H}_{ext}$)
F_D = Demagnetizing ($\boldsymbol{M} \cdot \boldsymbol{H}_d$)
F_K = Magnetocrystalline anisotropy
F_σ = Magnetostriction
F_e = Exchange ($J_{ij}\, \boldsymbol{S}_i \cdot \boldsymbol{S}_j$)
F_0 = Non-magnetic terms

Magnetic domains

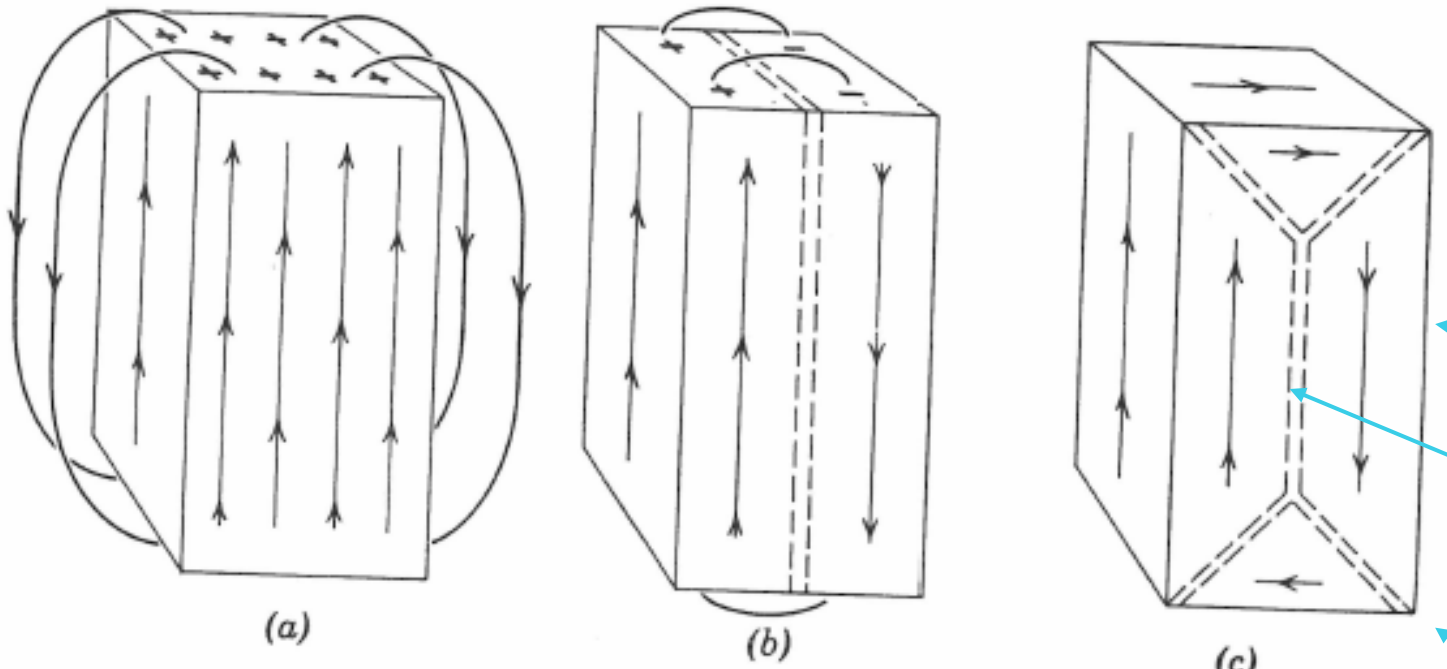


Fig. 7-1.2. Some hypothetical domain configurations.

Free energy minimum usually corresponds to the formation of **domains.**

Decreased magnetostatic energy

Increased exchange and magnetocrystalline

Domain walls

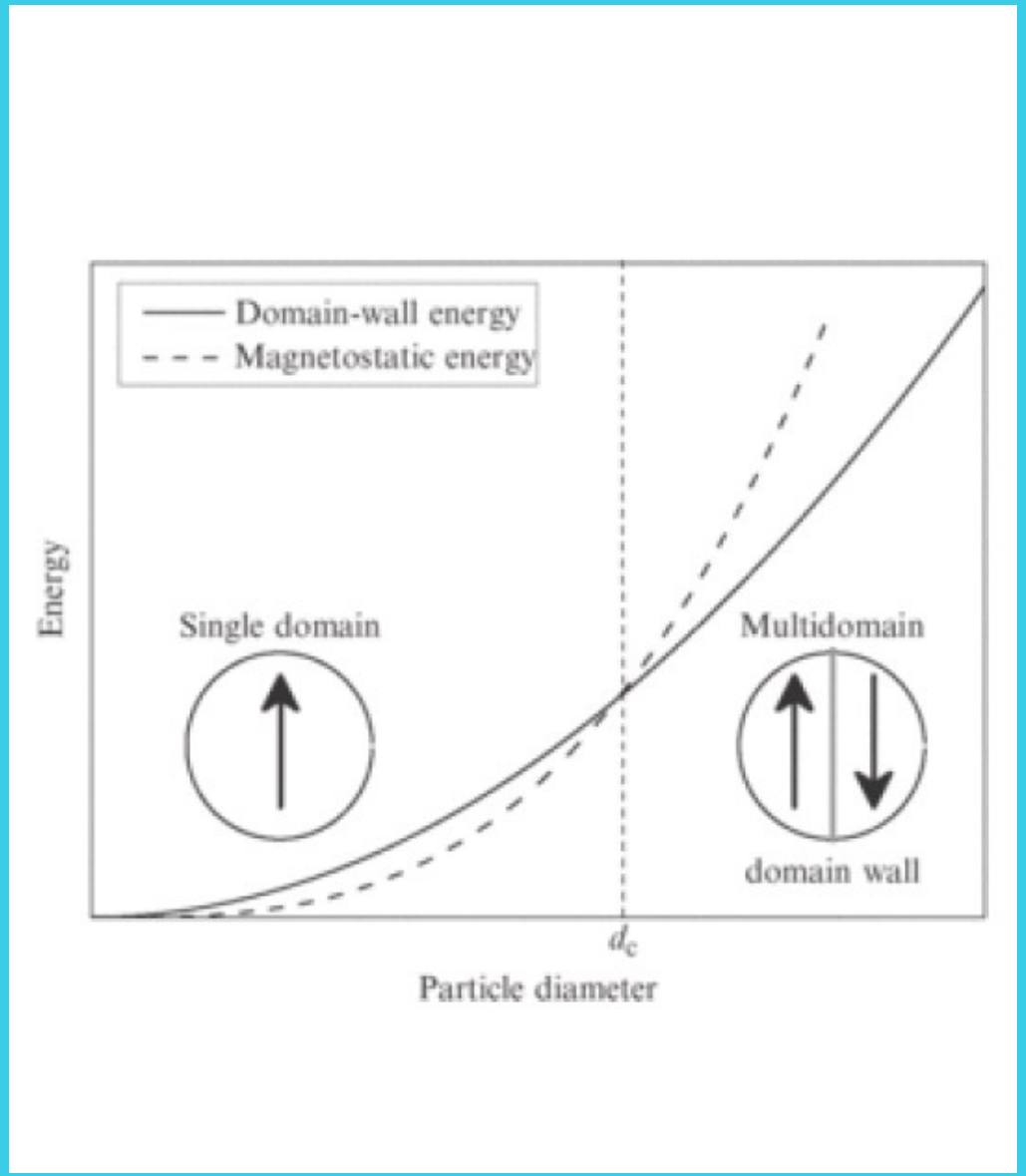
When a NP is single-domain?

When the Zeeman term dominates (**strong** applied field *H*)

or

$$F_H = -\int \mathbf{M} \cdot \mathbf{H}\, dv.$$

When the particle is **small**: the reduction of magnetostatic energy (*Volume*) does not compensate for the increase in exchange and magnetocrystalline (*Surface*, domain wall) energy



Length scales

Table 8.1. Characteristic magnetic length scales (in nm)

Length	Expression	Fe	Co	Ni	NiFe	$Fe_{90}Ni_{10}B_{20}$	CoPt	$Nd_2Fe_{14}B$	$SmCo_5$	$Sm_2Fe_{17}N_3$	CrO_2	Fe_3O_4	$CoFe_2O_4$	$BaFe_{12}O_{17}$
κ	$\sqrt{\lvert K_1\rvert/\mu_0 M_s^2}$	0.12	0.45	0.13	0.01	0.01	2.47	1.54	4.30	2.13	0.36	0.21	0.84	1.35
l_{ex}	$\sqrt{A/\mu_0 M_s^2}$	2.4	3.4	5.1	3.4	2.5	3.5	1.9	3.6	2.5	4.4	4.9	5.2	5.8
R_{coh}	$\sqrt{24}l_{ex}$	12	17	25	17	12	17	9.7	18	12	21	24	26	28
δ_w	$\pi l_{ex}/\kappa$	64	24	125	800	900	4.5	3.9	2.6	3.7	44	73	20	14
R_{sd}	$36\kappa l_{ex}$	10	56	24	1.6	0.7	310	110	560	190	48	38	160	280
R_{eq}	$(3k_BT/4\pi BM)$	0.8	0.8	1.2	1.0	0.9	1.0	0.9	1.0	0.9	1.3	1.2	1.2	1.3
R_b	$(6k_BT/K_1)^{1/3}$	8	4	17	55	63	1.7	1.7	1.1	1.4	11	13	5	4

κ, hardness parameter; l_{ex}, exchange length; R_{coh}, maximum particle size for coherent rotation; δ_w, Bloch wall width; R_{sd}, maximum equilibrium single domain particle size; R_{eq}, particle radius for which $mB = k_BT$ in 1 T at 300 K; R_b, superparamagnetic blocking radius at 300 K.

Length scales

$$d_0 = D_{\text{crit}} = \frac{4\gamma_w}{\mu_0 N_{SD} M_s^2}.$$

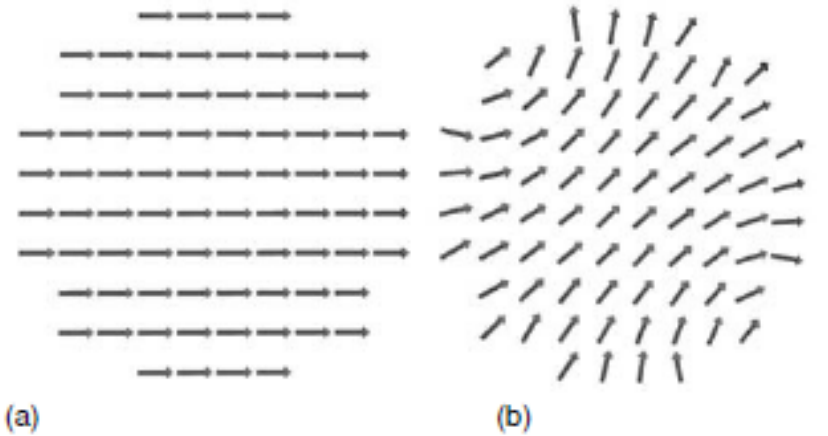
$$\gamma_W = 2\pi\left(\frac{JS^2}{a}K\right)^{1/2}$$

T gnetic leng

Length	Expression	Fe	Co	Ni	$Nd_2Fe_{14}B$	Fe_3O_4	$CoFe_2O_4$	$BaFe_{12}O_{17}$
κ	$\sqrt{\lvert K_1\rvert/\mu_0 M_s^2}$	0.12	0.45	0.13	1.54	0.21	0.84	1.35
l_{ex}	$\sqrt{A/\mu_0 M_s^2}$	2.4	3.4	5.1	1.9	4.9	5.2	5.8
R_{coh}	$\sqrt{24}l_{ex}$	12	17	25	9.7	24	26	28
δ_w	$\pi l_{ex}/\kappa$	64	24	125	3.9	73	20	14
R_{sd}	$36\kappa l_{ex}$	10	56	24	110	38	160	280
R_{eq}	$(3k_BT/4\pi BM)$	0.8	0.8	1.2	0.9	1.2	1.2	1.3
R_b	$(6k_BT/K_1)^{1/3}$	8	4	17	1.7	13	5	4

κ, hardness parameter; l_{ex}, exchange length; R_{coh}, m t rotation; δ_w n equilibrium single domain particle size; R_{eq}, particle radius for which m $B = k_BT$ in 1 tic blocking

Within a single domain NP



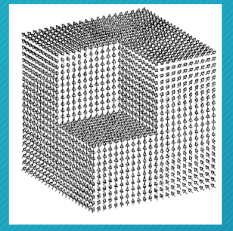
The spin configurations shown in Fig. 8.29 were determined numerically, by atomic scale Monte-Carlo simulations with simulated annealing from above the Curie point in order to find the lowest-energy state. The spin configurations have names: (b) is a throttled or flower state, (c) is a hedgehog and (d) is an artichoke.

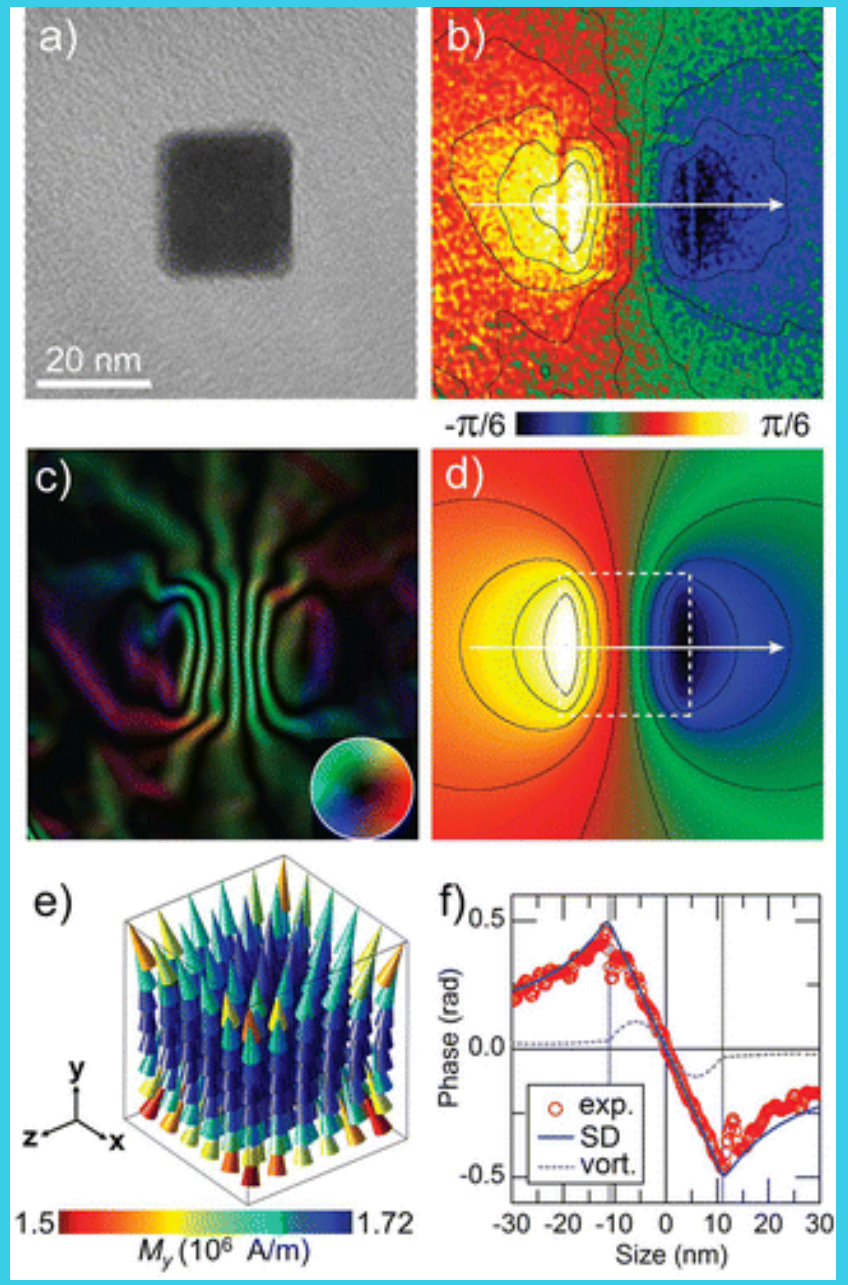
NANO LETTERS
Letter
pubs.acs.org/NanoLett

Size-Specific Spin Configurations in Single Iron Nanomagnet: From Flower to Exotic Vortices

Christophe Gatel,*,† Francisco Javier Bonilla,‡ Anca Meffre,‡ Etienne Snoeck,† Bénédicte Warot-Fonrose,† Bruno Chaudret,‡ Lise-Marie Lacroix,‡ and Thomas Blon*,‡

Within a single domain NP





(a) Electron hologram of a 24 × 26 × (25 ± 4) nm^3 Fe nanocube and (b) corresponding magnetic phase shift map with 78 mrad isophase contours (as for (d)). (c) Cosines of the experimental phase corresponding to the magnetic induction flux lines. The inset color wheel indicates the direction of the magnetic induction. (d) Magnetic phase shift map calculated from micromagnetic simulations (dashed box indicates the cube position). (e) 3D view of the calculated magnetization obtained at the equilibrium state for a simulated cube of a 24 × 26 × 24 nm^3 Fe nanocube (22 × 24 × 22 nm^3 Fe core surrounded with a 1 nm Fe_3O_4 shell). (f) Comparison of experimental and simulated profiles along the arrows indicated in (b) and (d) (the vertical dashed lines indicate the cube position). For comparison, the dashed line represents the profile obtained for a vortex configuration whose the core is aligned along the [010] (i.e., y) direction of the NC.

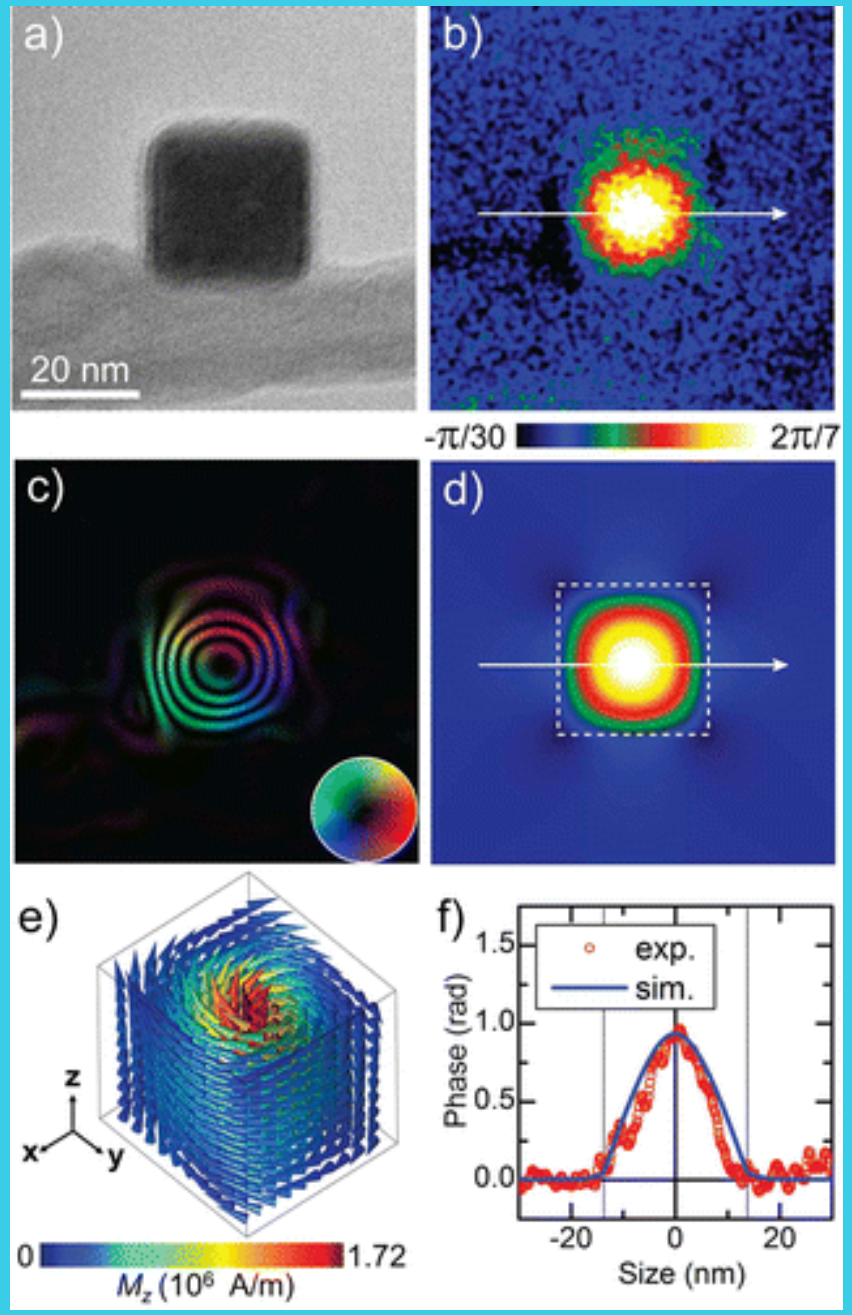
Flower state: 24 × 26 × (25 ± 4) nm^3 Fe nanocube

NANO LETTERS
Letter
pubs.acs.org/NanoLett

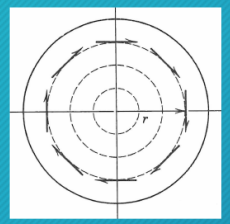
Size-Specific Spin Configurations in Single Iron Nanomagnet: From Flower to Exotic Vortices

Christophe Gatel,*,† Francisco Javier Bonilla,‡ Anca Meffre,‡ Etienne Snoeck,† Bénédicte Warot-Fonrose,† Bruno Chaudret,‡ Lise-Marie Lacroix,‡ and Thomas Blon*,‡

Within a single domain NP



Magnetic electron holography vs micromagnetic simulations of an isolated iron nanocube of 27 × 26 × (27 ± 5) nm3. (a) Experimental hologram and (b) resulting magnetic phase shift map. (c) Cosine of the experimental phase image corresponding to the magnetic induction flux lines (see Supporting Information). The inset color wheel indicates the direction of the magnetic induction. (d) Simulated magnetic phase shift map calculated from micromagnetic simulations (dashed box indicates the cube position). (e) 3D view of the magnetization obtained at the equilibrium state for a simulated cube of 29.53 nm3 (27.53 nm3 Fe core and a 1 nm Fe3O4 shell). (f) Comparison of experimental and simulated profiles along the arrows indicated in (b) and (d) (the vertical dashed lines indicate the cube position).

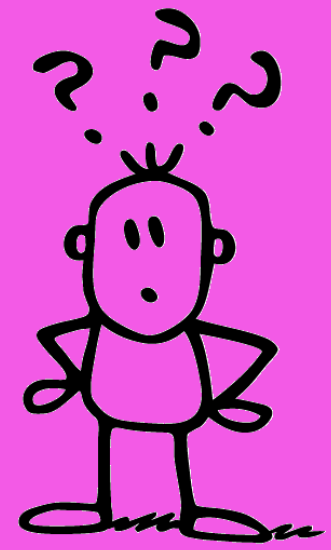


Vortex state: 27 × 26 × (27 ± 5) nm^3 Fe nanocube

4. The Stoner-Wohlfarth model

How's that?

Hysteresis with no domain wall??



Magnetization by coherent rotation

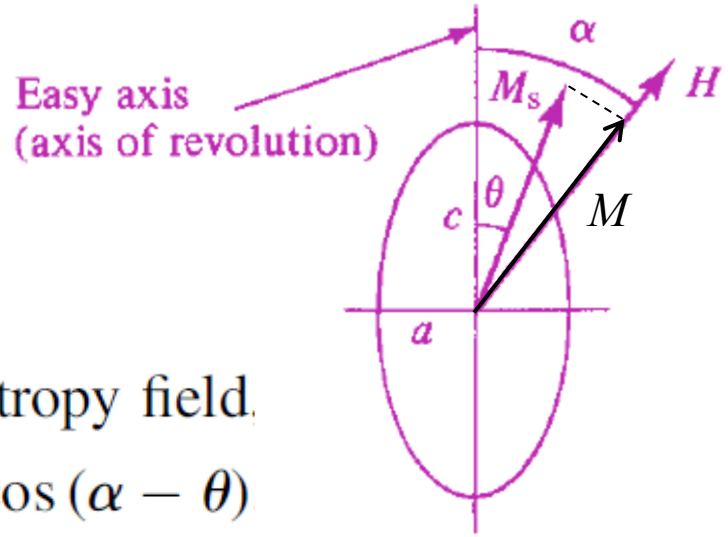
Model assumptions:

- Single domain nanoparticle (M_S)
- Fully saturated configuration
- Coherent magnetization rotation

Uniaxial anisotropy (K_u)

Field (H) is applied to any angle α to the easy axis

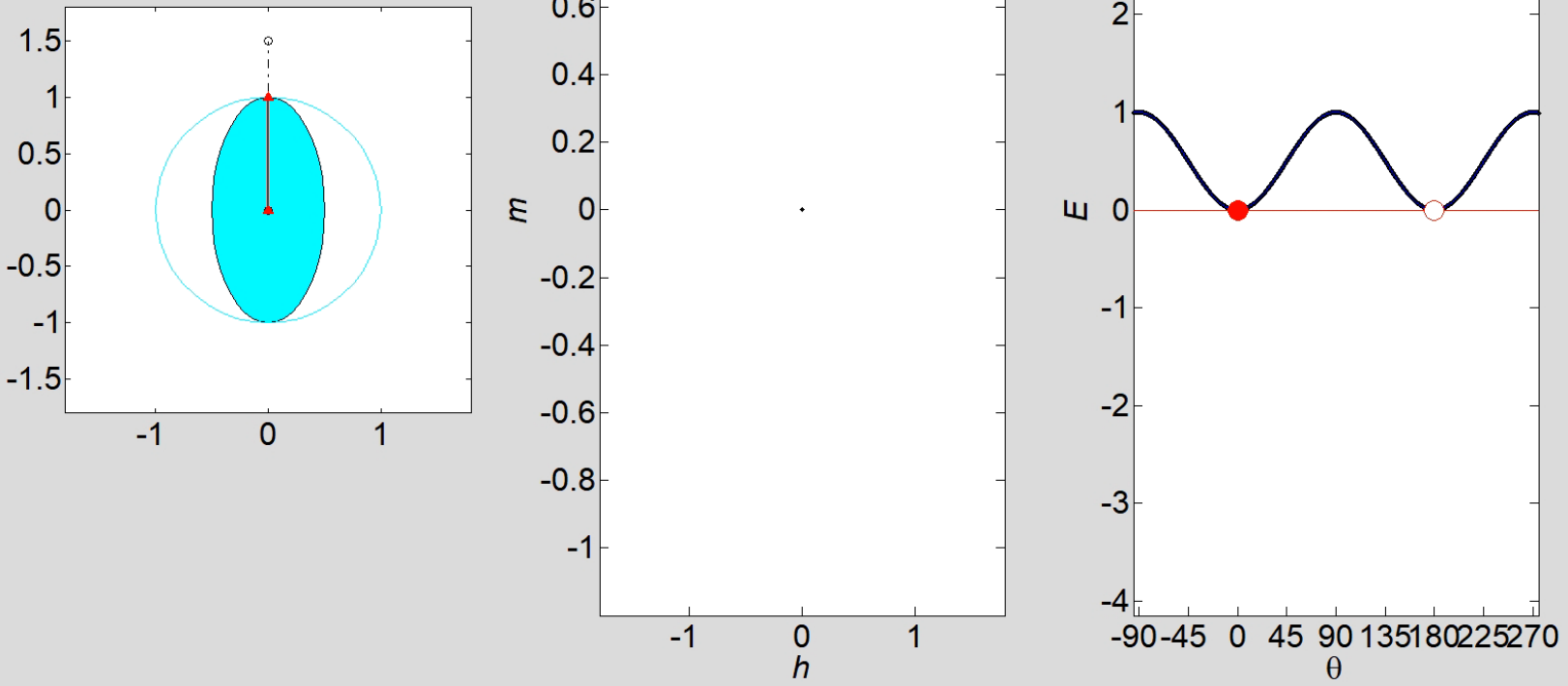
$$E = E_a + E_p = K_u \sin^2\theta - HM_s \cos(\alpha - \theta).$$



$$H_K = (2K_u/M_s) = \text{anisotropy field}$$

$$M = M_s \cos(\alpha - \theta)$$

Perpendicular case: Fully reversible



Perpendicular case: Fully reversible

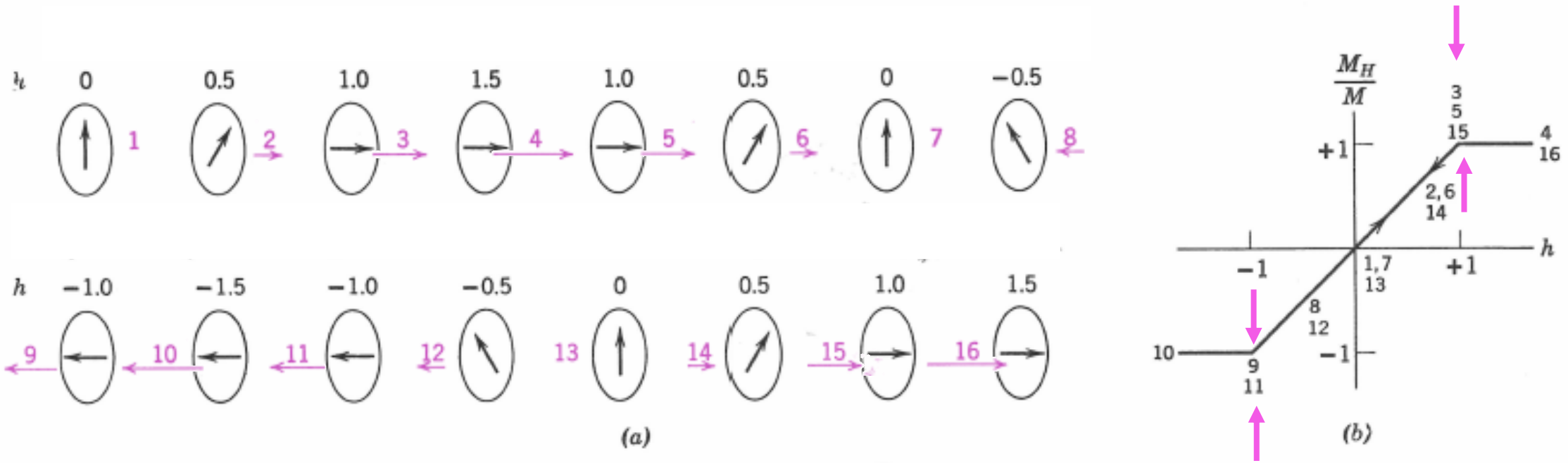
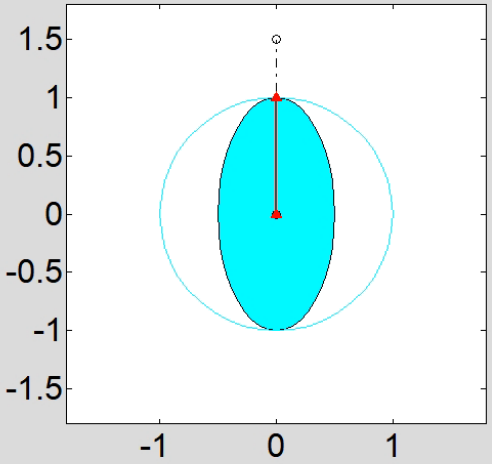
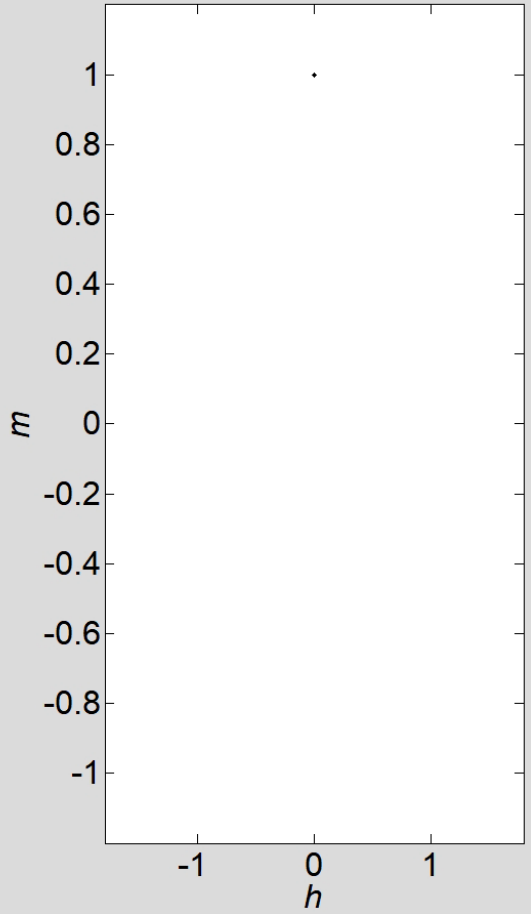
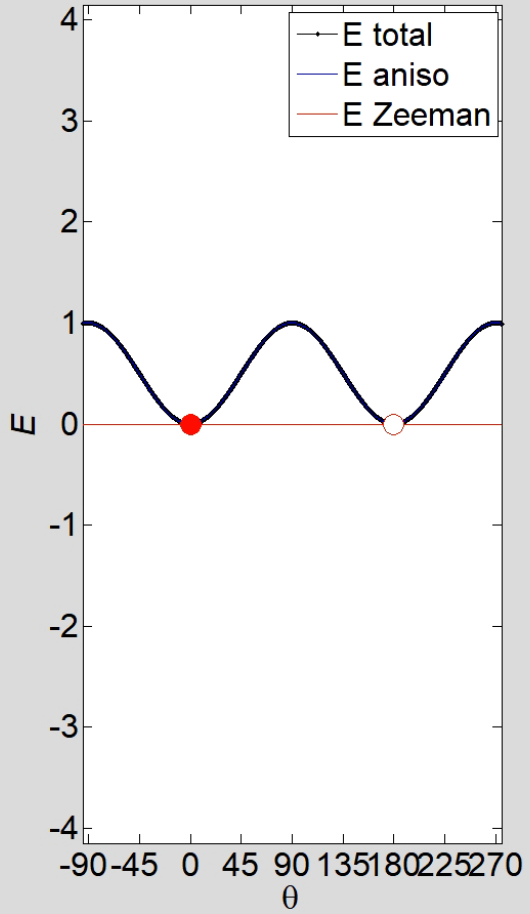


Fig. 7-2.5. The orientation of the magnetization **M** of a single-domain ellipsoidal particle as a function of a field applied perpendicular to the particle's polar axis ($\theta = \pi/2$) is illustrated. In (*a*) the vectors above the ellipses represent the field, whose magnitude is also indicated in units of h. The arrows within the ellipse represent the magnetization. The magnetization curve, plotted in the reduced units of M_H/M versus h, is shown at (*b*). The numbers 1, 2, 3, . . . , 16 correspond to successive stages in the application of the field. The hysteresis is zero.

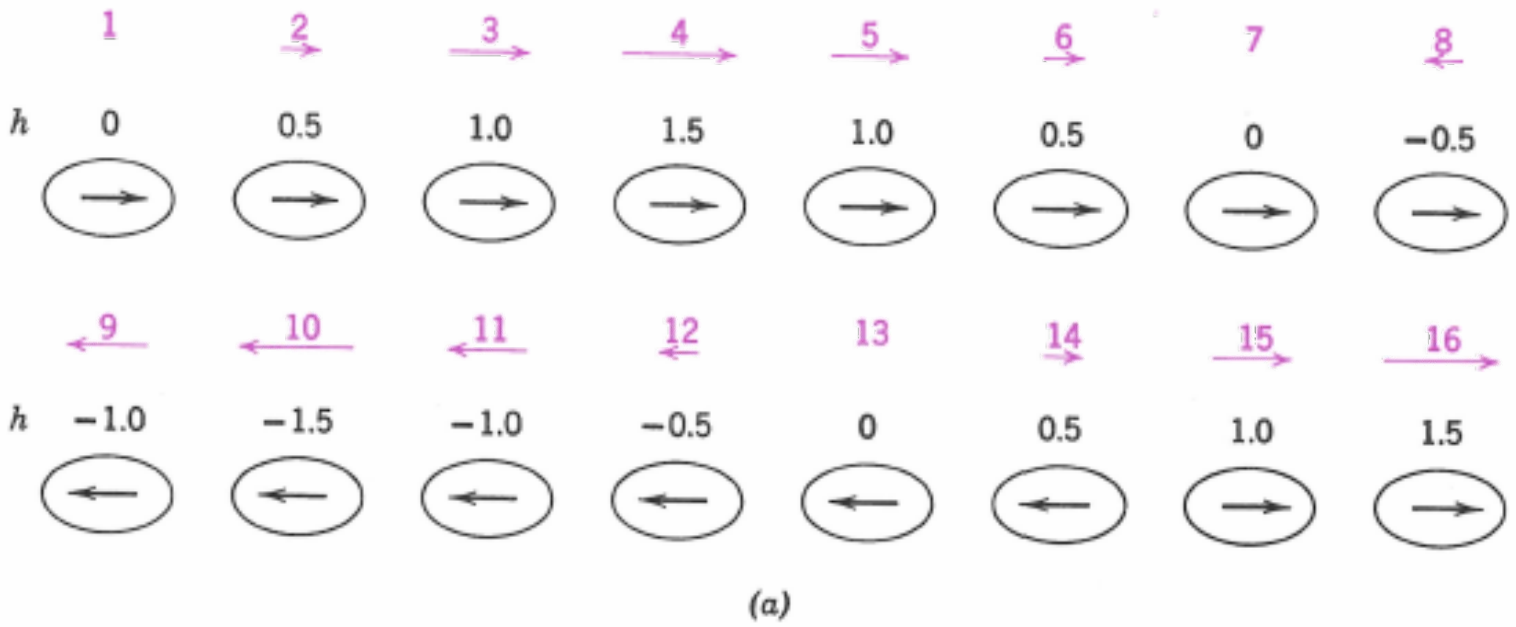
Parallel case: Fully irreversible







Parallel case: Fully irreversible



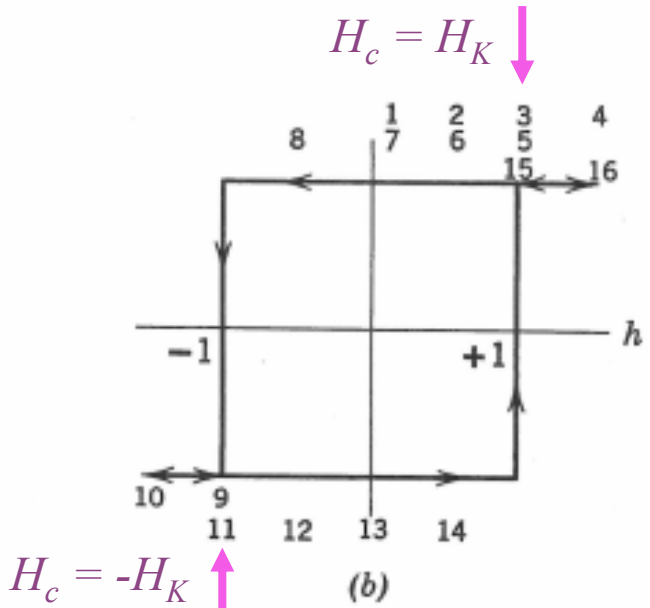
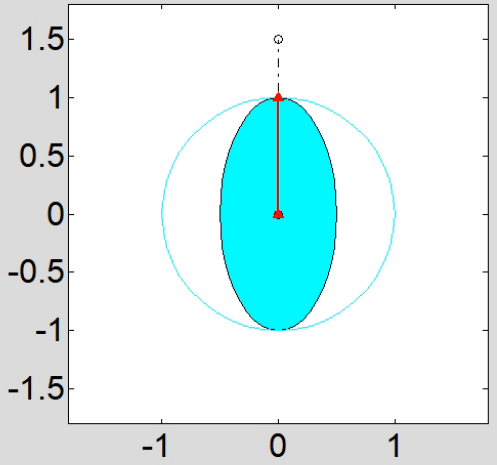
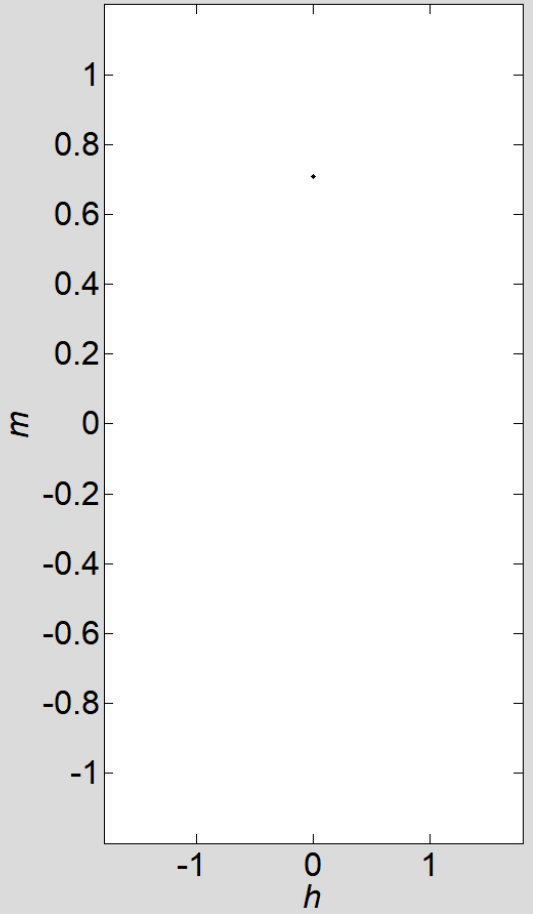
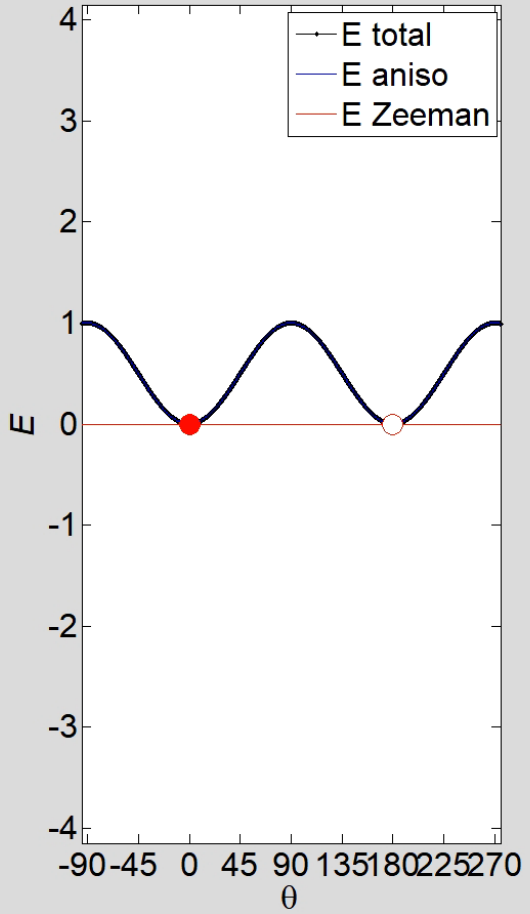


Fig. 7-2.6. Similar to Fig. 7-2.5, except that the field is applied along the polar axis ($\theta = 0°$). The jump in the magnetization occurs at $h = 1$. No reversible rotation occurs.

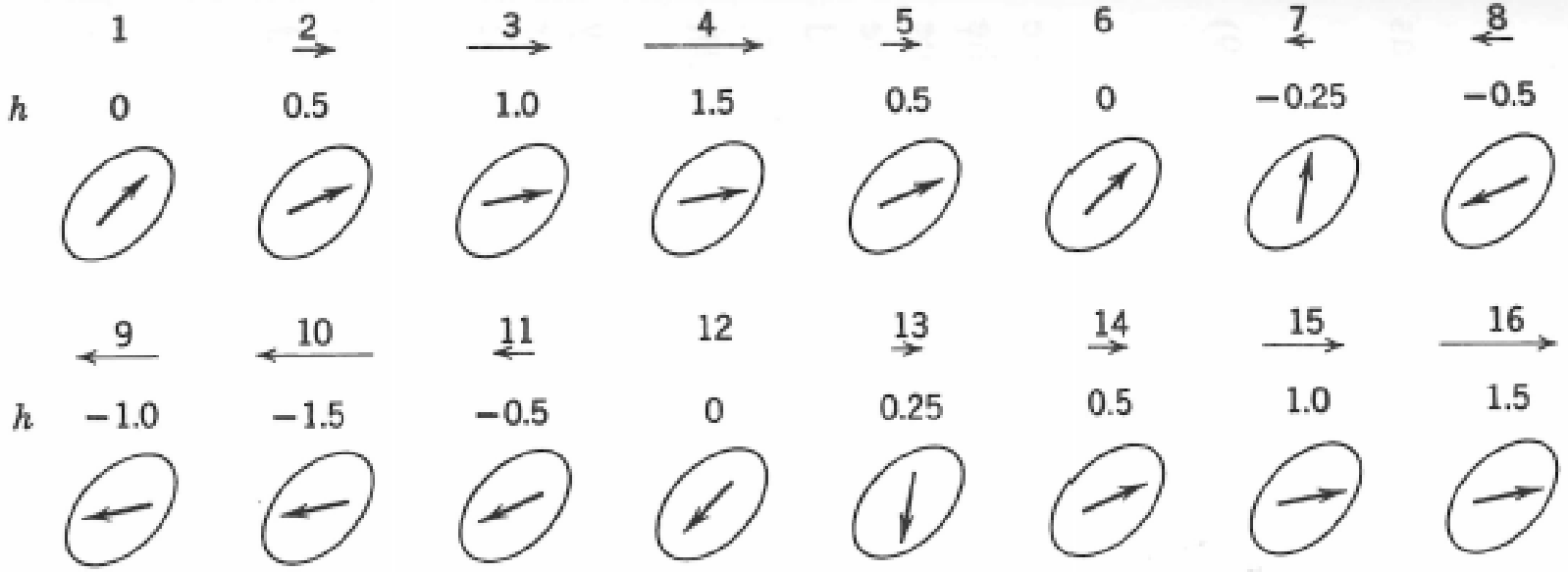
45° case: Reversible & irreversible







45° case: Reversible & irreversible



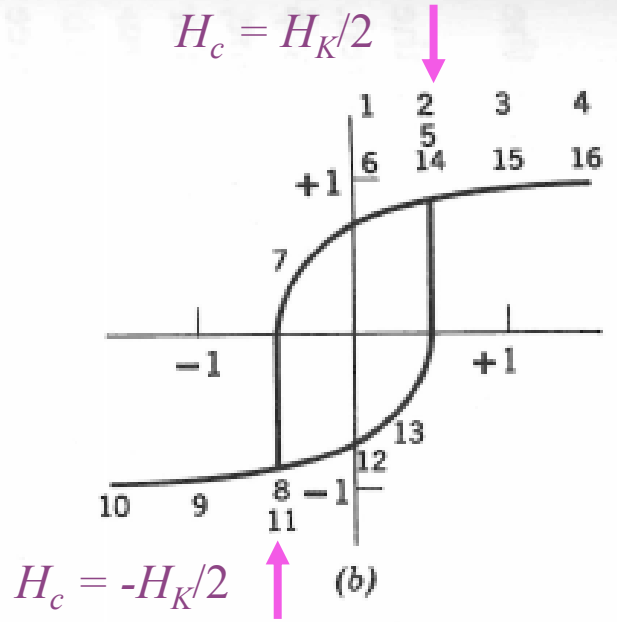
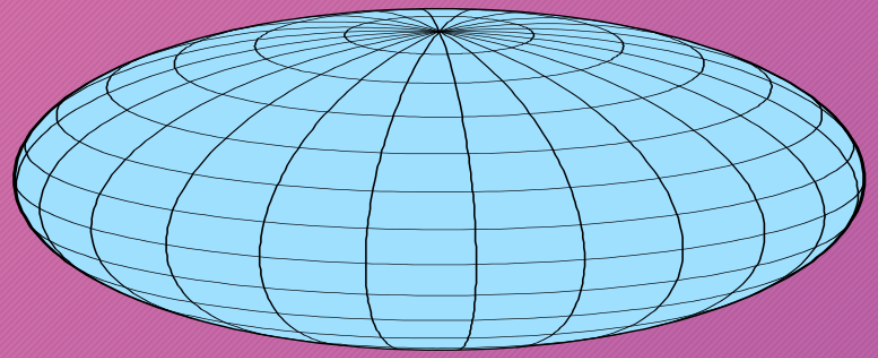


Fig. 7-2.8. $\theta = 45°$. The jump occurs at $h = 0.5$, which is the smallest field at which a jump takes place for any value of θ. The magnetization is double valued for $-0.5 < h < 0.5$.



No hysteresis for oblate S-W NPs

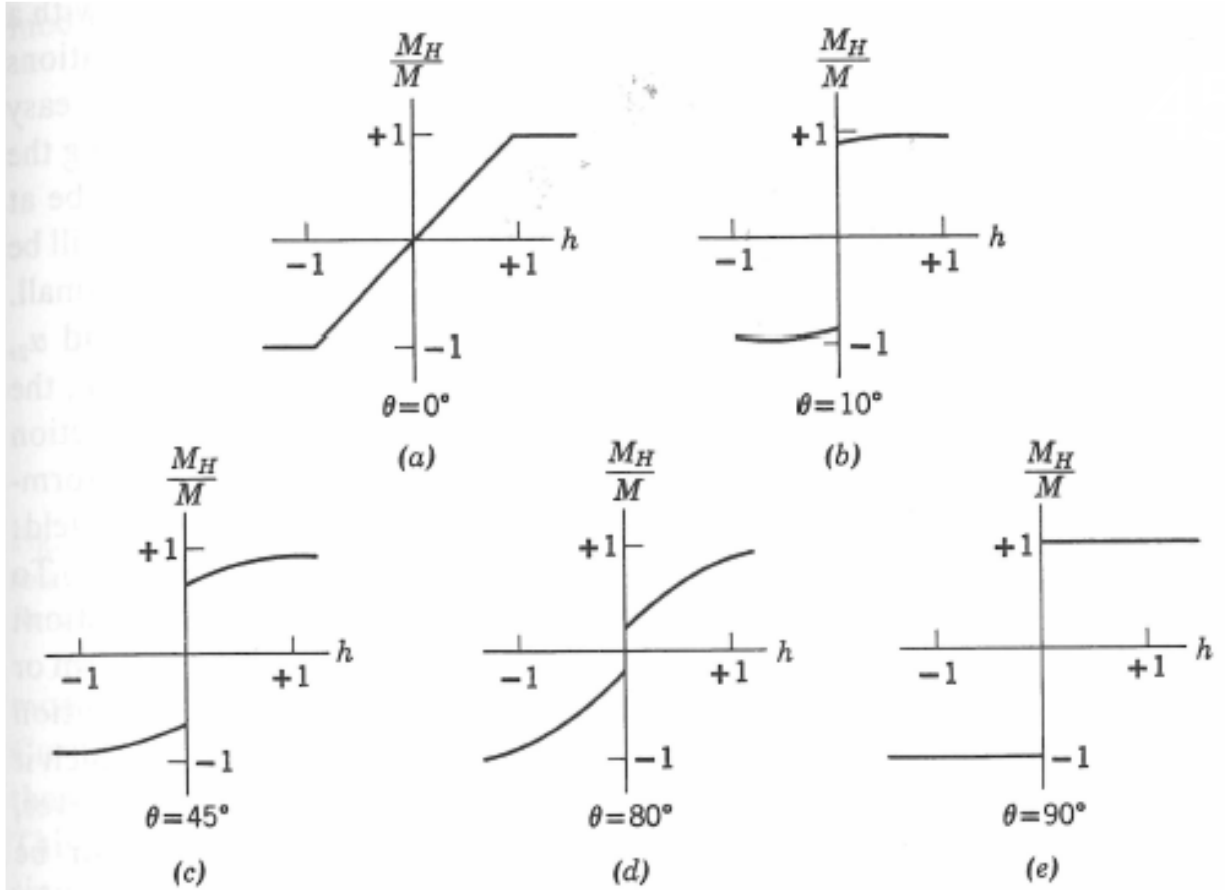


Fig. 7-2.11. Magnetization curves for an oblate ellipsoid of revolution plotted in reduced units. The successive curves are for various angles α between the applied magnetic field and the polar (a) axis, as indicated. In no case is there any hysteresis. [Based on calculations by E. C. Stoner and E. P. Wohlfarth, *Phil. Trans. Roy. Soc.* (*London*) **A-240,** 599 (1948).]

The magnitude of the anisotropy field

Table 7-2.1. Maximum Coercive Forces of Single-Domain Particles Assumed to Possess Only One Type of Anisotropy
(room temperature)

Material	Coercive Force (oersteds) Shape $2\pi M$	Crystalline $\frac{2K_1}{M}$ or $\frac{2K_1'}{M}$	Strain $\frac{3\lambda_s\sigma}{M}$
Fe	10,700	540	600
Ni	3,050	5850	4000
Co	8,800	200	600

$H_K = (2K_u/M_s)$

(shape) $H_K = h(N_a - N_c)M_s,$ (9.46)

(stress) $H_K = h\left(\frac{3\lambda_{si}\,\sigma}{M_s}\right),$ (9.47)

(crystal) $H_K = h\left(\frac{2K_1}{M_s}\right),$ (9.48)

where N_a and N_c are the demagnetizing factors parallel to the a and c axes, λ_{si} the saturation magnetostriction (assumed isotropic), σ the stress, and K_1 the crystal anisotropy constant. If

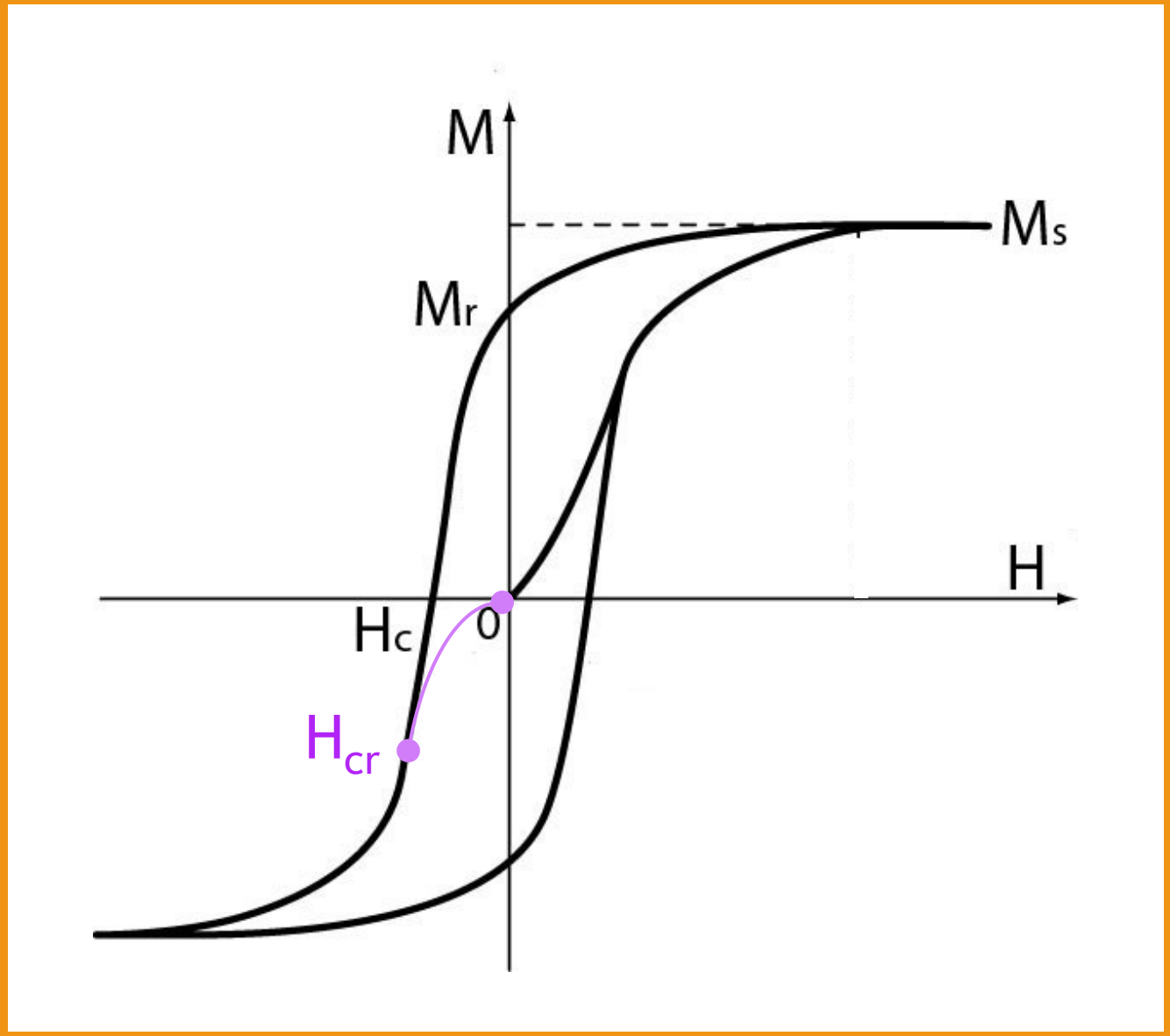
Very large!

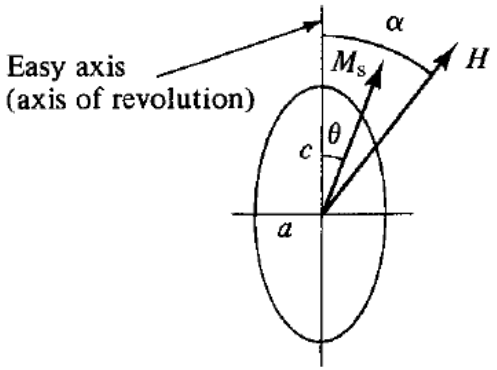


5. Coercivity and Hysteresis

Reversing the NP magnetization

Hysteresis loop





Residual magnetization $I_r = 0.5 I_s$

Coercive field $H_c \simeq 1.0 \dfrac{K_u}{I_s}$

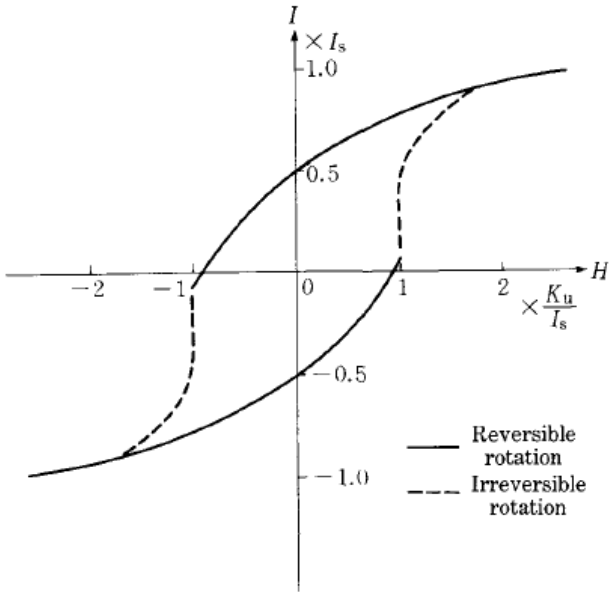


Fig. 18.39. Hysteresis loop of an assembly of randomly oriented single domain particles with uniaxial anisotropy, calculated by averaging the loops in Fig. 18.38.

Assembly of ramdomly oriented prolate NPs

Coercivity and remanence: SD vs. MD

SD NPs feature much larger remanence and coercivty because magnetization inversion occurs *via* magnetization rotation and not *via* domain wall displacement

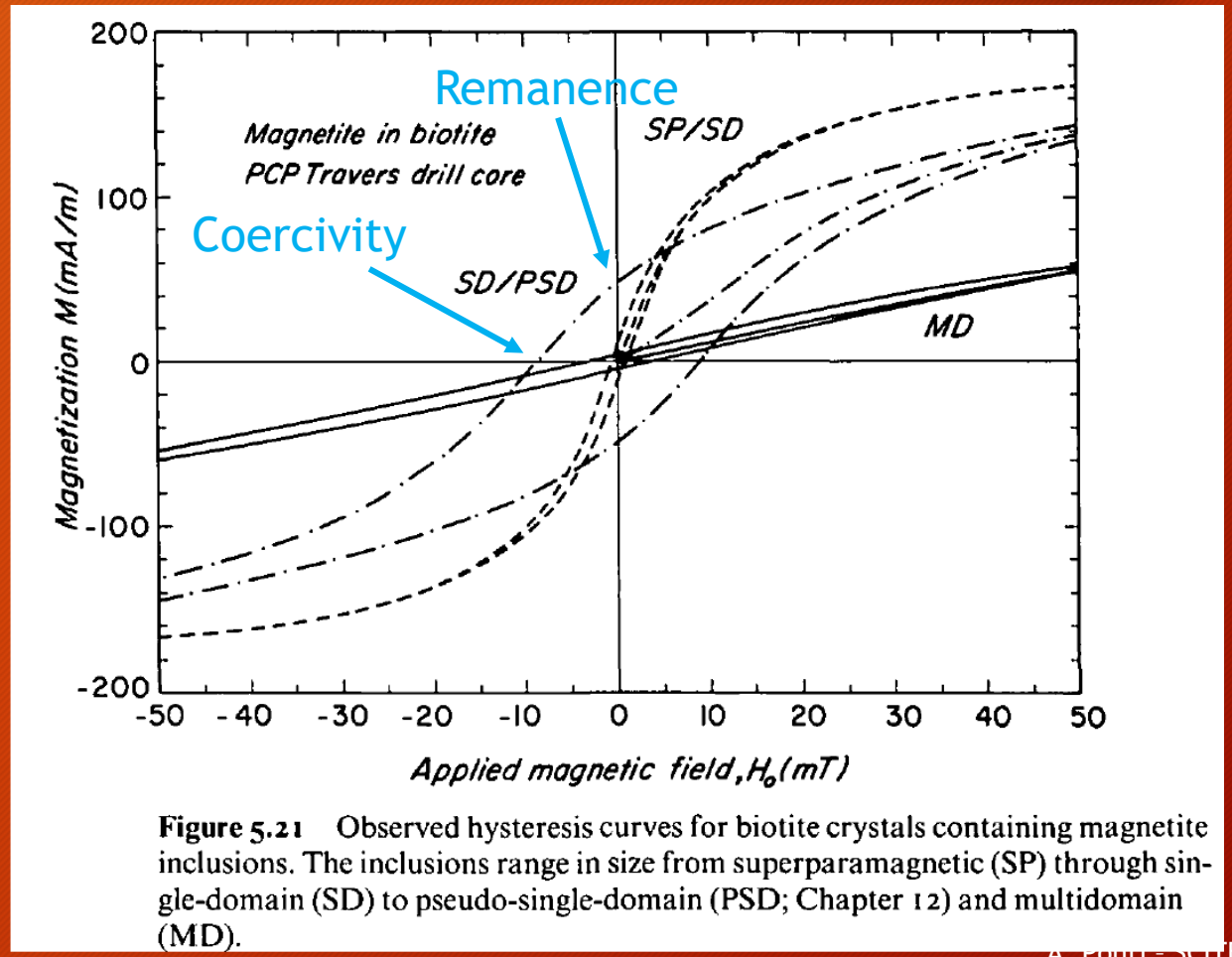


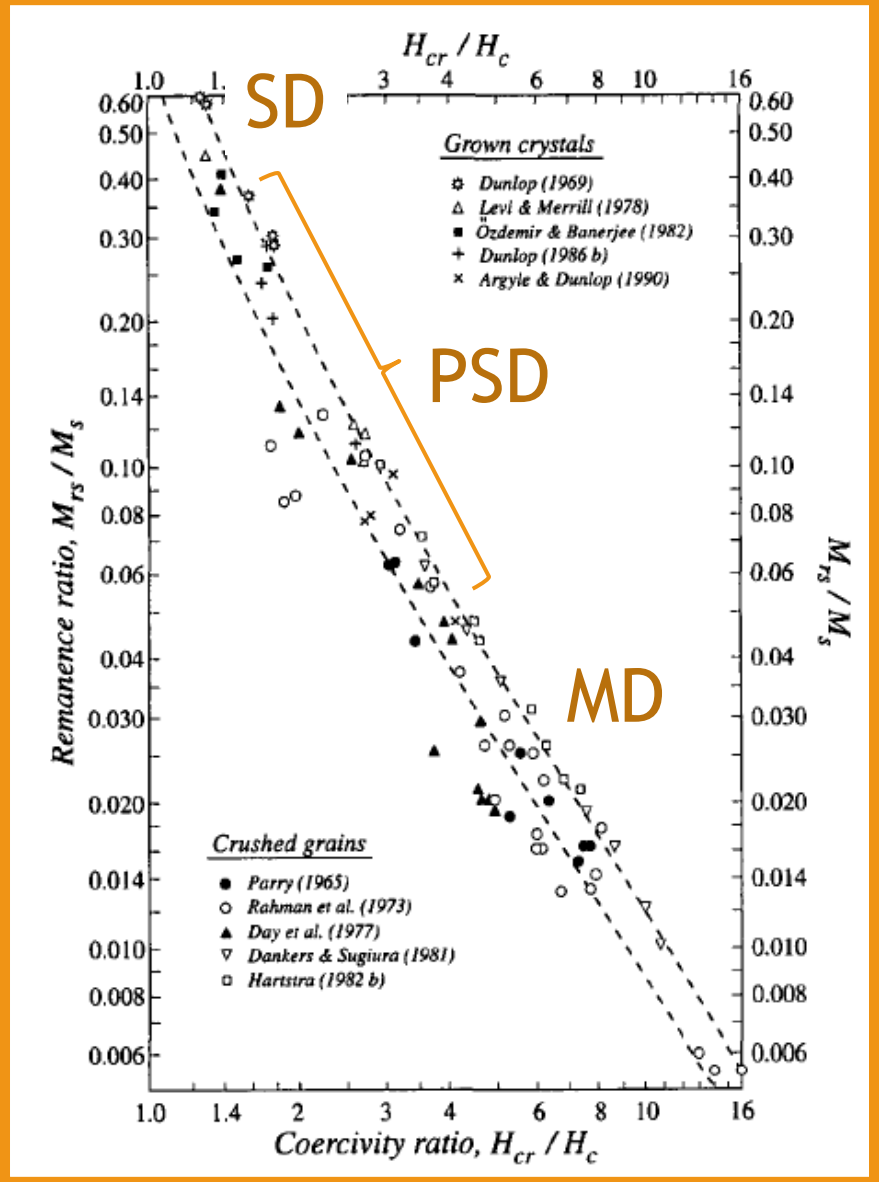
Figure 5.21 Observed hysteresis curves for biotite crystals containing magnetite inclusions. The inclusions range in size from superparamagnetic (SP) through single-domain (SD) to pseudo-single-domain (PSD; Chapter 12) and multidomain (MD).

$M_{rs}/M_s =$		
	0.500	uniaxial
	0.866	cubic, ⟨111⟩ easy axes (magnetite)
	0.832	cubic, ⟨100⟩ easy axes (TM60)
	0.500–0.637	uniaxial, easy plane (hematite)
	0.750–0.955	triaxial, easy plane (hematite)

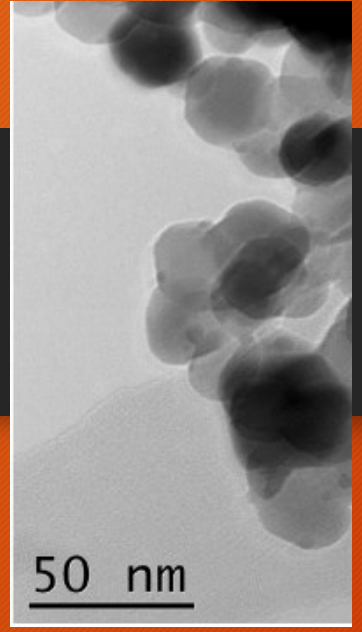
The estimation of H_{cr}/H_c is more problematic. For coherent rotation in randomly oriented grains of a single microscopic coercive force H_K, H_{cr}/H_K is 0.524 for uniaxial anisotropy (Wohlfarth, 1958), 0.204 and 0.333 for cubic anisotropy with ⟨111⟩ and ⟨100⟩ easy axes, respectively (Joffe and Heuberger, 1974), and 0.642 for uniaxial anisotropy within an easy plane (Dunlop, 1971). H_c has

What can we learn from hysteresis loops?

What can we learn from hysteresis loops?



Temperature

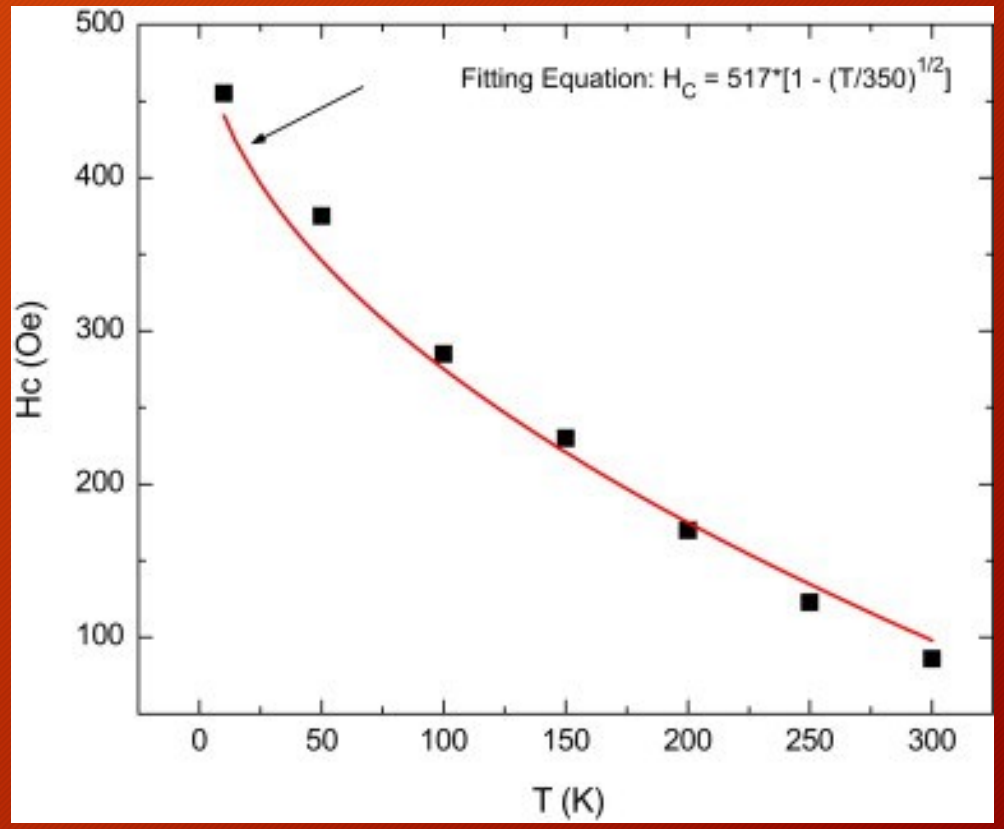


K.Maaz et al., JMMM 322 (2010) 2199-2202

$NiFe_2O_4$ NPs: <*D*> = 24 nm, std dev 4 nm

The coercivity follows a simple model of thermal activation of the NP moment over the anisotropy barrier in the temperature range 10–300 K, in accordance with *Kneller's law*

$$H_C = H_{C0}\,[1-(T/T_B)^{1/2}]$$



Temperature dependence of coercivity for the $NiFe_2O_4$ NPs. The red line shows the fit curve according to Kneller's law

Surface anisotropy

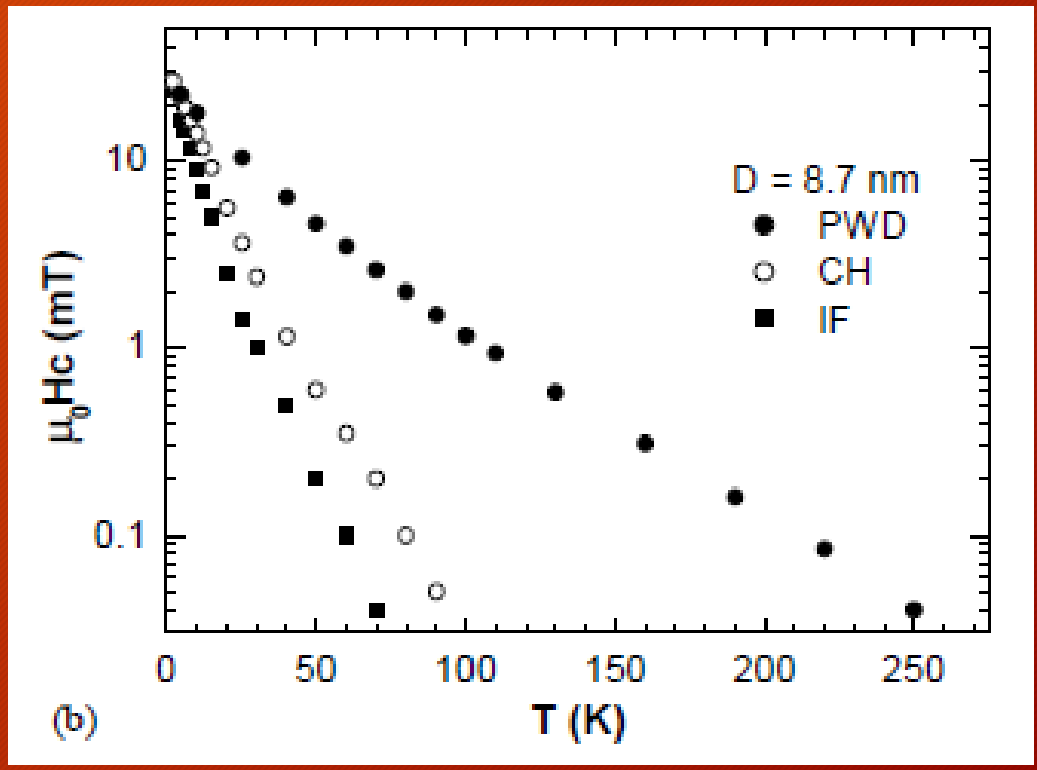
E. Tronc et al., JMMM 262 (2003) 6–14

γ-Fe_2O_3 NPs: 8.7, 4.6 and 2.7 nm

The temperature dependence of H_c is not in agreement with expectations.

The coercivity is due to **surface-to-core** exchange coupling, i.e., surface exchange anisotropy.

The uniaxial surface anisotropy $K_S = 1.5 \cdot 10^5$ J/m^2



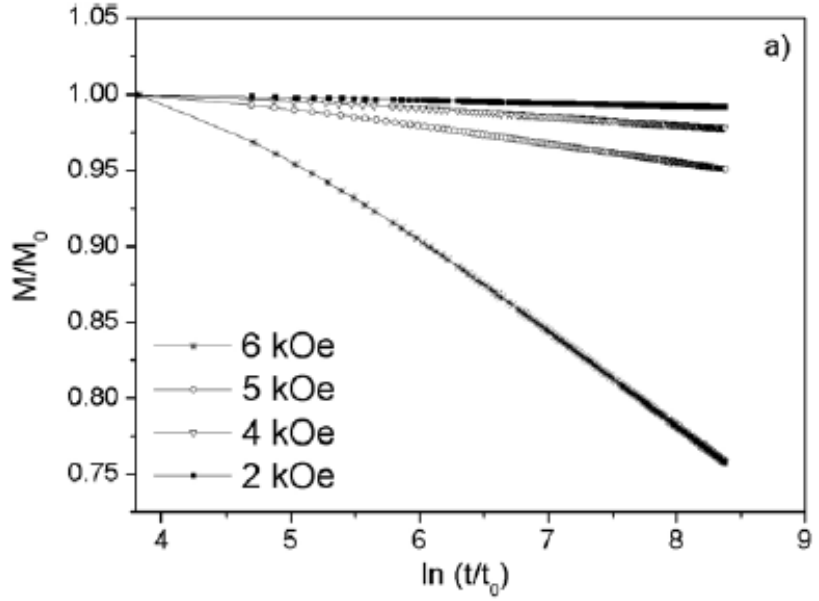
Magnetic viscosity and activation volume

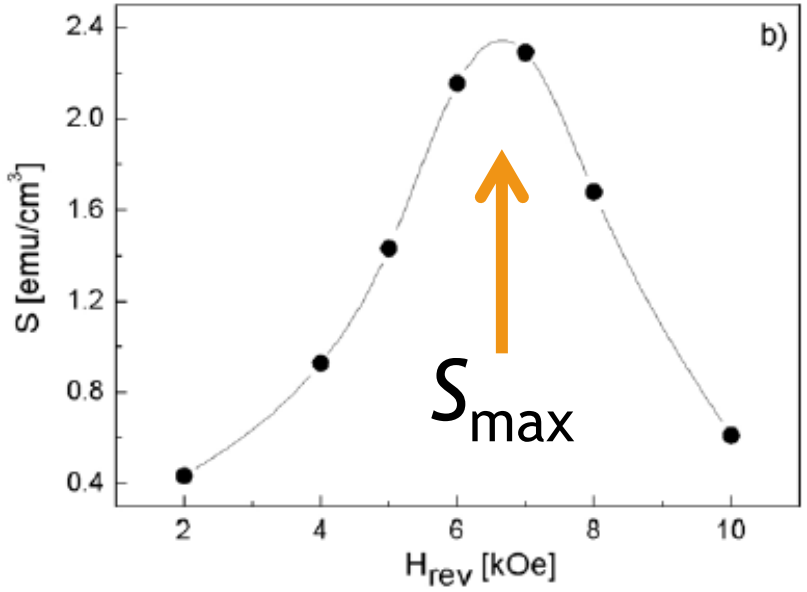
The time relaxation of magnetization arises from the thermally activated decay of metastable states over energy barriers. For a collection of non-interacting or weakly interacting particles, characterized by a distribution of energy barriers (or activation energies), a logarithmic decay of $M(t)$ is usually observed:

$$M(t) = \text{const} \pm S \ln\left(\frac{t}{t_0}\right) \qquad (3)$$

where S is the so-called magnetic viscosity coefficient, t_0 is the

The activation volume can be defined as the volume of the material involved in the process of overcoming the energy barrier for magnetization reversal. For very small single-domain non-interacting particles, the switching process occurs by coherent rotation and the activation volume corresponds to the entire particle physical volume V_f ($v_{act(u)} = V_f$), whereas





$$v_{act(u)} = \frac{k_B T}{M_s H_f} = \frac{k_B T \chi_{irr}}{M_s S_{max}}$$

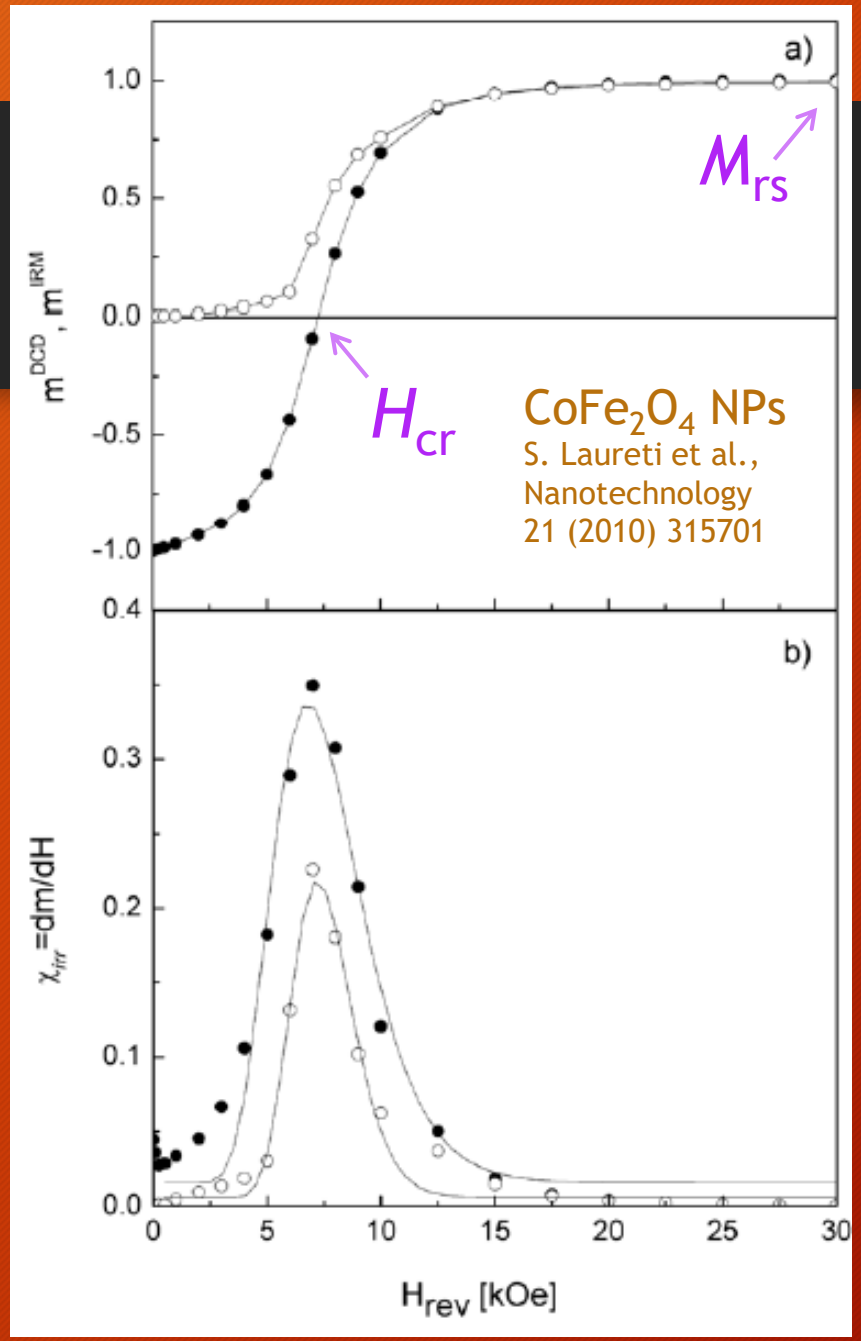
S_{max} from magnetic viscosity
M_s from hysteresis loop
x_{irr} from DCD

$CoFe_2O_4$ NPs
S. Laureti et al., Nanotechnology 21 (2010) 315701

IRM and DCD provide χ_{irr} and SFD

$$SFD \approx \left|\frac{dM(DCD)}{dH}\right| = \chi_{irr}^{DCD}$$

$$SFD \approx \left|\frac{dM(IRM)}{dH}\right| = \chi_{irr}^{IRM}$$



SFD represents the PDF of NP switching fields and provides clues into the coercivity

Brown's paradox

Coercive field $H_c \simeq 1.0 \frac{K_u}{I_s}$

If we insert the K_u and M_s values of hexaferrites (and even cubic ferrites) in this equation, we get coercive fields of the order of 1 tesla.

If one measures a SINGLE small single-domain NP, the coercivity is (sometimes) close to this value. However, a macroscopic magnet made up of NPs has coercivity typically **10-100 times smaller!**

- *Incoherent magnetization rotation*
- *Domain wall nucleation*
- *Shape imperfections*
- *Microstructural defects*
- *Easy axis misalignment*
- *Interparticle interactions*

Beyond coherent rotation

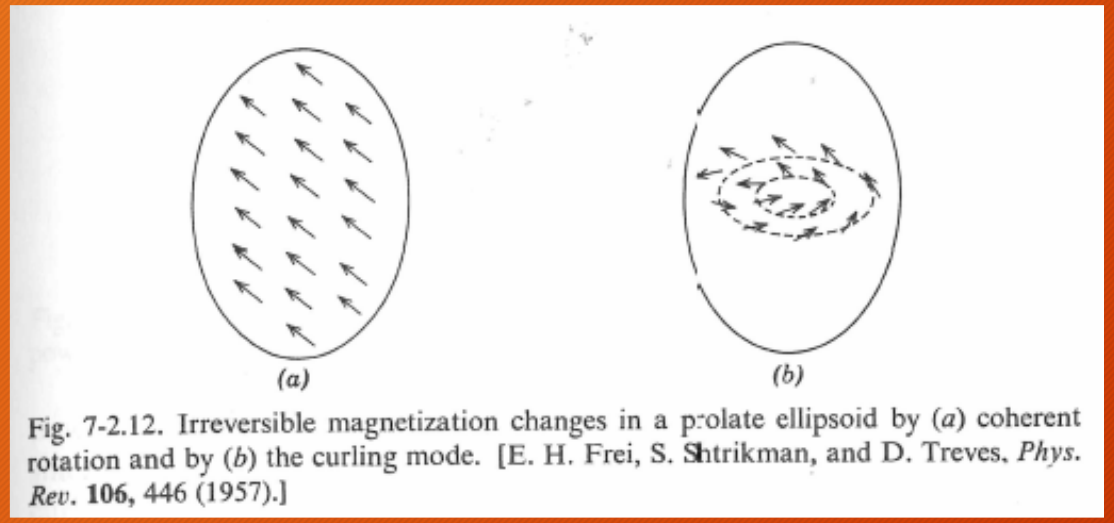


Fig. 7-2.12. Irreversible magnetization changes in a prolate ellipsoid by (*a*) coherent rotation and by (*b*) the curling mode. [E. H. Frei, S. Shtrikman, and D. Treves, *Phys. Rev.* **106,** 446 (1957).]

Coherent Curling

Buckling Fanning

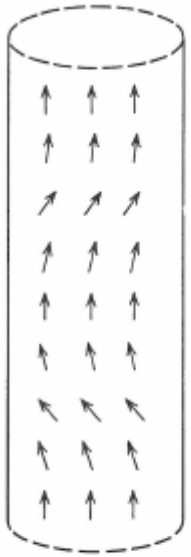


Fig. 7-2.13. The change of magnetization in an infinite circular cylinder by the buckling mode. [E. H. Frei, S. Shtrikman, and D. Treves, *Phys. Rev.* **106,** 446 (1957).]

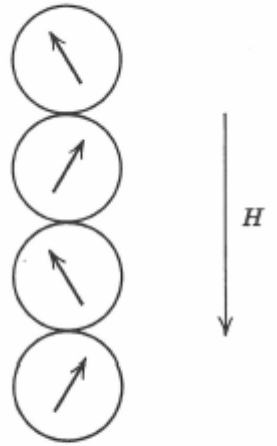


Fig. 7-2.14. Magnetization reversal by "fanning" in a chain of spheres. (After I. S. Jacobs and C. P. Bean.)

The coherent critical size

$$\frac{R_{sd}}{R_{coh}} = \frac{18}{\sqrt{6}}\sqrt{\frac{|K_u|}{M_S^2}}$$

T gnetic leng

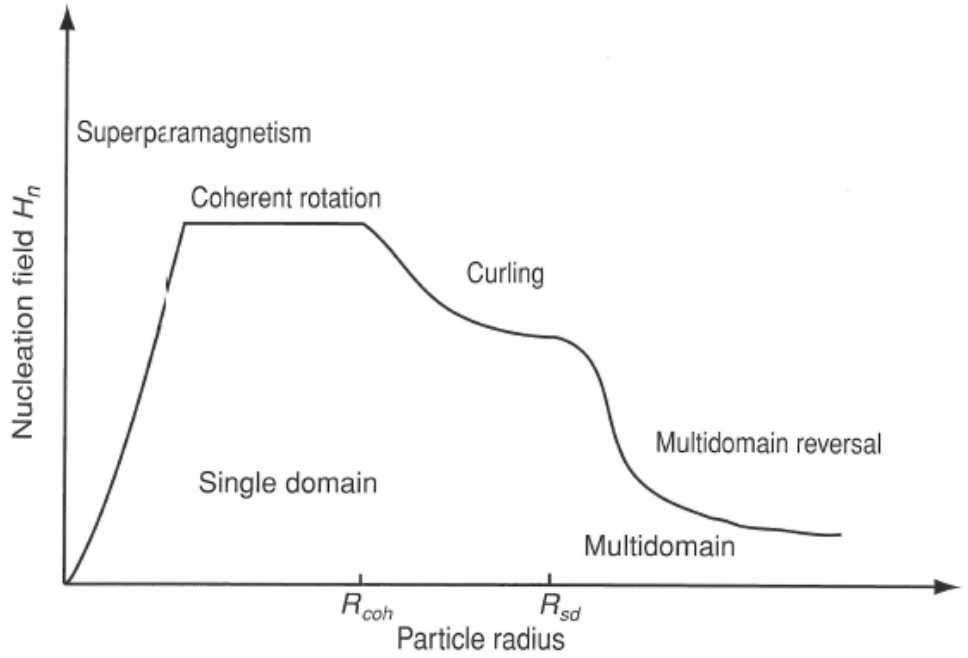
Length	Expression	Fe	Co	Ni	$Nd_2Fe_{14}B$	Fe_3O_4	$CoFe_2O_4$	$BaFe_{12}O_{17}$
κ	$\sqrt{\lvert K_1\rvert/\mu_0 M_s^2}$	0.12	0.45	0.13	1.54	0.21	0.84	1.35
l_{ex}	$\sqrt{A/\mu_0 M_s^2}$	2.4	3.4	5.1	1.9	4.9	5.2	5.8
R_{coh}	$\sqrt{24}l_{ex}$	12	17	25	9.7	24	26	28
δ_w	$\pi l_{ex}/\kappa$	64	24	125	3.9	73	20	14
R_{sd}	$36\kappa l_{ex}$	10	56	24	110	38	160	280
R_{eq}	$(3k_BT/4\pi BM)$	0.8	0.8	1.2	0.9	1.2	1.2	1.3
R_b	$(6k_BT/K_1)^{1/3}$	8	4	17	1.7	13	5	4

κ, hardness parameter; l_{ex}, exchange length; R_{coh}, m t rotation; δ_w n equilibrium single domain particle size; R_{eq}, particle radius for which m $B = k_BT$ in 1 tic blocking

Beyond coherent rotation: size effects

Figure 7.18

Nucleation field as a function of particle size, showing superparamagnetism, coherent rotation, curling and multidomain reversal. The nucleation field is an upper limit on the coercivity. (After Kronmüller and Fähnle (2003).)



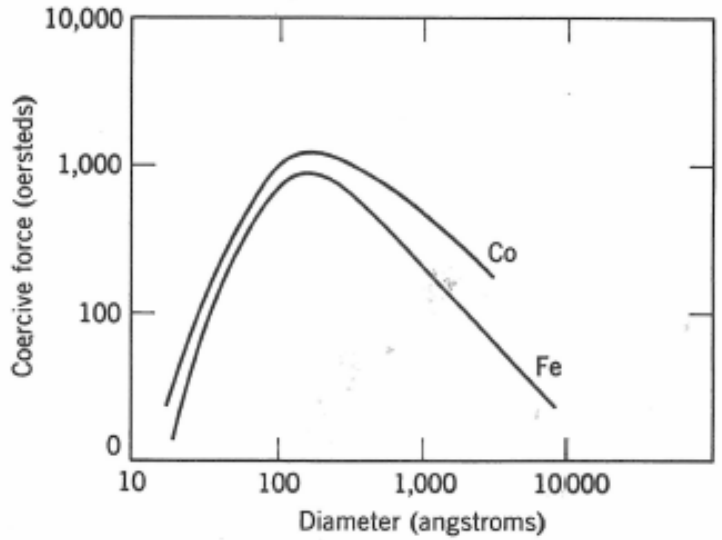
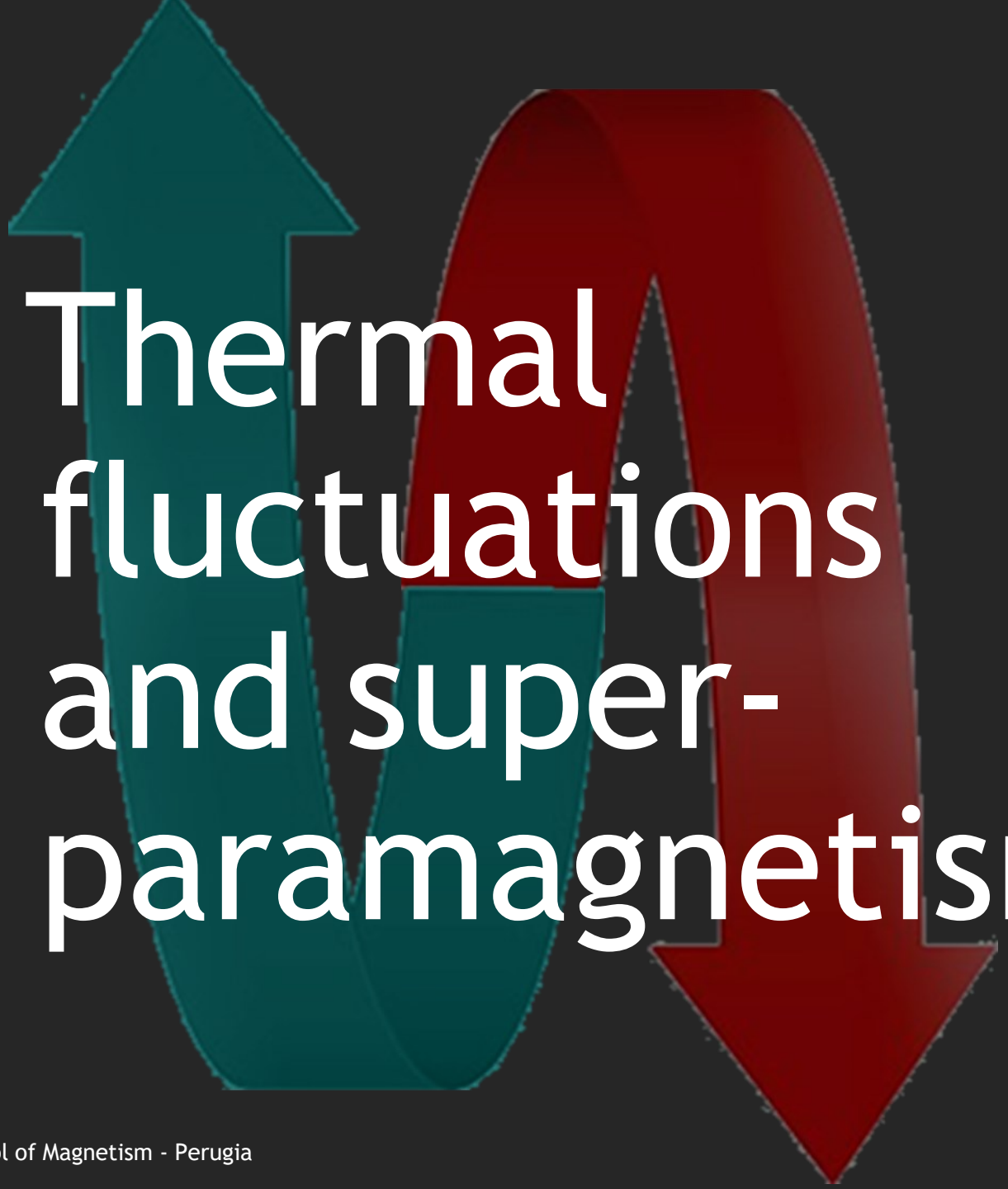


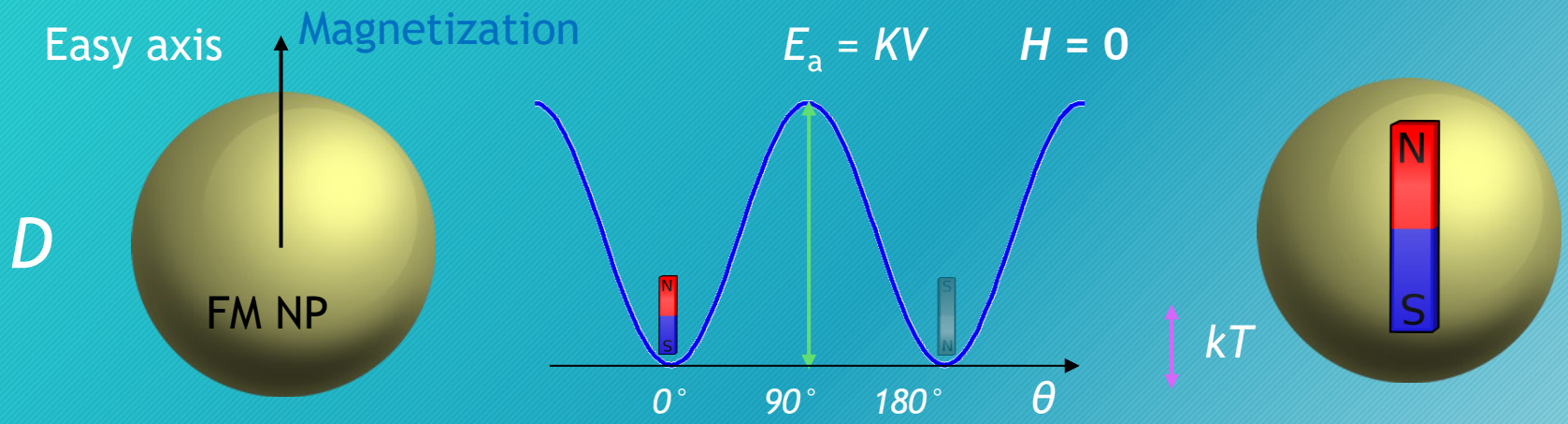
Fig. 7-2.15. Coercive force as a function of particle size. The coercive force of the powders develops from both crystalline and shape anisotropy. $T = 76°K$.

6. Thermal fluctuations and super-paramagnetism

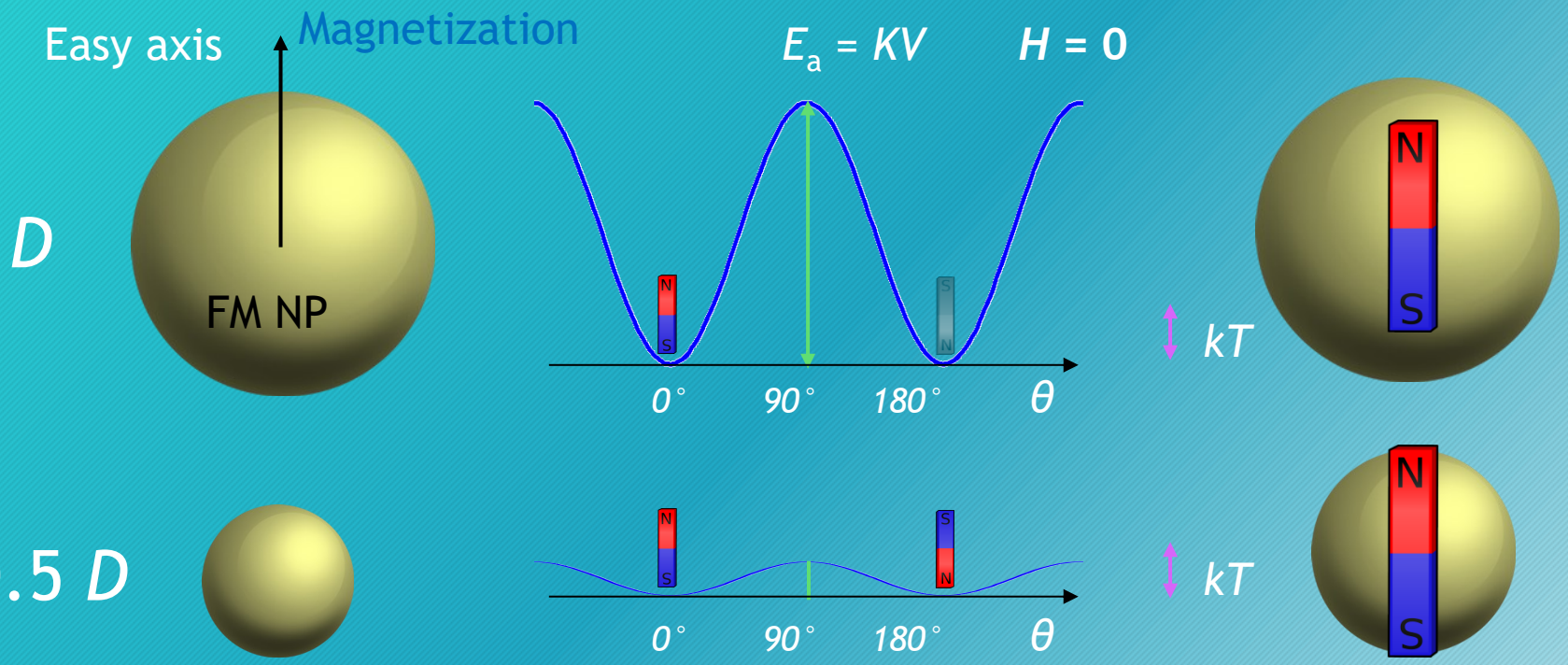


The eye of the beholder

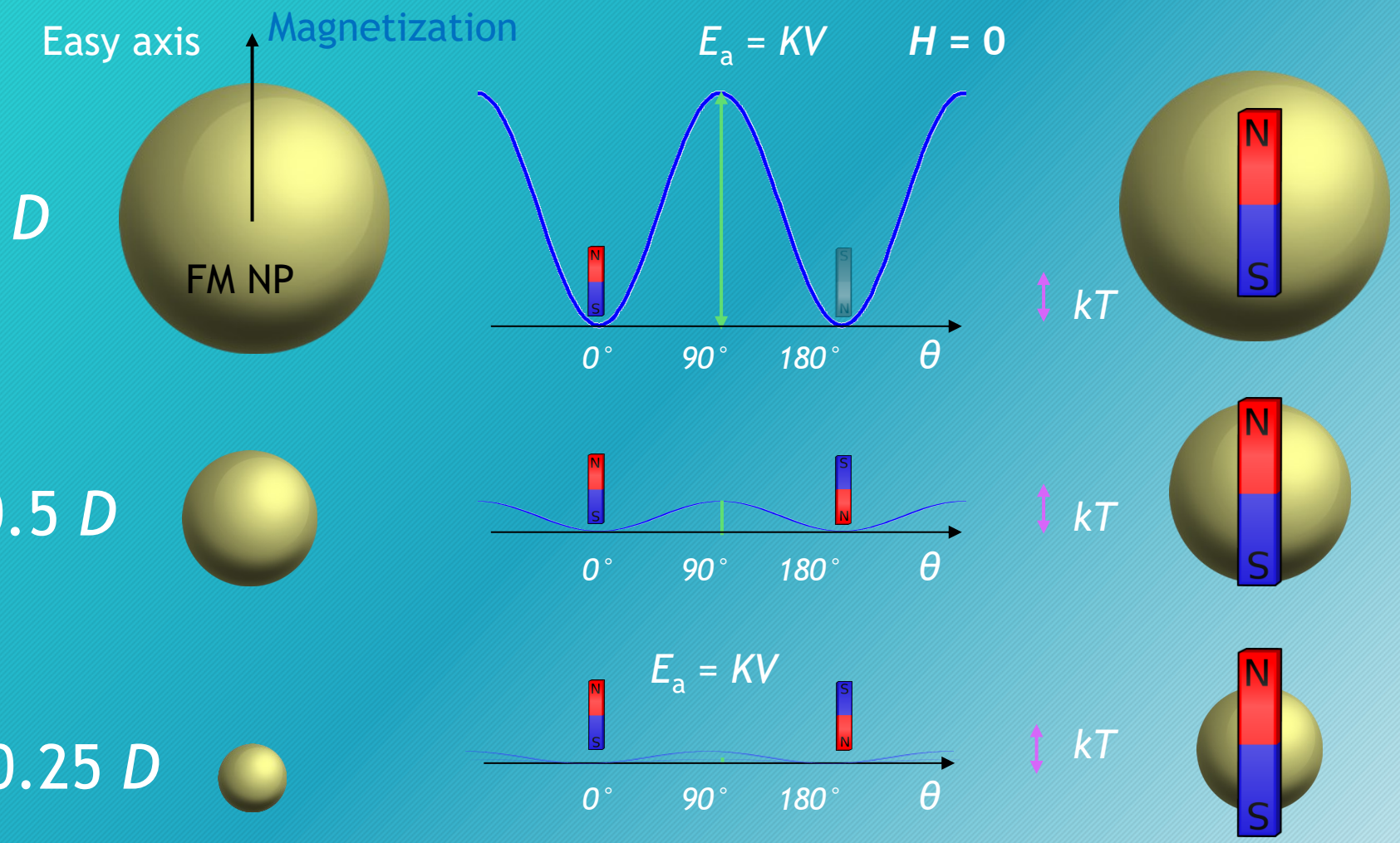
Fluctuation and size



Fluctuation and size



Fluctuation and size



Superparamagnetism

Superparamagnetism occurs when the thermal energy is larger than the barrier to inversion and thus rapid magnetization **fluctuation is observed**, ie, when the magnetic relaxation time is smaller than the timescale that is **important to me.**

Magnetization relaxation time

$$\tau = \tau_0 \, exp\left(\frac{\Delta E}{kT}\right) = \tau_0 \, exp\left(\frac{KV}{kT}\right)$$

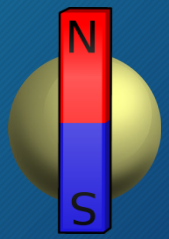
$$\tau_0 = 10^{-9} - 10^{-11} \, s$$

Superparamagnetism is a **dynamical regime of FM/FIM NPs**, it is **not** a thermodynamic phase.

SPM and anisotropy

Key to understand how SPM affects the magnetic behavior

Fast thermal relaxation washes out all anisotropies,
i.e., superparamagnetism = no effective anisotropy

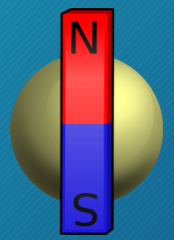


In the NP free energy, only two terms are not averaged to isotropy:

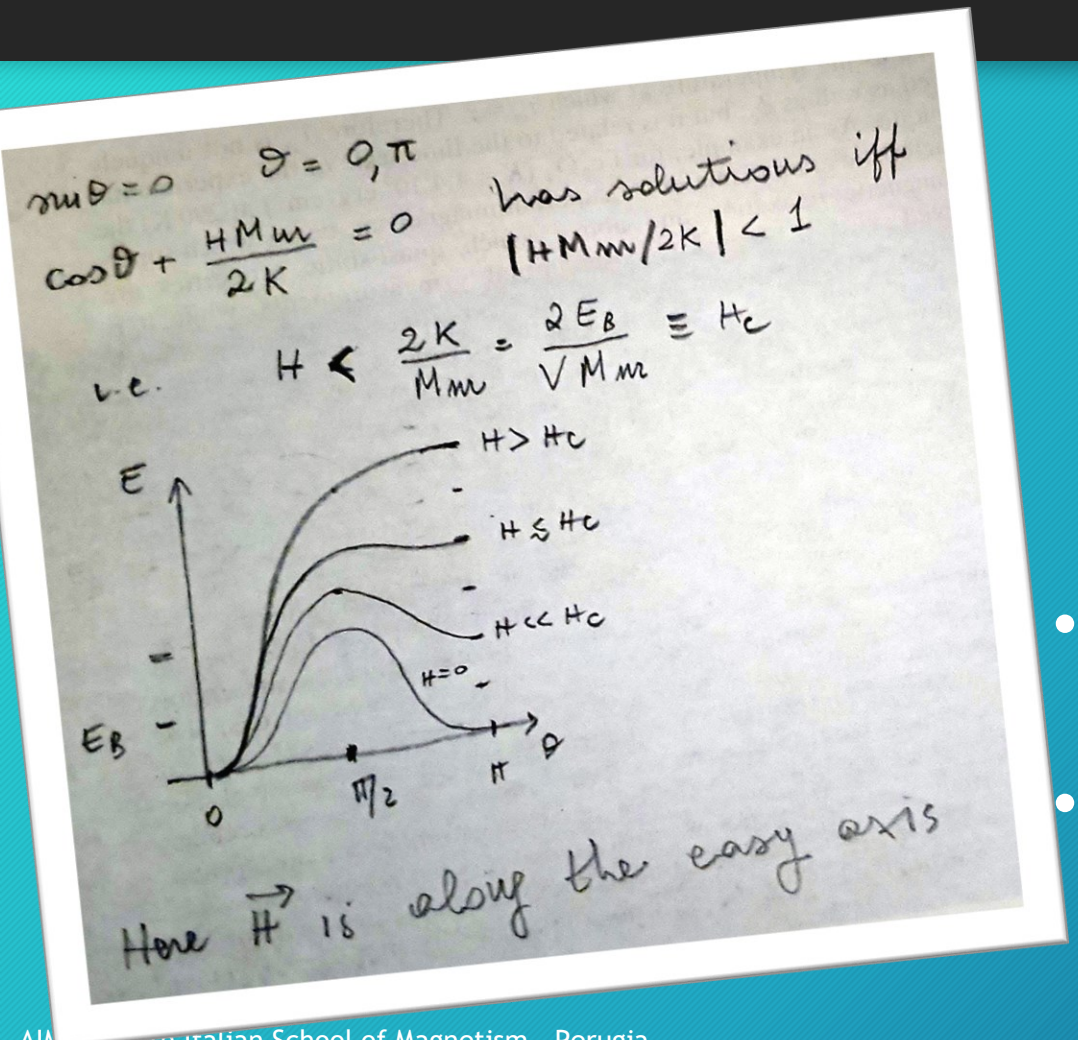
- Exchange: ferromagnetic order
- Zeeman: magnetization responds to applied field

SPM and magnetic properties

- Remanence $M_r = 0$
  despite FM order present
- Coercivity $H_c = 0$
  thermal equilibrium readily reached
  (absolute minimum of free energy)



SPM in the presence of field



- Saturation $M_s = n\,\mu$ (Strong exchange & strong Zeeman)
- $M(H) = M_s\,L(\alpha)$, $\alpha = n\mu H / kT$ (classic paramagnet)

- *n* is large, α is large, M can saturate in relatively low *H*
- *n* is large, initial susceptibility is large, i.e., *M* responds very strongly to *H*

Superparamagnetism is subjective

SUPERPARA-
MAGNETISM
IS
IN THE EYE
OF THE
BEHOLDER

Superparamagnetism depends

- on the **experiment timescale:**
  how long does it take to measure the system properties, eg, its magnetic moment?

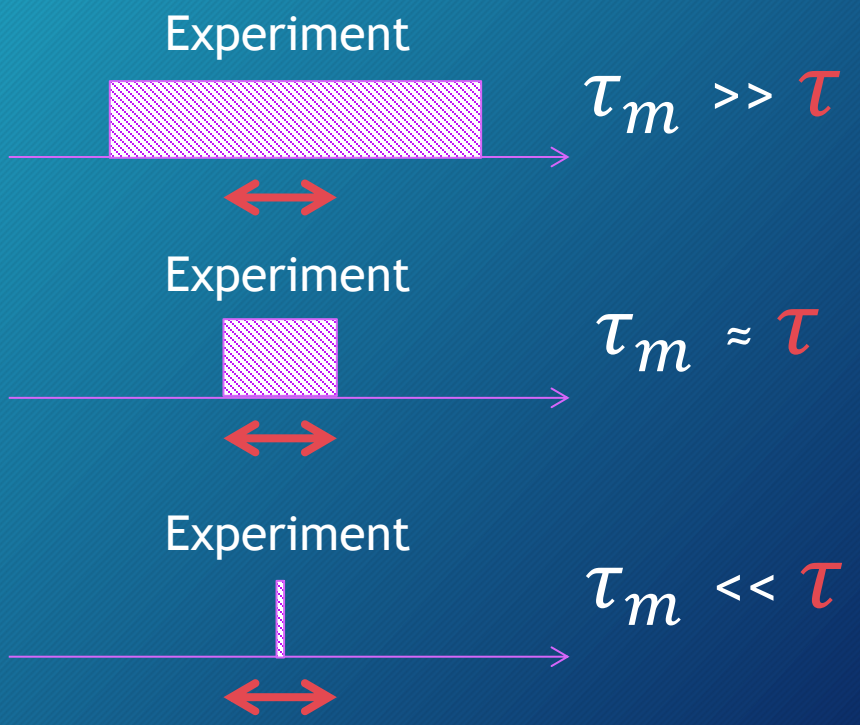
  or

- on the **stability timescale:**
  how long must the magnetization stay put to achieve your goal

Timescales

τ_m as the experiment timescale

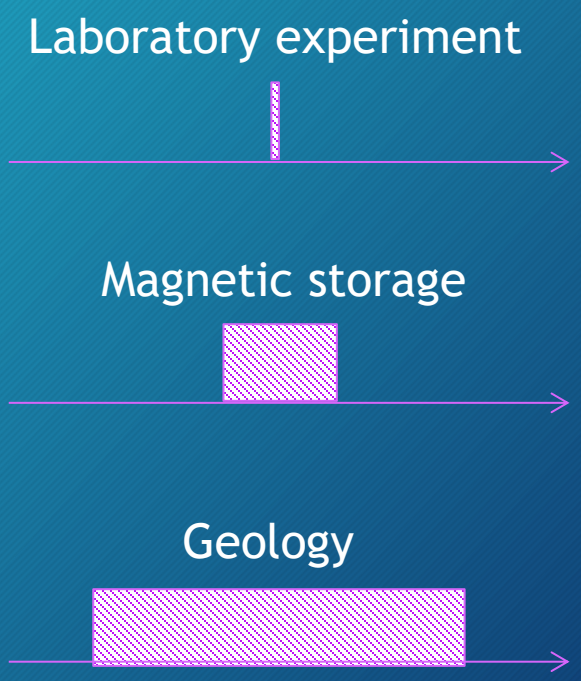
- DC magnetization — 1-100 s, depends on detector
- AC magnetization — $1/\omega$ (10^{-1} to 10^{-5} s)
- Mössbauer spectroscopy — 10^{-7} to 10^{-9} s (for ^{57}Fe)
- Ferromagnetic resonance — ≈ 10^{-9} s
- Neutron diffraction — 10^{-8} to 10^{-12} s



Timescales

τ_m as the stability timescale

- Laboratory experiments ≈ 1 s $E_a \approx 25\ kT$
- Magnetic recording media > a few years $E_a \approx 40\ kT$
- Paleointensity ≈ billions years $E_a \approx 60\ kT$



Blocking temperature

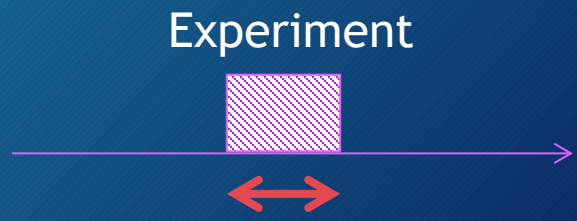
T_B such that $\tau(T_B) = \tau_m$

For **monodisperse, non-interacting** uniaxial NPs with identical volume *V*:

$$T_B = \frac{K\,V}{k\,log\frac{\tau_m}{\tau_0}}$$

T_B increases when barrier increases (anisotropy or volume increase)

T_B decreases when τ_m increases



Blocking volume

V_B such that $\tau(V_B) = \tau_m$

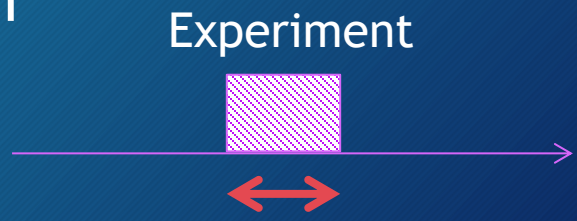
For **monodisperse, non-interacting** uniaxial NPs at a given *T*:

$$V_B = \frac{k\,T}{K} log \frac{\tau_m}{\tau_0}$$

V_B gets larger when *T* increases

V_B gets larger when *K* decreases

V_B gets larger when τ_m increases



The blocking critical size

$$R_b = \left(\frac{3V_B}{4\pi}\right)^{1/3} = \left(\frac{6kT}{K}\right)^{1/3} = d_S/2$$

Length	Expression	Fe	Co	Ni	$Nd_2Fe_{14}B$	Fe_3O_4	$CoFe_2O_4$	$BaFe_{12}O_{17}$
κ	$\sqrt{\lvert K_1\rvert/\mu_0 M_s^2}$	0.12	0.45	0.13	1.54	0.21	0.84	1.35
l_{ex}	$\sqrt{A/\mu_0 M_s^2}$	2.4	3.4	5.1	1.9	4.9	5.2	5.8
R_{coh}	$\sqrt{24}l_{ex}$	12	17	25	9.7	24	26	28
δ_w	$\pi l_{ex}/\kappa$	64	24	125	3.9	73	20	14
R_{sd}	$36\kappa l_{ex}$	10	56	24	110	38	160	280
R_{eq}	$(3k_BT/4\pi BM)$	0.8	0.8	1.2	0.9	1.2	1.2	1.3
R_b	$(6k_BT/K_1)^{1/3}$	8	4	17	1.7	13	5	4
Blocking diameter (nm)		16	8	34	3.4	26	10	8

300 K

κ, hardness parameter; l_{ex}, exchange length; R_{coh}, m t rotation; δ_w n equilibrium single domain particle size; R_{eq}, particle radius for which m $B = k_BT$ in 1 tic blocking

Hysteresis and SPM

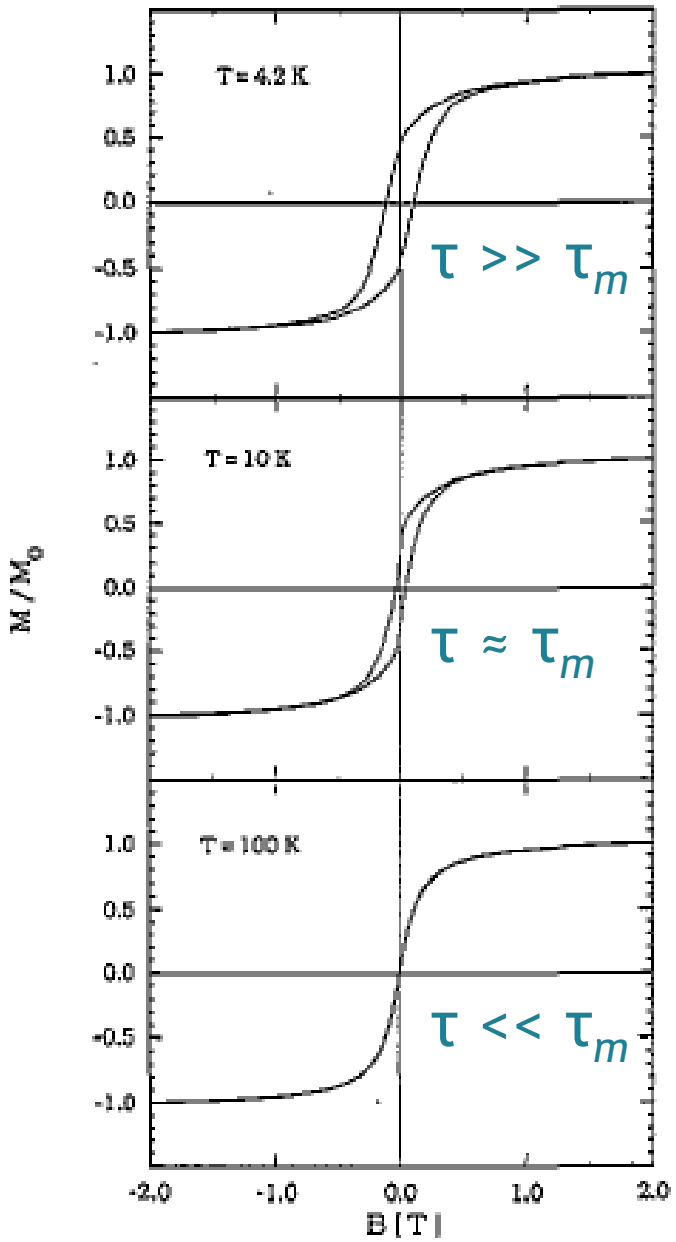


Figure 3. Hysteresis curves at 100 K, 10.0 K and 4.2 K for the magnetic liquid with amorphous iron–carbon particles. The curves are normalized to the magnetization measured in $B = 2$ T.

Property	Blocked regime $\tau >> \tau_m$	Intermediate regime $\tau \approx \tau_m$	SPM regime $\tau << \tau_m$
Magnetic moment	Stable	Slowly fluctuating	**Rapidly fluctuating**
Coercivity (Hc)	$H_c > 0$	Reduced H_c	**$H_c = 0$**
Remanence (Mr)	$M_r > 0$	Reduced M_r	**$M_r = 0$**
Saturation (Ms)	$M_s = n\ \mu$	$M_s = n\ \mu$	$M_s = n\ \mu$
Hysteresis	Present	Reduced	**Absent**
Initial susceptibility	Moderate	Moderate/High	**Very high**

M Hanson et al., J Phys Cond Matter, 7, 9263-9268,1995

Relaxation time: size and temperature

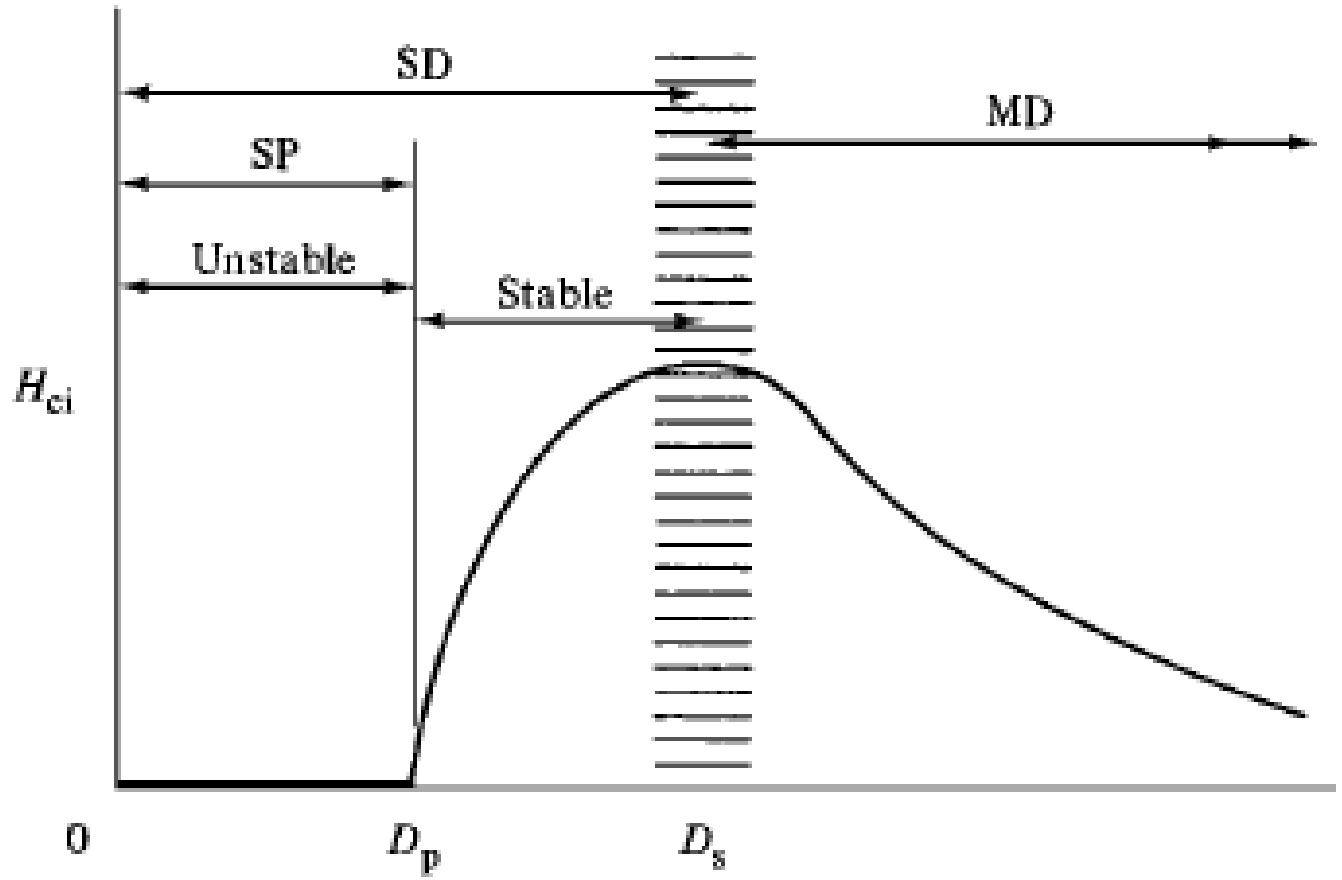
Due to the activated nature of the SPM, τ varies rapidly with temperature and very rapidly with size

$$\tau = \tau_0 \, exp\left(\frac{KV}{kT}\right)$$
$$= \tau_0 \, exp\left(\frac{4\pi K R^3}{3kT}\right)$$

Table 8.5. Superparamagnetic relaxation times for cobalt particles

Radius (mm)	Temperature (K)	Relaxation time
3.5	260	332 s
3.5	300	10 s
3.5	340	0.6 s
3.5	380	76 ms
3.0	300	1.9 ms
4.0	300	223 h
5.0	300	10^{12} y

Coercivity and size

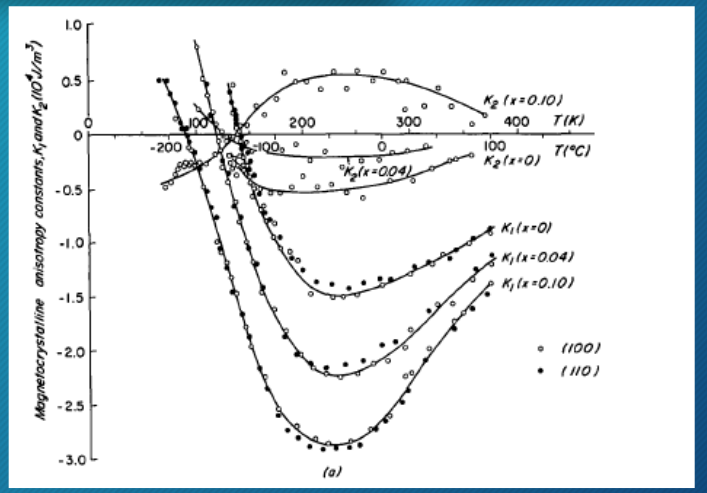


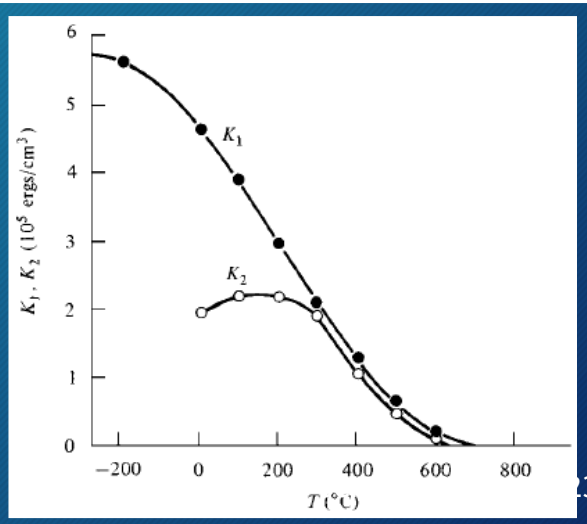
Variation of coercivity H_c with particle diameter D.

MD = multi-domain
SD = single-domain
SP = superparamagnetic

Anisotropy and temperature

The SP threshold size d_s is only weakly dependent on mineral properties such as anisotropy constant and grain shape. It is also time dependent, but again only weakly. The coefficient 25 in (5.29) approximately doubles for a 1 Ga time scale, leading to a mere 30% increase in d_s (Fig. 5.15a). On the other hand, d_s is strongly dependent on temperature T. K due to crystalline, magnetoelastic, or shape anisotropy (cf. eqns. (5.34), (5.35)) decreases rapidly to zero near the Curie point (Figs. 2.11, 3.13). Even the largest grains then become SP. This ability to pass readily between stable and thermally unstable conditions at high temperatures is at the heart of thermoremanent magnetization (Chapter 8).





K in *KV*/k*T* does depend on temperature

τ and T_B in practical cases

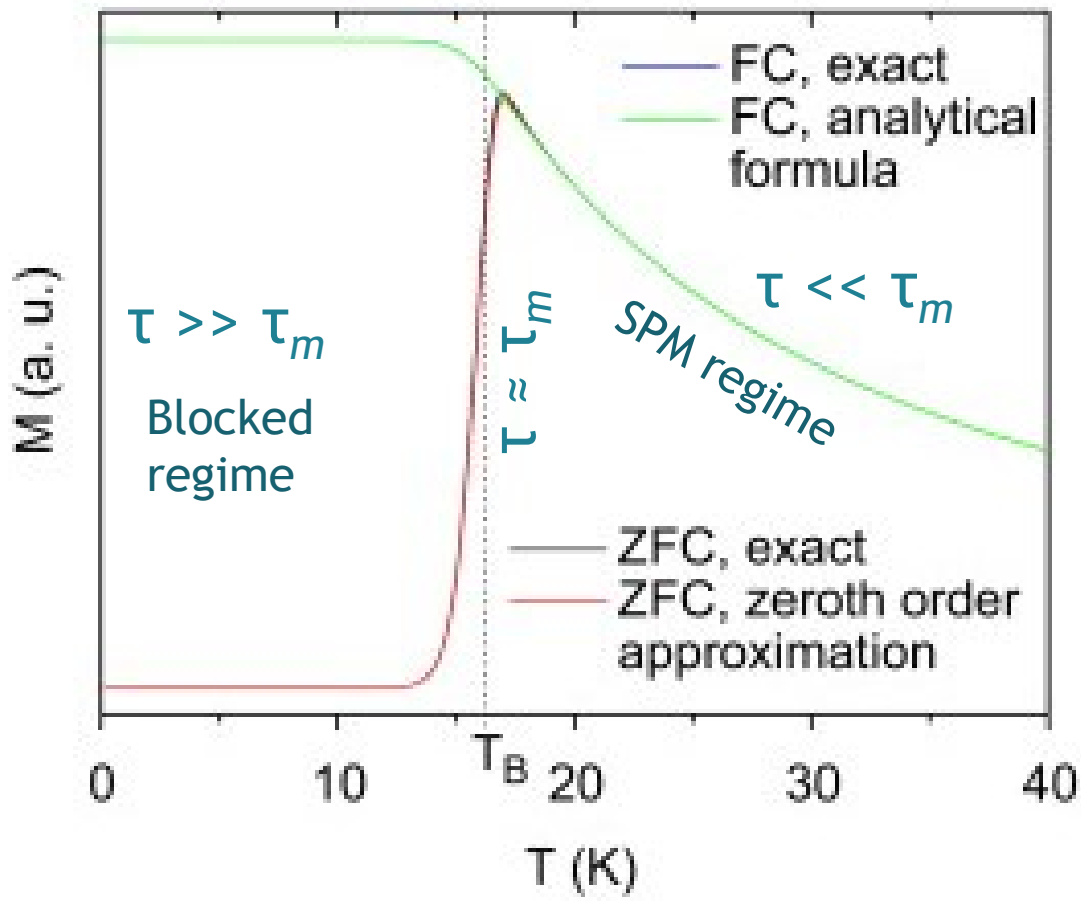
The relationship between **τ** and the anisotropy parameters are (very) complex.

It is far from easy to understand the relation between **τ** (τ_0 and ΔE) and the NP properties (size, magnetic parameters, etc.), even for non-interacting NPs

NPs are populations comprising individual NPs with different size, hence **different T_B**

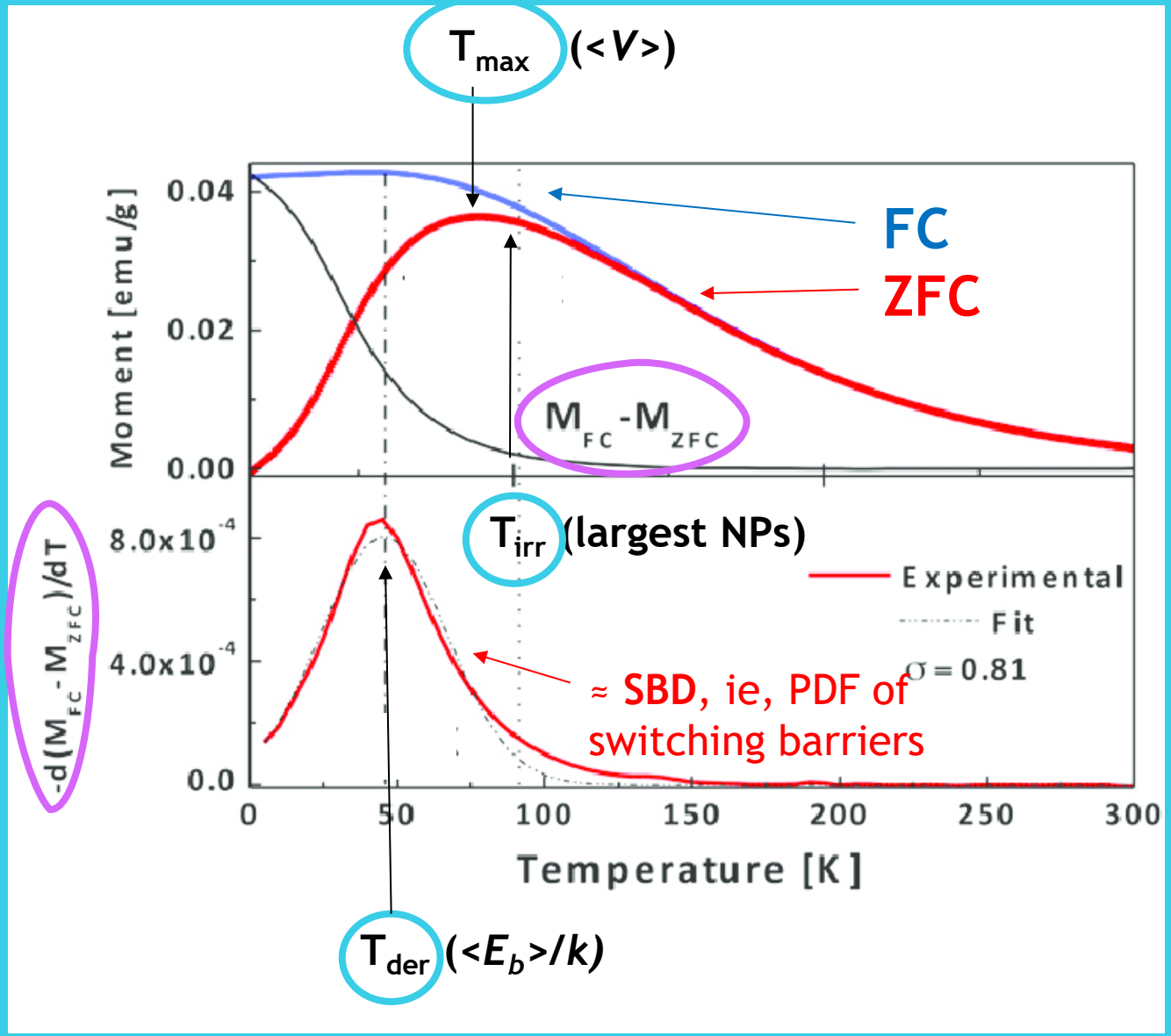
In ensembles of NPs, T_B is the resultant of the T_B's of each NP.

Can we measure T_B? ZFC and FC experiments



Simulated ZFC/FC curves for **mono-disperse**, **non-interacting** uniaxial NPs

Can we measure T_B? ZFC and FC experiments



F.4.3.2. Time Dependence. For a single particle an exponential decay of the remanent magnetization was predicted by Néel[1,187]:

$$\mathrm{TRM}(t) = \mathrm{TRM}(0)\exp(-t/\tau) \qquad \text{(F.4.10)}$$

The TRM relaxation data have been very often analyzed in terms of a logarithmic law[188–190]:

$$\mathrm{TRM}(t) = C - S\ln(t/t_0) \qquad \text{(F.4.12)}$$

However, there are no physical reasons for using the above relationship.

Magnetization time decay experiments provide τ

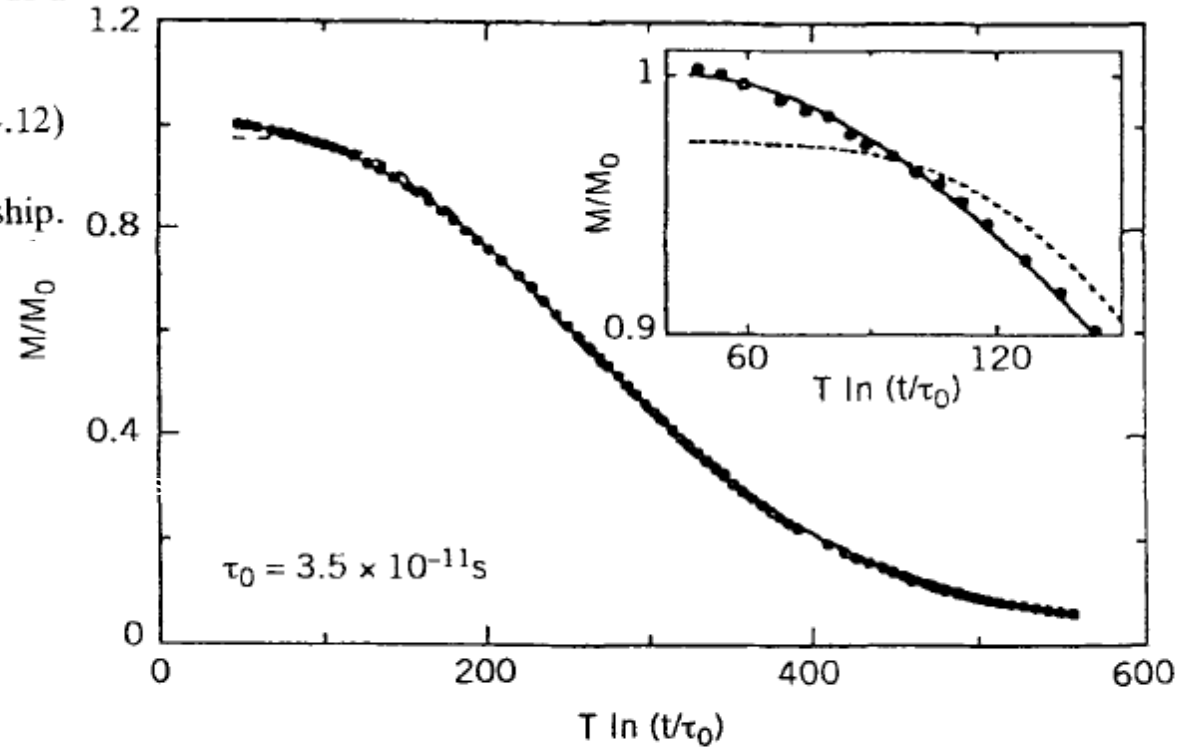


Figure F.4.4. Time decay of the remanent magnetization for FeC particles dispersed in a hydrocarbon oil in the temperature range 1.8–18 K. Dashed and solid lines correspond to the fits with one or two lognormal distributions. (Reproduced with permission from Ref. 194.)

194. O. Iglesias, F. Badia, A. Labarta, and Ll. Balcells, *J. Magn. Magn. Mat.* **140–144**, 399 (1995).

Amorphous $Fe_{1-x}C_x$ NPs
$\langle D \rangle$ = 3.2 nm, std dev 0.3 nm
dispersed in decalin

AC experiments provide τ

A sample is subjected to a time-varying magnetic field

$$h(t) = h_0 \cos(\omega t)$$

The resulting magnetization of the sample is

$$M(t) = \chi_{ac}(\omega, T)\, h(t)$$

where the susceptibility can be written as

$$\chi_{ac}(\omega, T) = \chi'(\omega, T) + i\,\chi''(\omega, T)$$

Usually, one measures the AC susceptibility as a function of temperature at different frequencies.

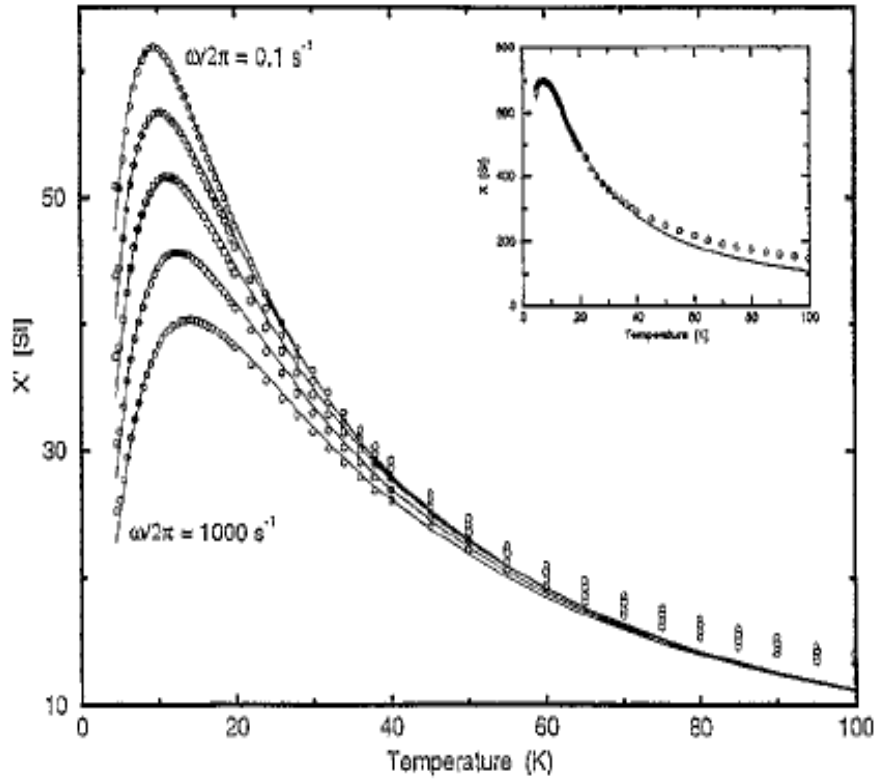
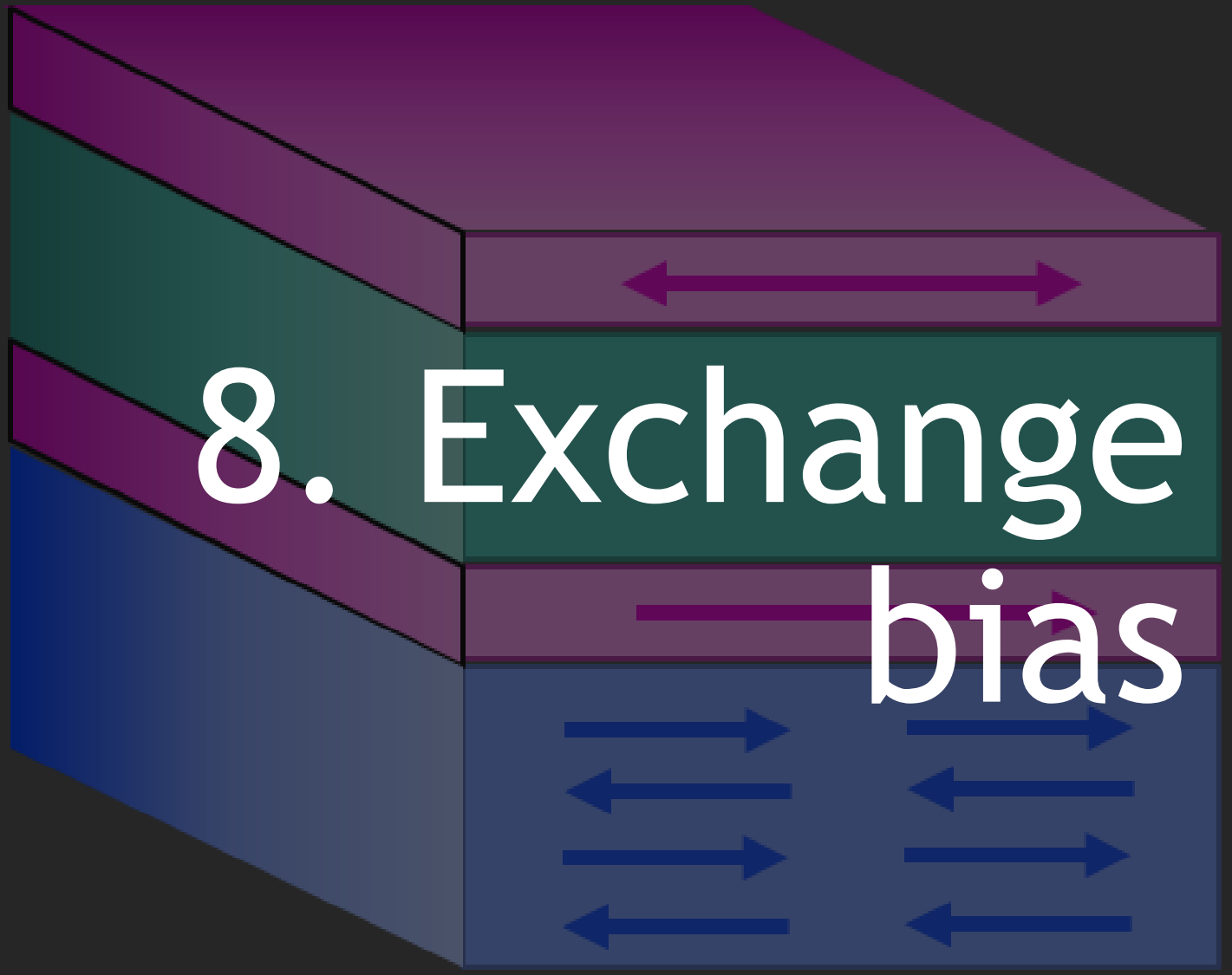


Fig. 2. The real part of the AC susceptibility obtained at frequencies of 0.1, 1, 10, 120, 1000 s^{-1}. The inset shows the ZFC magnetization curve. The full lines are the best fits as described



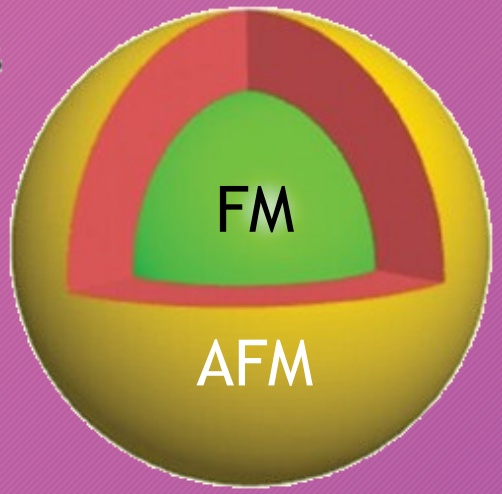
8. Exchange bias

The neighbor's spin is always stronger

or

Your friendly neighborhood antiferromagnet

Hysteresis loop of FM-AFM NPs



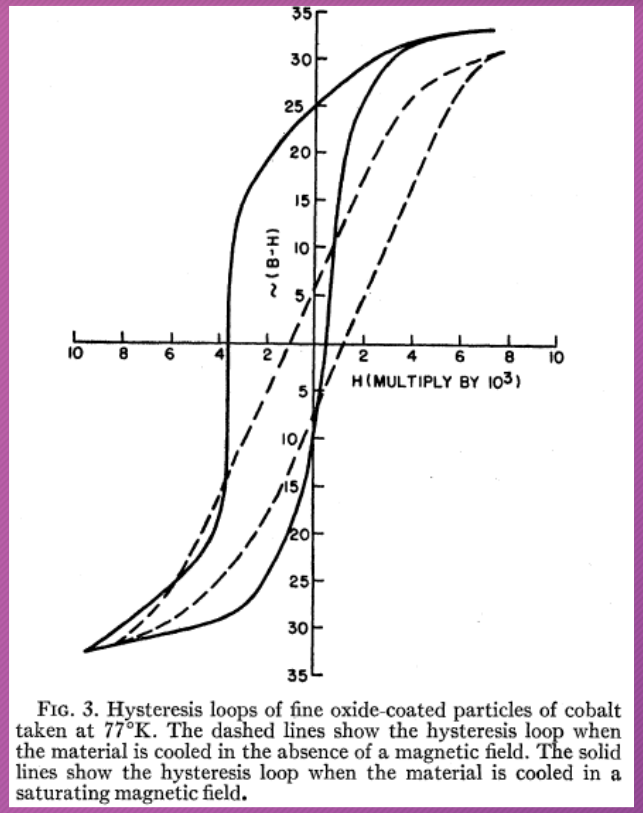


FIG. 3. Hysteresis loops of fine oxide-coated particles of cobalt taken at 77°K. The dashed lines show the hysteresis loop when the material is cooled in the absence of a magnetic field. The solid lines show the hysteresis loop when the material is cooled in a saturating magnetic field.

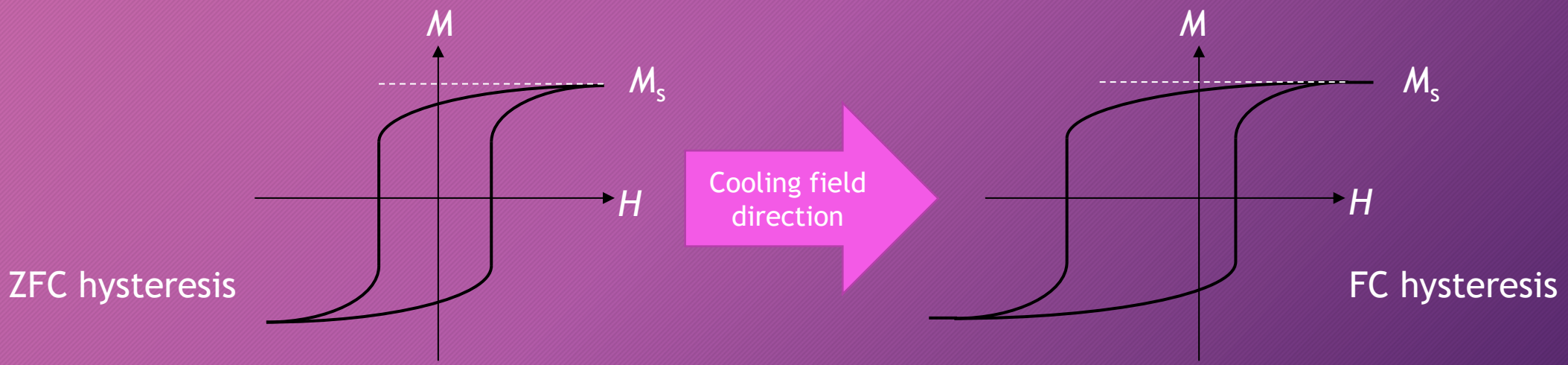
The usual (ie, zero-field cooled) hysteresis loop (dashed curve) is **very** different from the hysteresis loop (solid curve) recorded after **cooling the sample in a magnetic field!**

Unidirectional anisotropy!

Oxidized Co particles
W.H. Meiklejohn, C.P. Bean, Phys. Rev. **102**, 1413 (1956)

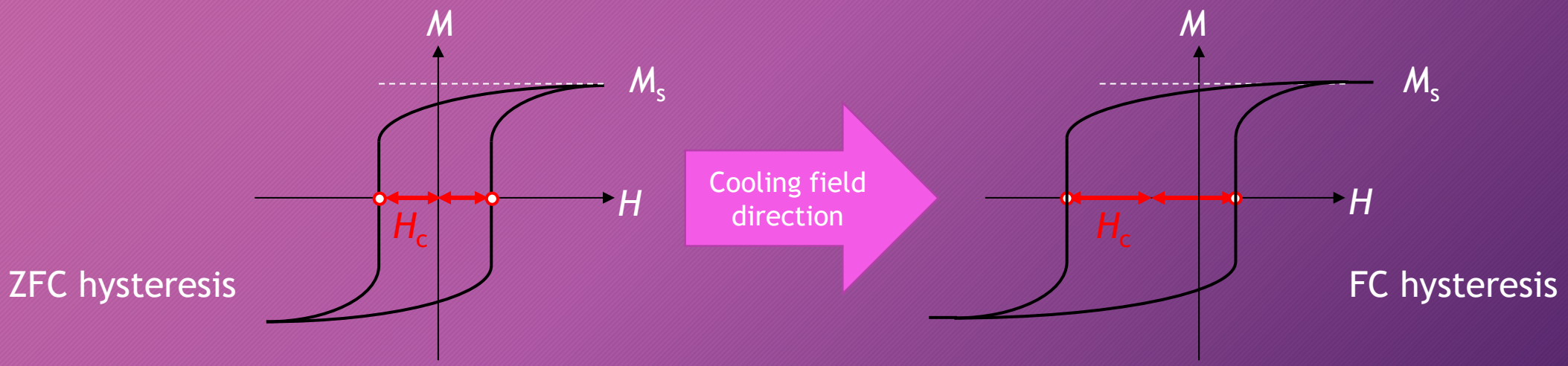
What are the effects of field cooling before recording hysteresis loop?

- Coercivity (H_c) increases: broader loop
- M_r/M_s ratio increases: more “square” loop
- Exchange bias (H_b): shifted loop



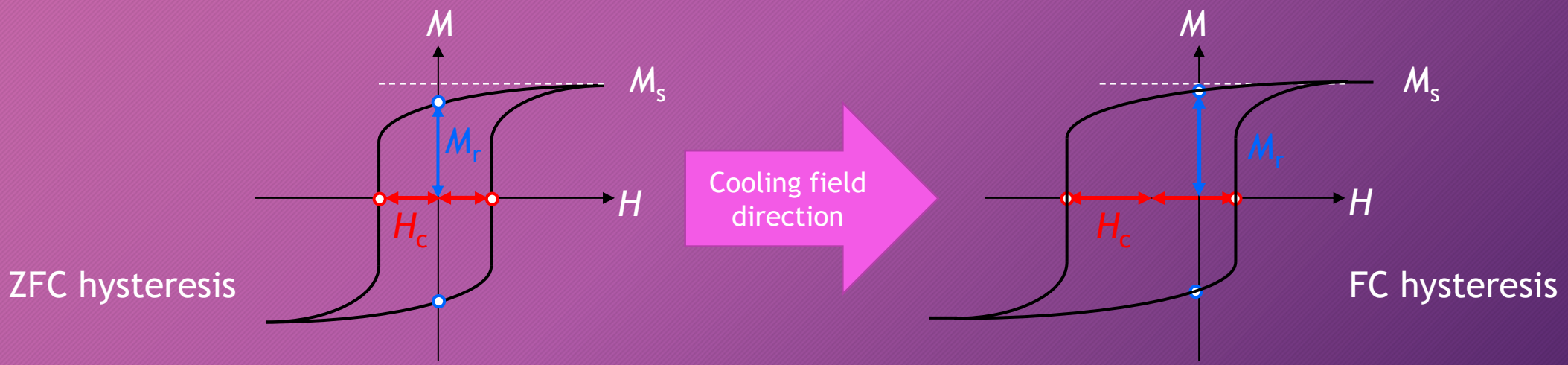
What are the effects of field cooling before recording hysteresis loop?

- Coercivity (H_c) increases: broader loop
- M_r/M_s ratio increases: more “square” loop
- Exchange bias (H_b): shifted loop



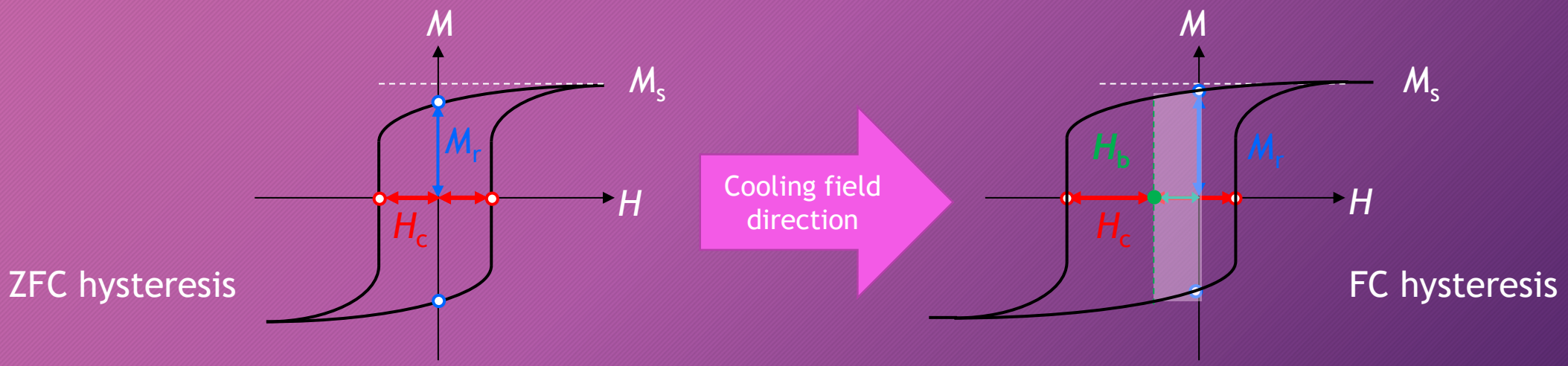
What are the effects of field cooling before recording hysteresis loop?

- Coercivity (H_c) increases: broader loop
- M_r/M_s ratio increases: more “square” loop
- Exchange bias (H_b): shifted loop



What are the effects of field cooling before recording hysteresis loop?

- Coercivity (H_c) increases: broader loop
- M_r/M_s ratio increases: more "square" loop
- **Exchange bias** (H_b): shifted loop



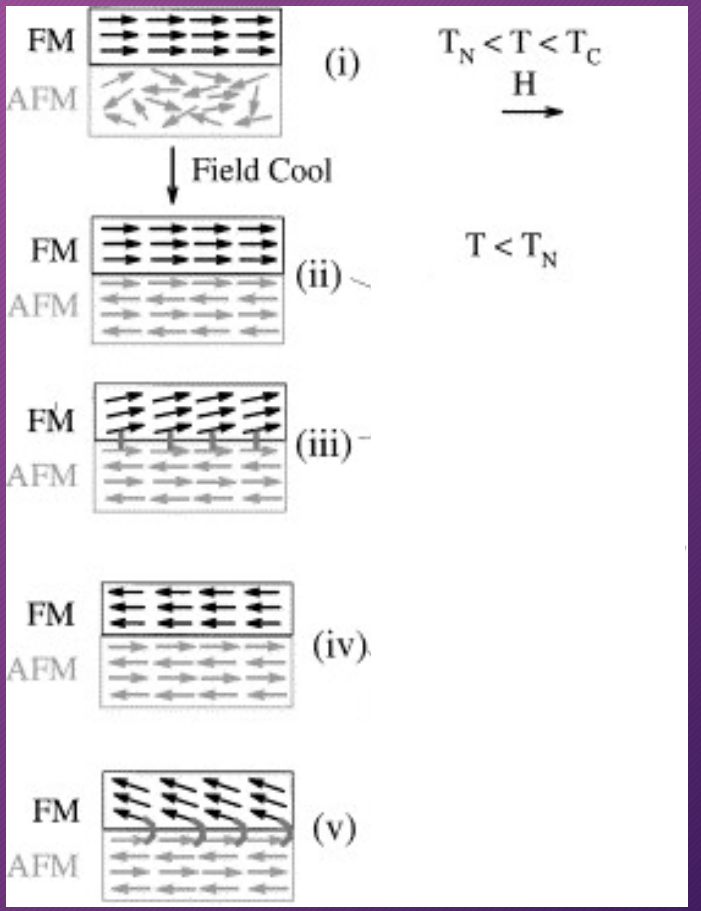
ZFC hysteresis

FC hysteresis

What's the mechanism of EB?

It has long been clear that the observed bias that locks the ferromagnet (FM) into a preferred direction must originate from the **exchange coupling** between uncompensated spins near the FM–AFM interface, which are frozen in by the setting field.

The Meiklejohn and Bean model predicts H_B fields about 100x larger than observed

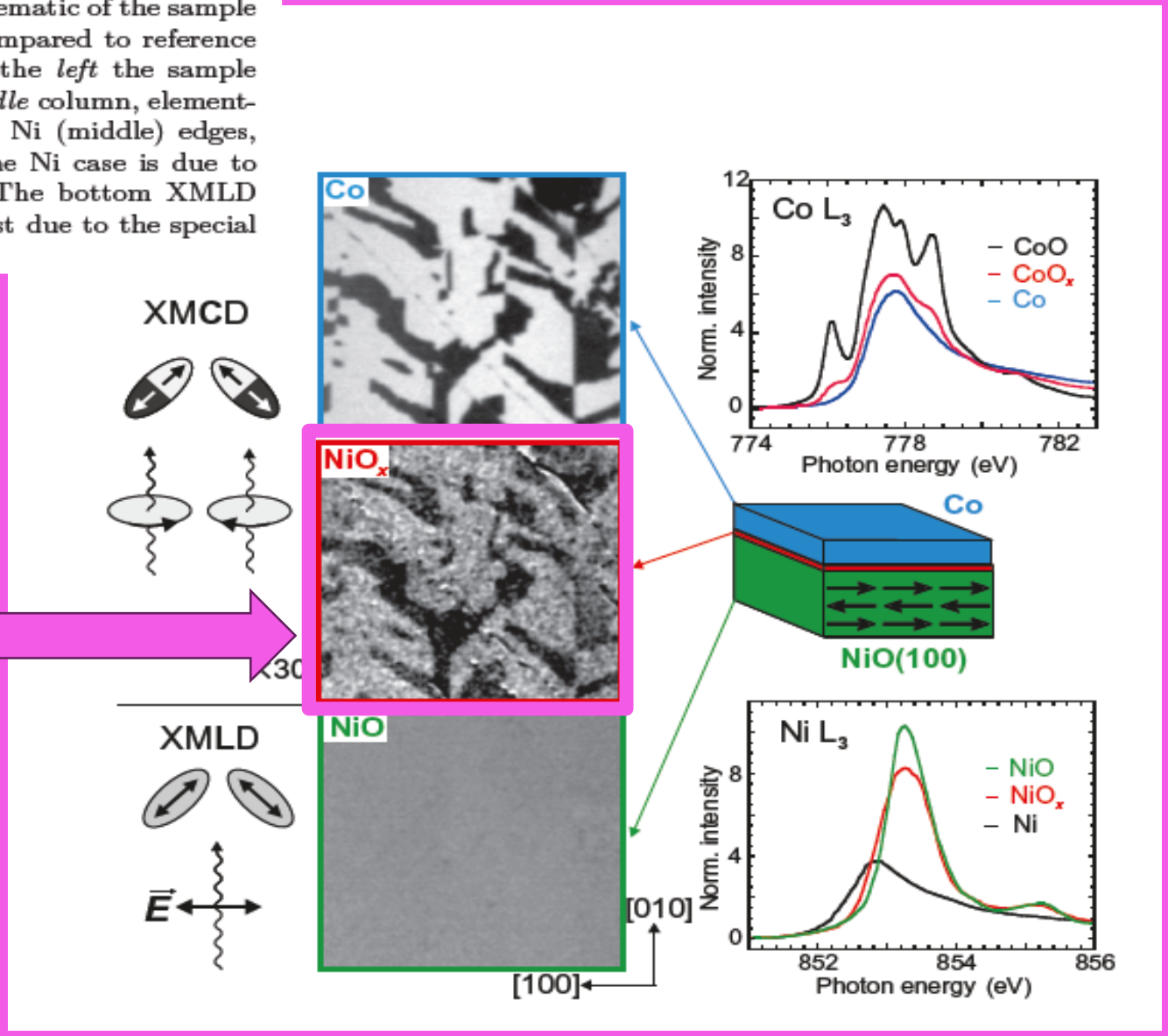


Recent interpretation of EB

1. In the biased ground state the FM and AFM spins are aligned along the same axis.
2. **Near the interface, there are uncompensated spins that originate from magnetic atoms in the AFM.**
3. **A fraction of the uncompensated interfacial spins are pinned. They are responsible for the existence of exchange bias and their number is proportional to the size of the bias.**
4. The size of the bias decreases with the antiferromagnetic domain size.
5. The sign of the bias is determined by the sign of the exchange coupling between the pinned interfacial spins and the FM.
6. The interfacial pinned spins are anchored in the bulk AFM through a Bloch domain wall. The size of exchange bias is proportional to the exchange stiffness of this domain wall and the magnetocrystalline anisotropy of the bulk AFM.

Fig. 13.19. X-PEEM images of the magnetic domain structure in a sandwich of 0.8 nm of Co deposited on NiO(100). On the *right* we show the X-ray absorption fine structure near the Co and Ni L_3 absorption edges and a schematic of the sample structure. Spectra for the actual Co/NiO sample (red) are compared to reference spectra recorded for pure metal and monoxide samples. On the *left* the sample orientation and the X-ray polarization is illustrated. In the *middle* column, element-specific XMCD PEEM images recorded at the Co (top) and Ni (middle) edges, respectively, show *ferromagnetic domain contrast*, which in the Ni case is due to uncompensated interfacial Ni spins in NiO (labeled NiO_x). The bottom XMLD image taken at the Ni edge shows no antiferromagnetic contrast due to the special sample orientation (compare Fig. 10.25)

Uncompensated spins in the AFM



Few uncompensated spins are pinned

2 nm Co on 50 nm of $Ir_{20}Mn_{80}$

The XMCD Mn loop displays a **vertical shift**:

- The number of uncompensated Mn moments corresponds to **0.6 monolayer** at the FM-AFM interface
- Just about **7%** of them are **pinned**.
- It is the **pinned 0.04 monolayer Mn moments** that are held responsible for the exchange bias.

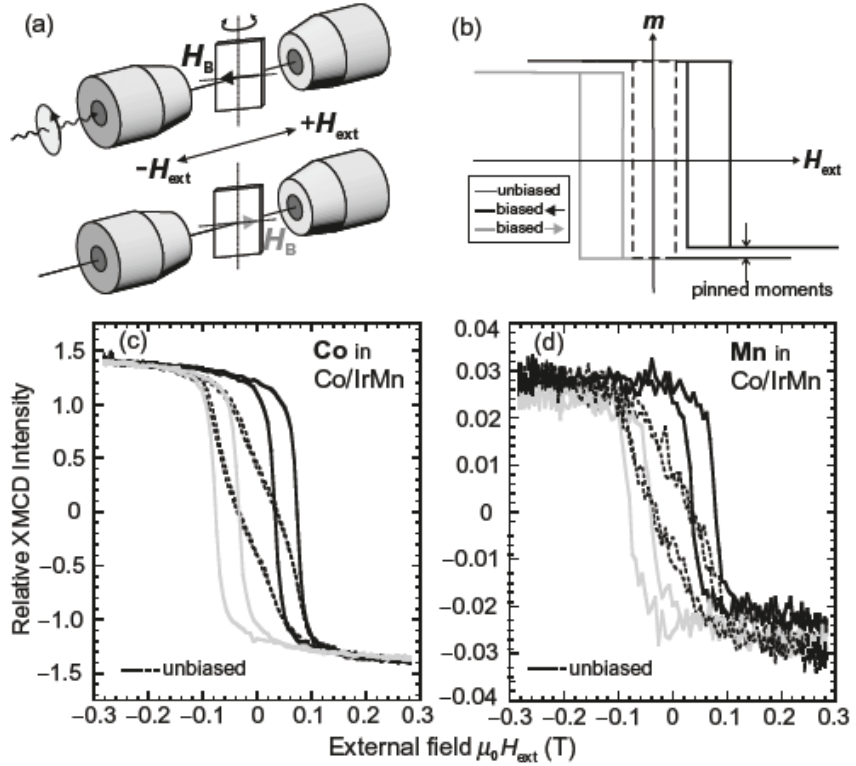
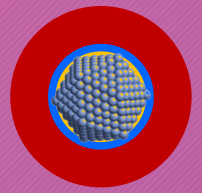
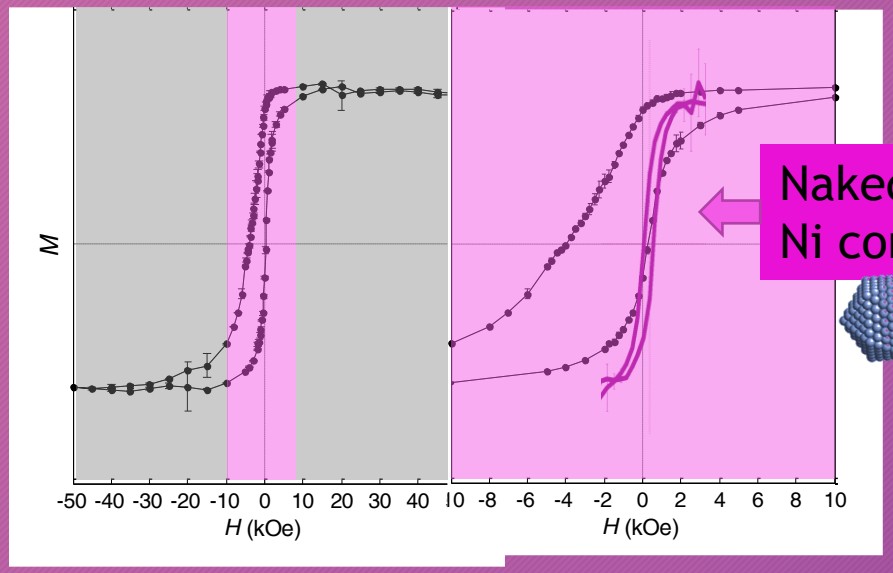


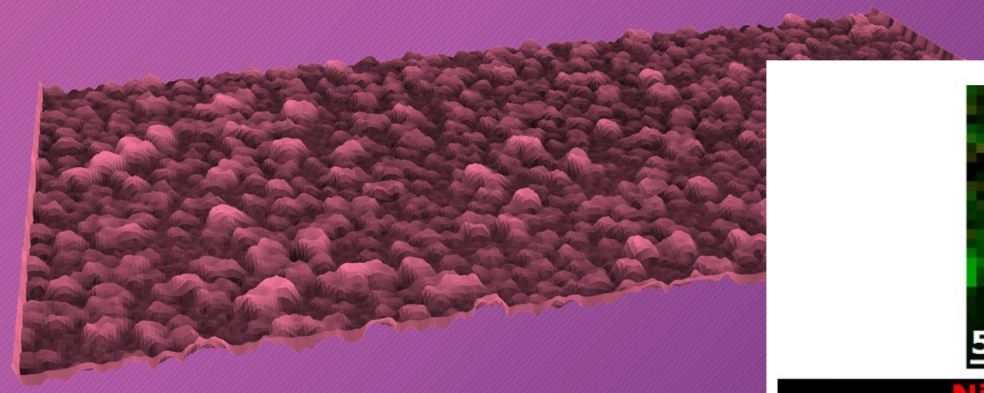
Fig. 13.20. (a) Experimental geometry for XMCD spectroscopy measurements. (b) Illustration of expected XMCD-intensity loops for the two experimental geometries in (a), assuming a small fraction of pinned moments pointing into the bias direction. (c) Element-specific Co loops for unbiased and biased samples for the two geometries in (a). (d) Element-specific Mn loops for unbiased and biased samples for the two geometries in (a)

Exchange bias in Ni @ NiO @ CoO NPs



t_{NiO} = 0.2 nm
t_{CoO} = 2.7 nm





Ni(11 nm) @ NiO @ CoO

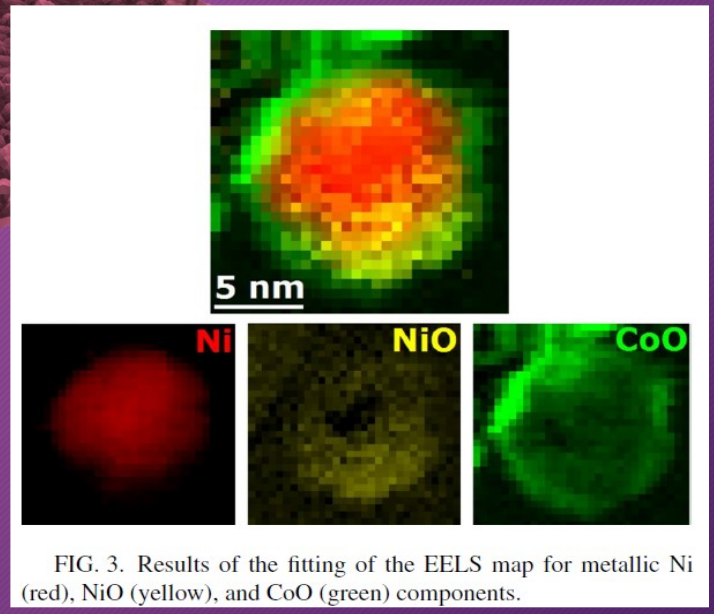
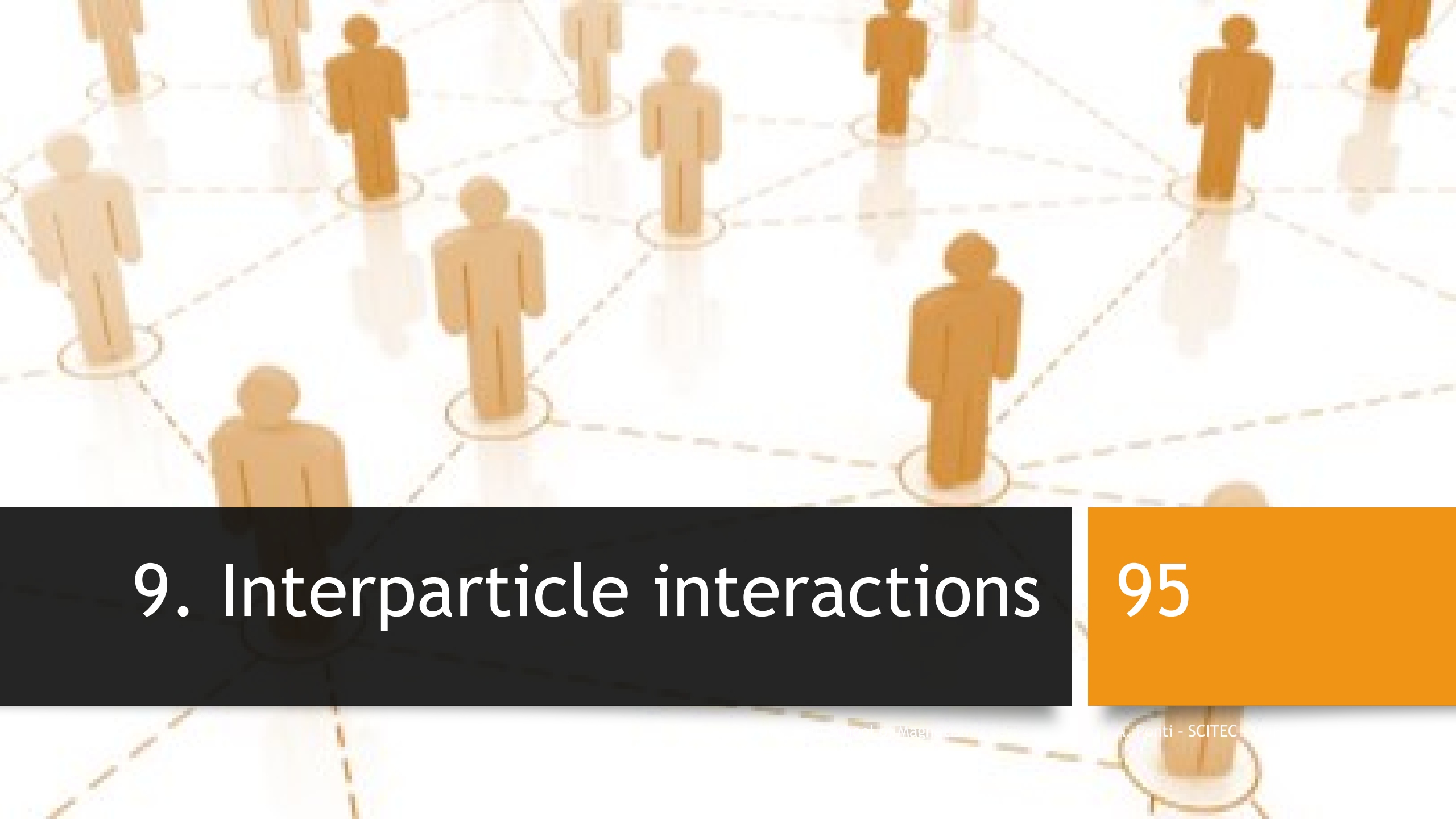


FIG. 3. Results of the fitting of the EELS map for metallic Ni (red), NiO (yellow), and CoO (green) components.

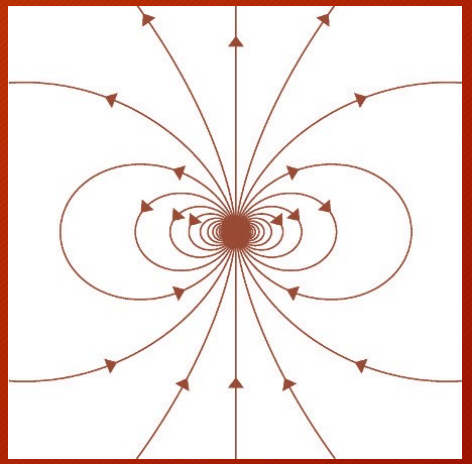
A. Ponti et al., *Phys Rev Materials*, 1, 036001 (2017)



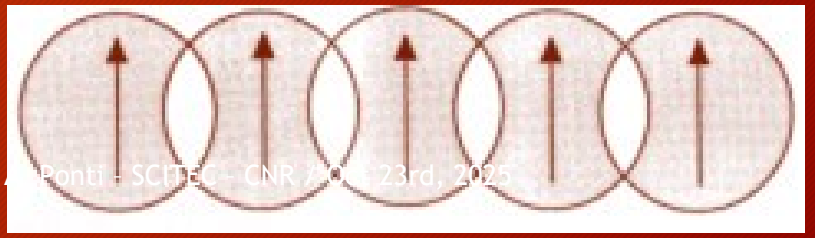
9. Interparticle interactions

Types of interparticle interactions

- Long-range **magnetostatic (dipole) interactions** can have a strong influence on the dynamics of magnetic NPs.



- If NPs are in very close proximity, **exchange interactions** between surface atoms can be significant. An important example is exchange bias.



Magnetostatic dipole interaction

Dipole interactions have a negligible influence on the magnetic order in bulk materials at finite temperatures.

In magnetic NPs, dipole interactions between nanoparticles can have a significant influence on the magnetic properties.

In a sample of randomly distributed nanoparticles with average magnetic moment μ and average separation $d \approx N^{-1/3}$, the dipole interaction energy of a NP is of the order of

$$E_d \approx \frac{\mu_0}{4\pi}\frac{\mu^2}{d^3}$$

Wohlfarth relation

$$m^{\mathrm{DCD}}(H) = 1 - 2m^{\mathrm{IRM}}(H)$$

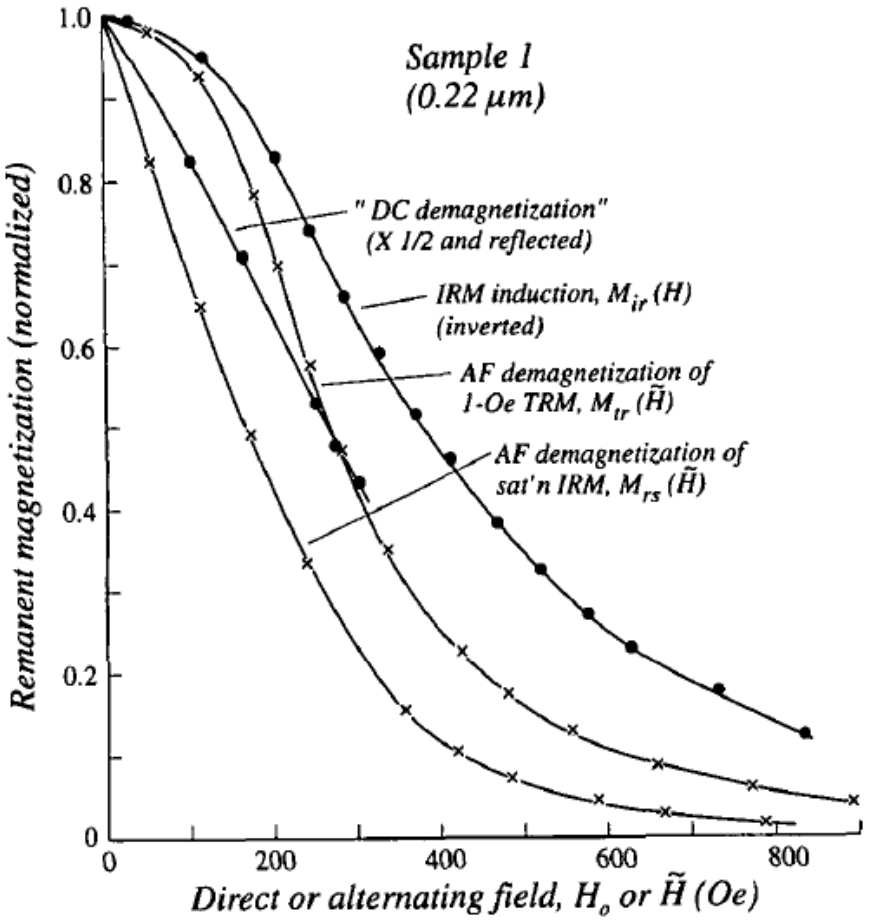


Figure 11.16 Comparison of DC 'demagnetization', IRM acquisition, and AF demagnetization curves, suitably reflected, rescaled or inverted for the purposes of testing the Wohlfarth relations (eqns. (11.10), (11.11)). The curves are all of approximately the same form, but the offsets between them are evidence of grain interactions. The sample contains magnetite grains somewhat above critical SD size. [Reprinted from Dunlop (1986a), with kind permission of the author and Elsevier Science – NL, Sara

Wohlfarth (1958) proposed formal relations among the IRM acquisition curve, $M_{\mathrm{ir}}(H_0)$, the 'DC demagnetization' curve, $M_{\mathrm{r}}(-H_0)$ (see Fig. 11.5), and the AF demagnetization curve, $M_{\mathrm{r}}(\tilde{H})$. On the asumption that the three curves give identical measures of the coercivity spectrum for non-interacting SD grains,

$$M_{\mathrm{r}}(-H_0) = M_{\mathrm{rs}} - 2M_{\mathrm{ir}}(H_0) \quad \text{and} \quad M_{\mathrm{r}}(\tilde{H}) = M_{\mathrm{rs}} - M_{\mathrm{ir}}(H_0). \tag{11.10}$$

Deviation from these relations indicates particle interaction. When normalized

A. Omelyanchik at al., *Chem. Mater.* 2024, 36, 7976–7987

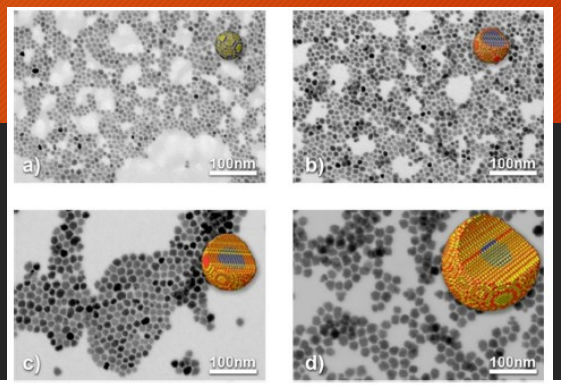
The δ*m* method

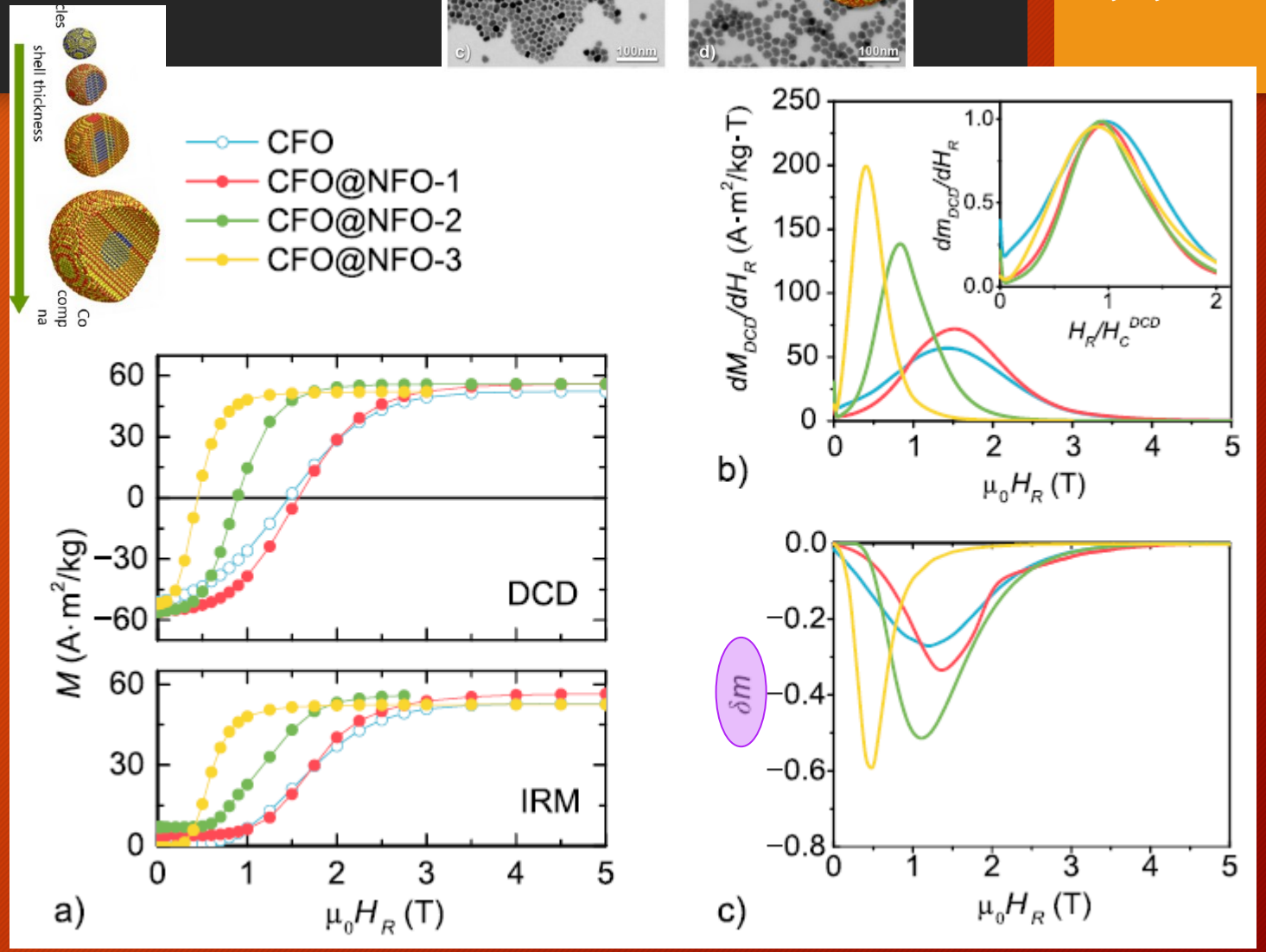
Hard $CoFe_2O4$ NPs coated with one or more layers of soft $NiFe_2O_4$

$$\delta m = m_{DCD} - (2\, m_{IRM} - 1)$$

gives insight into the PDF of interparticle interactions, which are

- demagnetizing (eg dipolar) for $\delta m < 0$
- magnetizing (eg surface exchange) for $\delta m > 0$





(Z)FC magnetization

Dipole interactions can result in a shift of the maximum of the **ZFC** magnetization to either lower or higher temperature.

Dipole interactions can result in an almost temperature independent **FC** magnetization at low temperature.

In samples with a high NP concentration, the frustrated inter-NP interactions can result in formation of a **frozen collective state**.

If the NPs are randomly distributed, the frozen collective state can have many similarities to a **spin glass** (spin-glass-like-state)

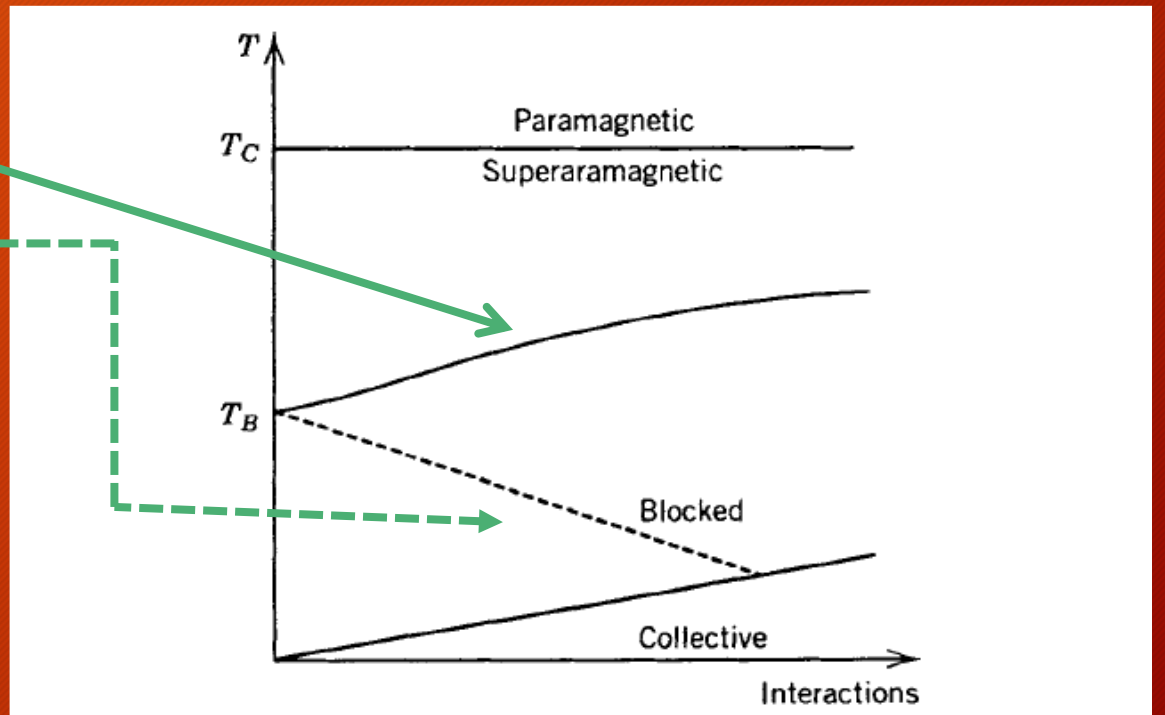
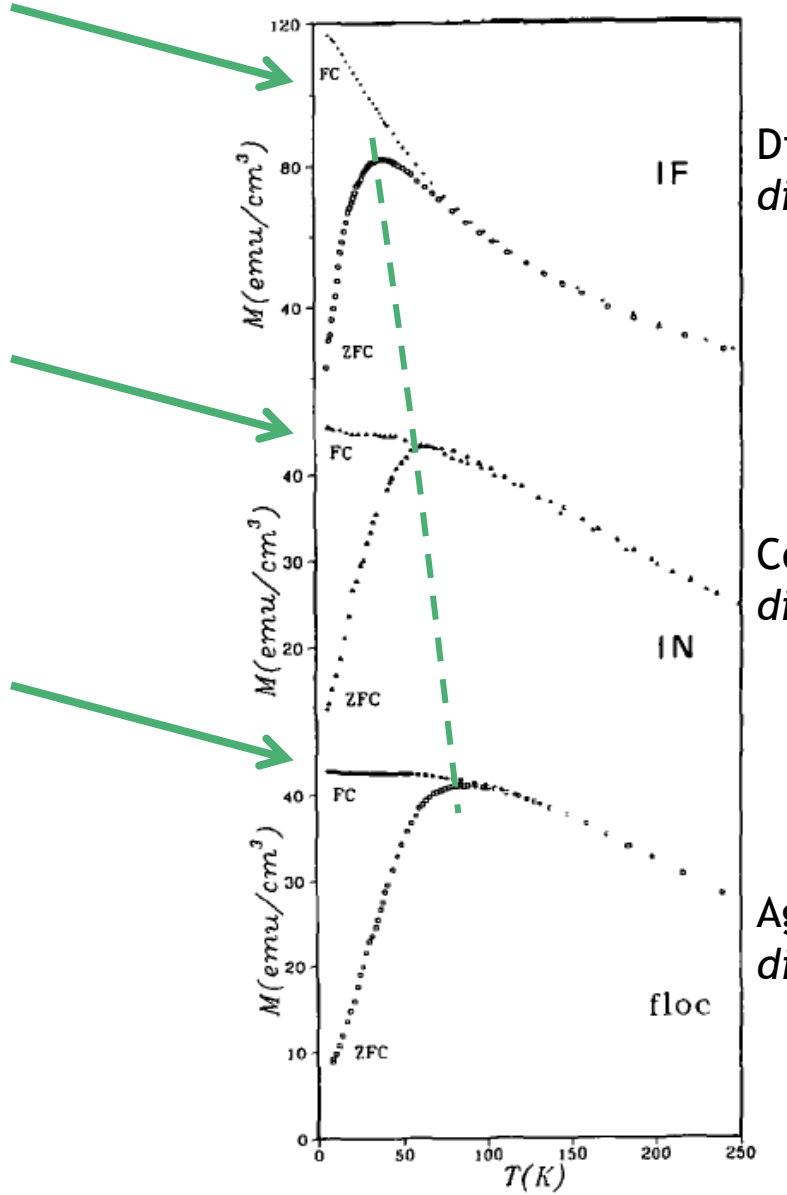


Figure E.1. Schematic phase diagram for fine particles with magnetic interparticle interactions. Case 1, the blocking temperature T_B increases with interactions (continuous line). Case 2, T_B decreases with interactions (dashed line) (see text).

Tronc, E. *et al.*, *Hyperfine Interact.* **95**, 129–148 (1995)

(Z)FC magnetization



Diluted NPs
distance = 5 <D_{NP}>

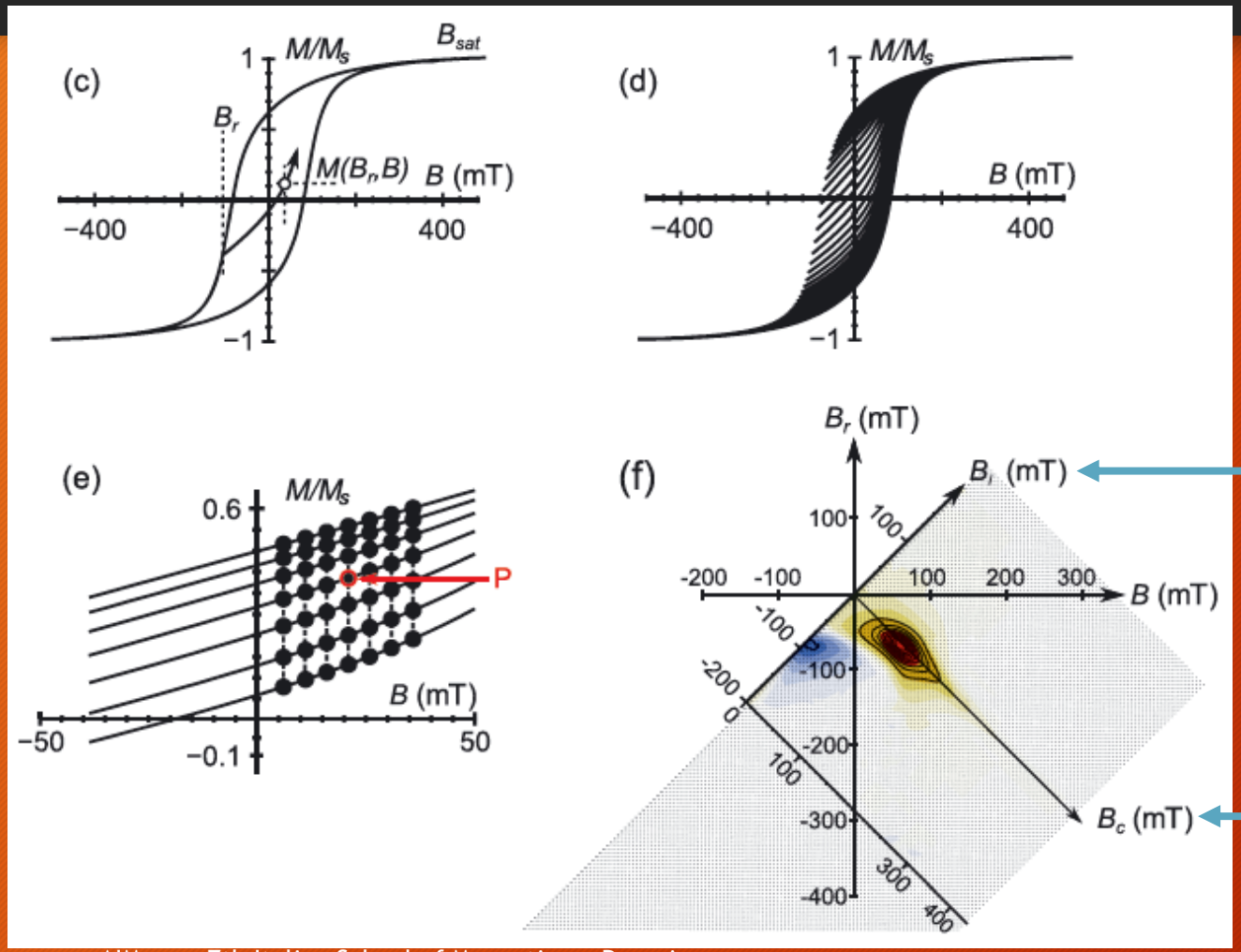
Concentrated NPs
distance = 1.4 <D_{NP}>

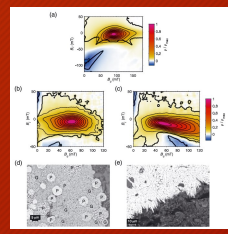
Aggregated NPs
distance = <D_{NP}>

Fig. 10. Thermal variation of zero field cooled and field cooled magnetization of γ-Fe_2O_3 particles dispersed in polyvinylic alcohol. The averaged diameter corresponding to the mean volume is $\langle D \rangle = 7.1$ nm. Interparticle spacing of $5\langle D \rangle$ (IF), and $1.4\langle D \rangle$ (IN); strong aggregation (FLOC).

AP Roberts et al., Rev. Geophys., 52, 557–602 (2014)

First-order reversal curves (FORCs)

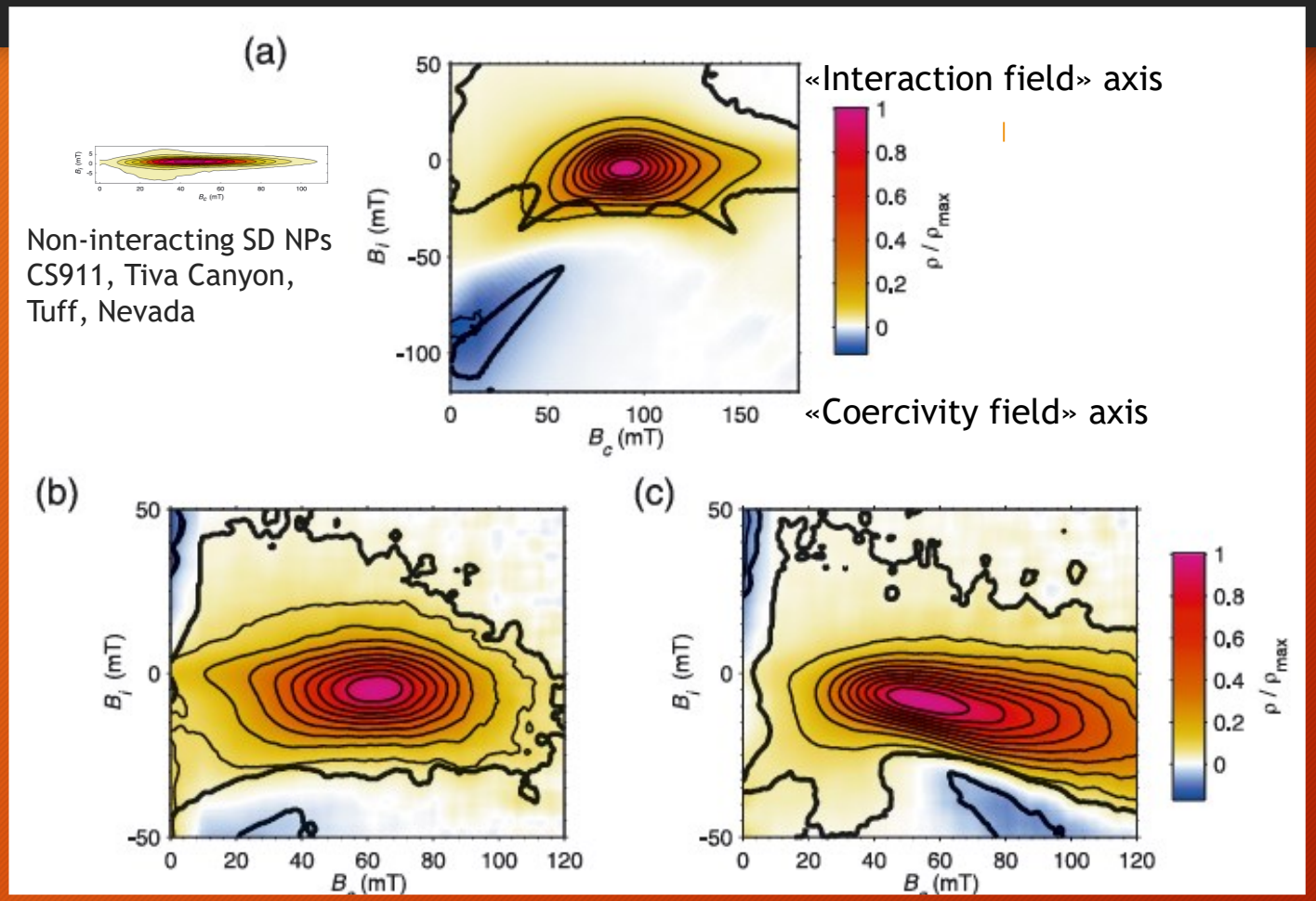




«Interaction field» axis

«Coercivity field» axis

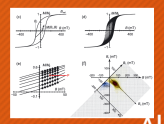
First-order reversal curves (FORCs)



Non-interacting SD NPs
CS911, Tiva Canyon,
Tuff, Nevada

Floppy disk with closely packed SD particles

Strongly interacting greigite Fe_3S_4 (left) and pyrrhotite $Fe_{(1-x)}S$ (right) NPs in samples from Vrica, Italy



If I have created this presentation, it is by *standing on the shoulders of Giants*

- J. M. D. **Coey**, *Magnetism and Magnetic Materials*, CUP, 2010.
- R. **Skomski**, *Simple Models of Magnetism*, OUP, 2008.
- B. D. **Cullity** and C. D. **Graham**, *Introduction to Magnetic Materials*, Second Edition, The IEEE, 2008.
- J. **Stöhr**, H.C. **Siegmann**, *Magnetism - From Fundamentals to Nanoscale Dynamics*, Springer, 2006.
- A. **Aharoni**, *Introduction to the Theory of Ferromagnetism*, Second Edition, OUP, 2000.
- L. **Dormann**, D. **Fiorani**, and E. **Tronc**, *Magnetic Relaxation in Fine-particle Systems*, Adv Chem Phys, 98, 283, 1997.
- David J. **Dunlop** and Özden **Özdemir**, *Rock Magnetism - Fundamentals and Frontiers*, CUP, 1997.
- S. **Chikazumi**, *Physics of Ferromagnetism*, Second Edition, Clarendon Press, 1997.
- A. H. **Morrish**, *The Physical Principles of Magnetism*, Wiley, 1965.
- S. **Mørup**, C. **Frandsen**, M. F. **Hansen**, *Magnetic properties of nanoparticles*, in Oxford Handbook of Nanoscience and Technology, 2010.



Encyclopedic manuscript containing allegorical and medical drawings, Library of Congress, Rosenwald 4, Bl. 5r

Thanks!

Consiglio Nazionale delle Ricerche

ISTITUTO DI SCIENZE E TECNOLOGIE CHIMICHE "GIULIO NATTA"

Anna M. Ferretti
Fulvio Bellato
Gaia Nascimben
Emanuele Corno
Ruben Ruggiero
Sara Mondini
Elena Capetti
Primiano D'Ambrosio
Sandro Usseglio Nanot
Carmelo Drago
Alessandra Puglisi
Simone Cenedese
Mauro Parini

AIMagn Associazione Italiana di Magnetismo

School Directors
G. Carlotti, M. Madami,
G. Gubbiotti, S. Tacchi

Organising Committee
L. Ciaccarini, R. Pellegrini,
R. Silvani, A. Stollo

Suppose you fell for the NP peddler, now what?

***My third** free advice nobody asked for*

Suppose you know nothing about the NPs you intend to measure. What should you do?

1. Write a list of the **answers** to want to get and the experiments that will give you those answers
2. Do a preliminary **ZFC/FC**: What are the **critical** temperatures? Can a **reversible** regime (superpara- or para-magnetic) be achieved? (If not, you must be very careful)
3. Do a preliminary **hysteresis loop: Can saturation** be achieved? (If not, you must be very careful)



Suppose you fall for the NP peddler, now what?

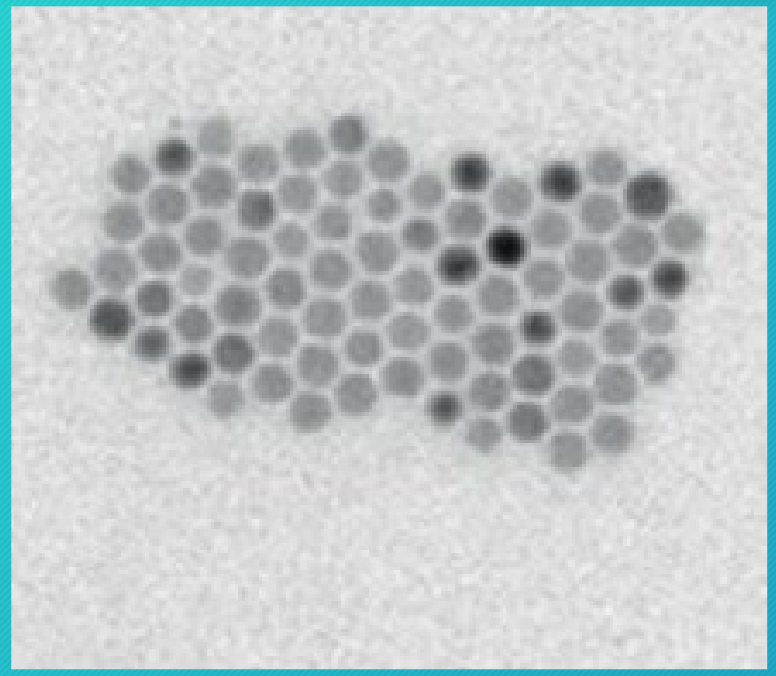
***My fourth** free advice nobody asked for*

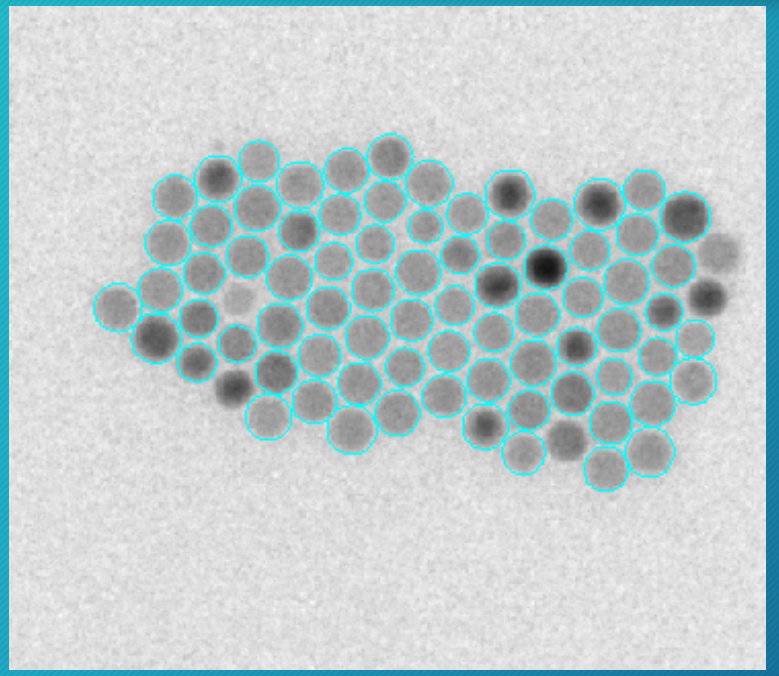
A possible experimental plan for NPs I do not know anything about

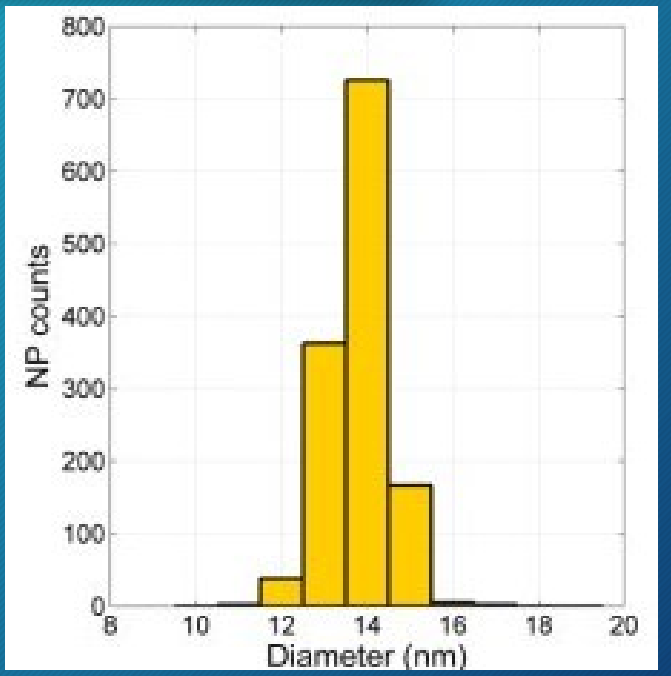
1. **ZFC/FC** at 10 and 100 Oe, from min to max *T*
2. Saturation vs. *T* (max *H*, min to max *T*)
3. Remanence vs. *T* ("TRM", max *H* then *H*=0, min to max *T*)
4. Several hysteresis loops at temperatures of interest
5. Isothermal remanence (IRM: stepwise create remanence)
6. Direct-current demagnetization (DCD: stepwise invert remanence)
7. Magnetic viscosity (time relaxation of magnetization, best around coercivity)
8. AC susceptometry (several frequencies)



Morphology: analyzing TEM images







PEBBLES (S. Mondini, A. M. Ferretti, A. Puglisi, A. Ponti, *Nanoscale*, 2012, **4**, 5356-5372) is a user-friendly software which implements an accurate, unbiased, reproducible, and fast method to measure the morphological parameters of a population of nanoparticles (NPs) from TEM micrographs.

Freely available from pebbles.istm.cnr.it or pebbles.scitec.cnr.it

Composition: macroscale

NM-212: industry-made CeO_2 NPs

EDX

NM212	Element	C	O	Si	Cl	Ce
	Mean	1.86%	19.80%	0.13%	0.10%	78.10%
	Std Dev	0.13%	0.58%	0.04%	0.01%	5.68%

O : Ce = 2.2 ± 0.2

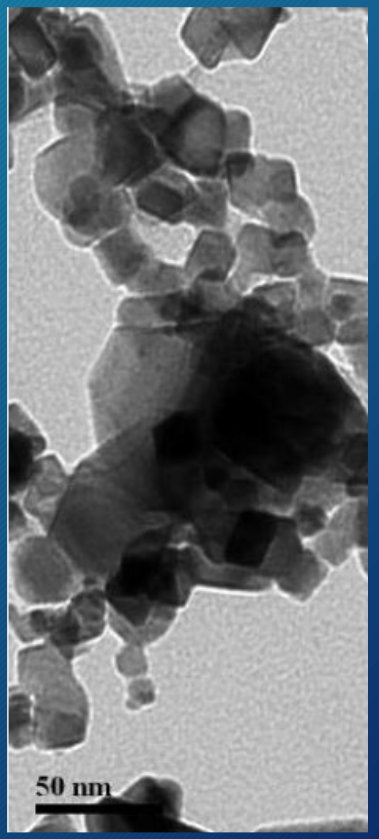
ICP-OES

ppm	Ag	Al	Ba	Be	Bi	Ca	Cd	Co	Cr	Cu	Fe	Ga	In	K	Li	Mg	Mn	Mo	Na	Ni	Pb	Sr	Tl	V	Zn	Purity (%)
NM-212		61.2				24.8				15.7			33	168		204		23.4	1081		6.7				53.4	99.83

CHN

Impurity (ppm)	C	H	N
NM212 (JRCNM02102a)	1000	600	1200

Organic compounds

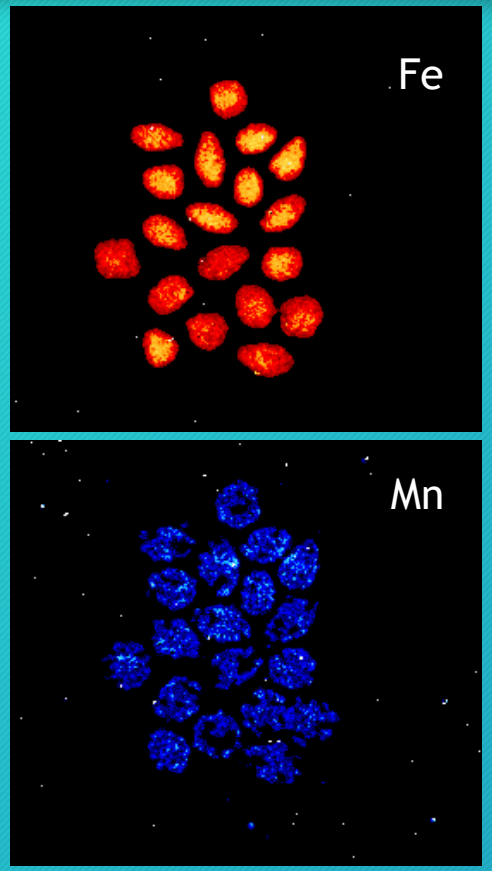


A common European approach to the regulatory testing of nanomaterials

Composition: nanoscale maps

EF-TEM maps

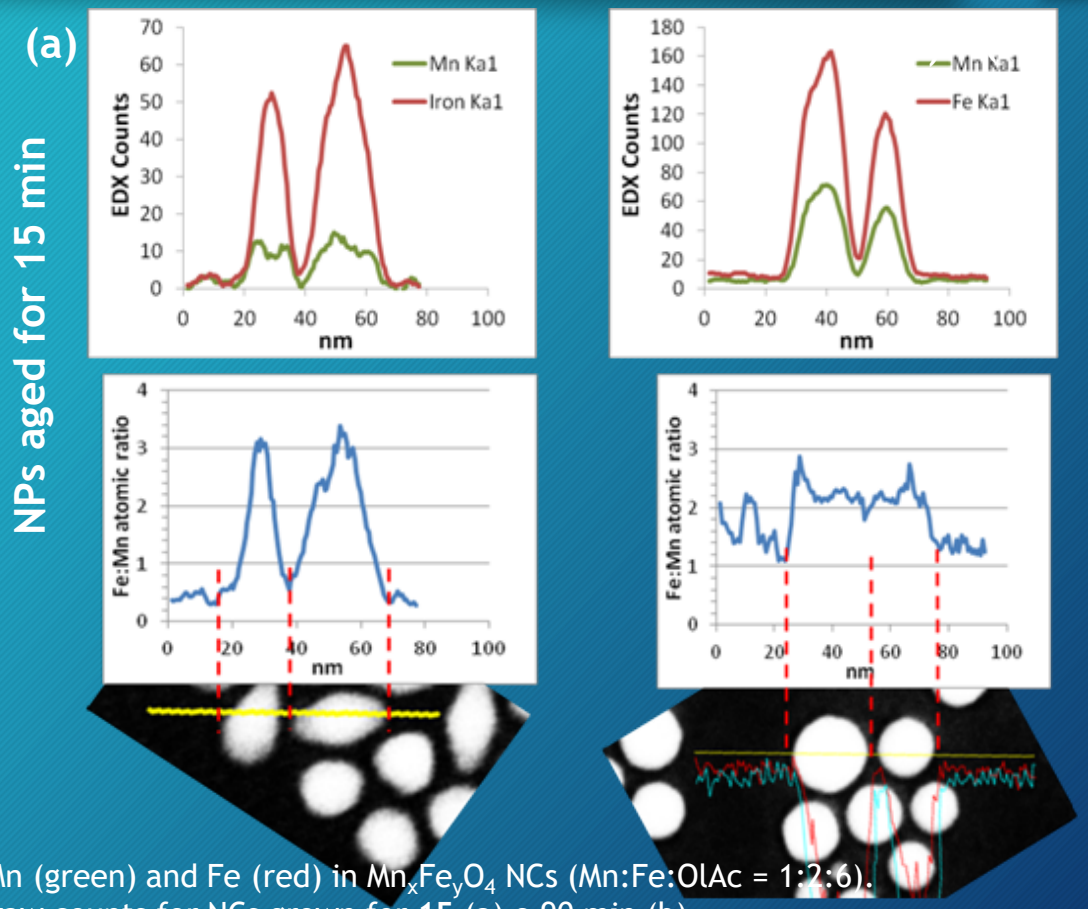
NPs aged for 15 min



$Mn_xFe_yO_4$ NCs (Mn:Fe:OlAc = 1:2:6) after **15 min** growth

Chemical inhomogeneity in $MnFe_2O_4$ NPs prepared by decomposition of $Mn(Ol)_2$ and $Fe(CO)_5$ in the presence of oleic acid (OlAc)

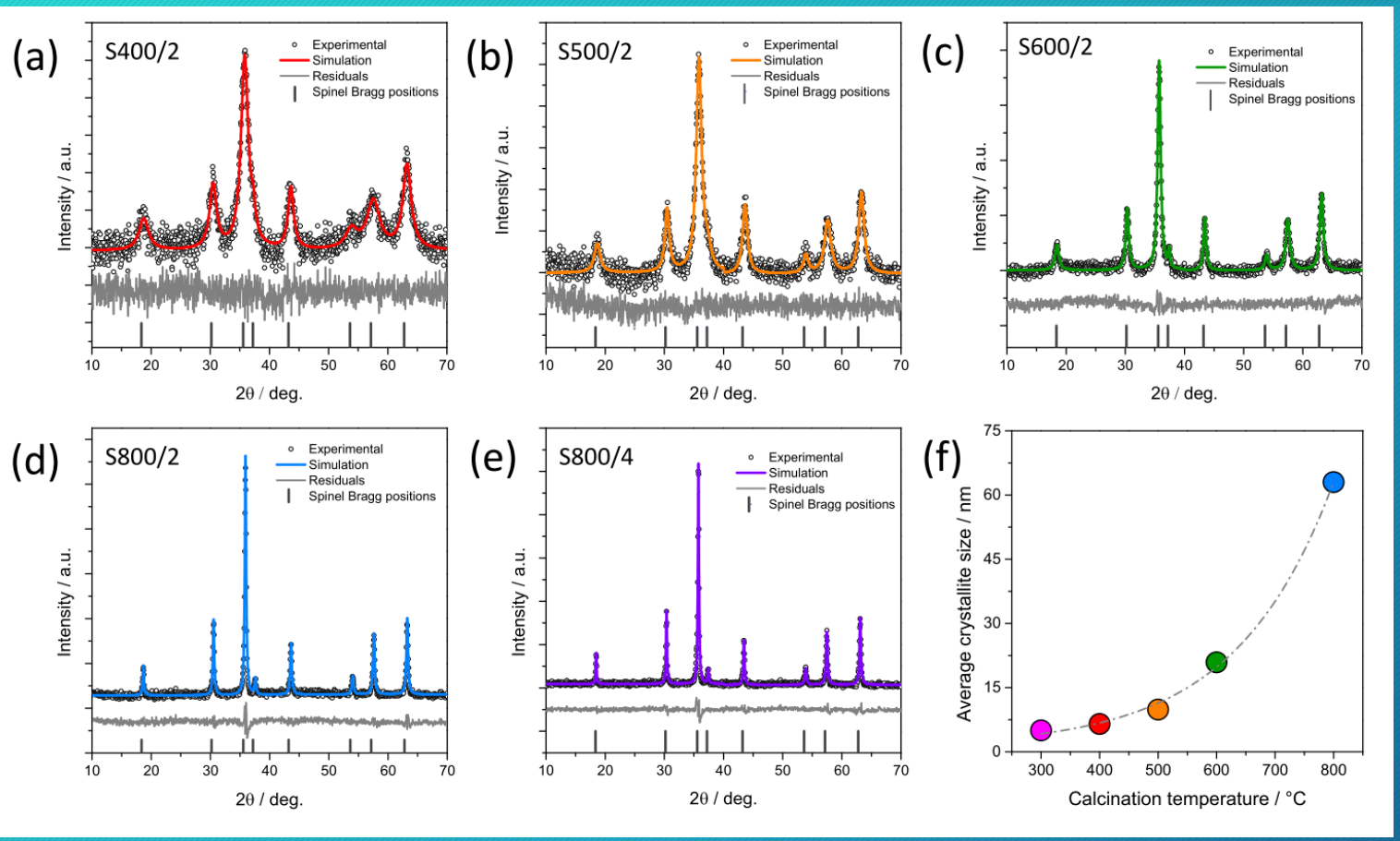
STEM - EDX



STEM-EDX profiles of Mn (green) and Fe (red) in $Mn_xFe_yO_4$ NCs (Mn:Fe:OlAc = 1:2:6).
Top: EDX raw counts for NCs grown for **15** (a) e 90 min (b)
Bottom: Fe:Mn atomic ratio of for NCs grown for **15** (c) e 90 min (d), superimposed to the corresponding STEM images

Crystal Structure - XRD and Rietveld

K Vezzù et al, Small. (2025), 2408319



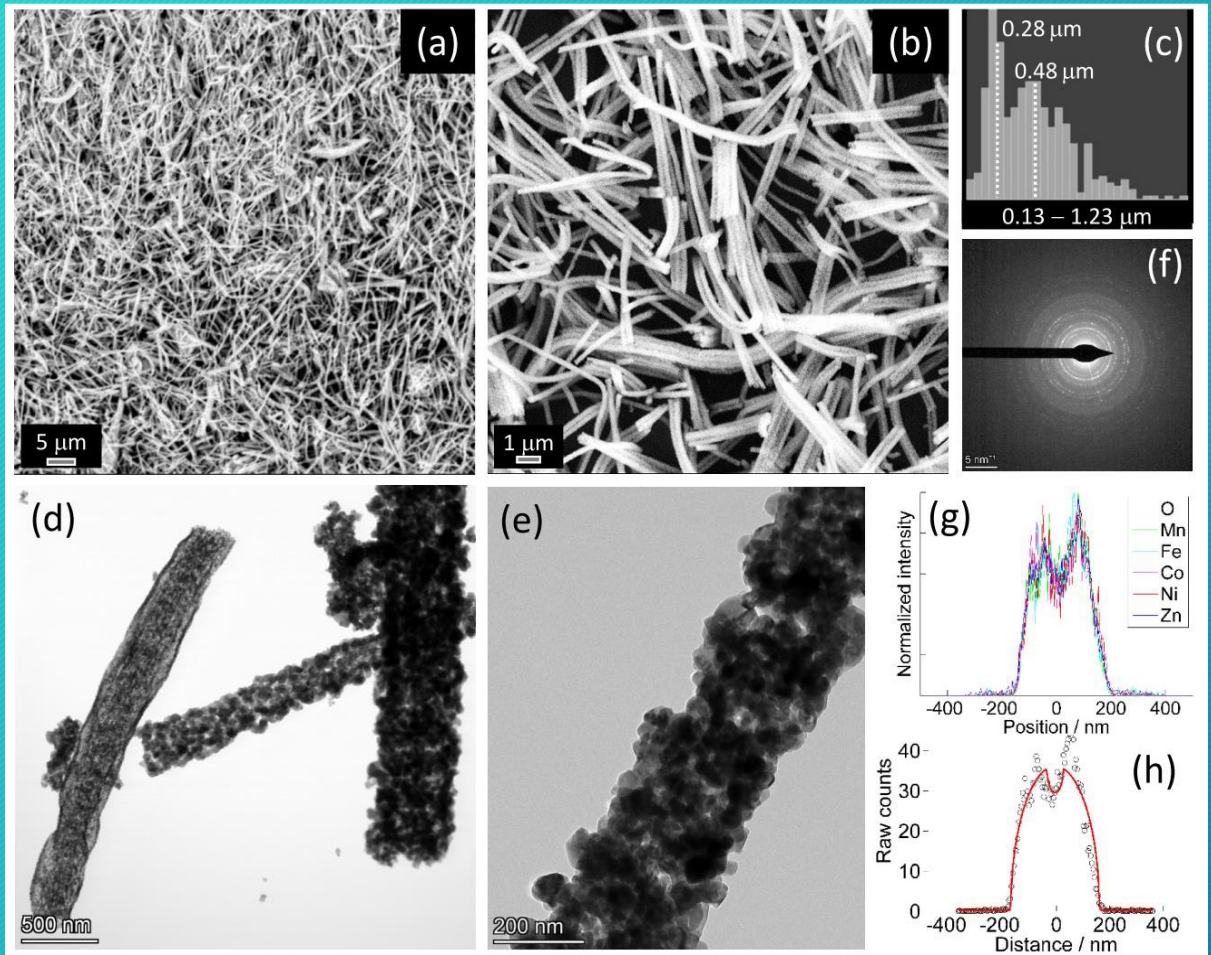
High-entropy $(Cr_{0.2}Mn_{0.2}Fe_{0.2}Co_{0.2}Ni_{0.2})_3O_4$ oxide nanofibers, calcined under different conditions.

Rietveld analysis of powder XRD provides

- phase identification
- phase quantification
- crystallite size
- crystallite microstrain

Crystal Structure - HRTEM and GPA

C. Triolo et al, Small (2023) 2304585

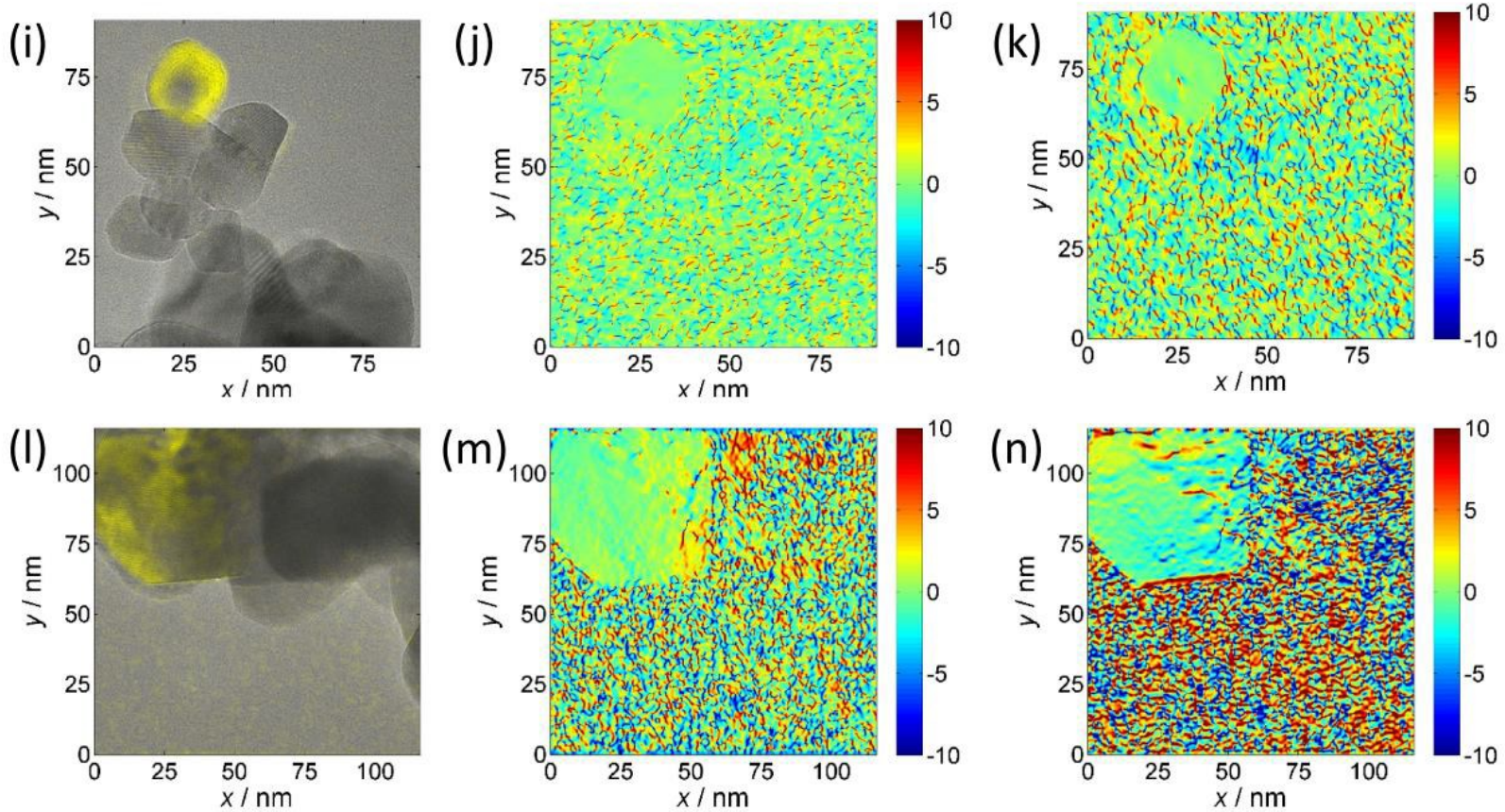


High-entropy $(Mn_{0.2}Fe_{0.2}Co_{0.2}Ni_{0.2}Zn_{0.2})_3O_4$ oxide nanofibers

(a,b) SEM micrographs,
(c) bimodal NF diameter distribution,
(d,e) TEM micrographs,
(f) SAED pattern for an isolated NF,
(g) projection analysis of the EDX maps and
(h) fitting of an oxygen projected profile revealing a quasi-solid NF.

Crystal Structure – HRTEM and GPA

C. Triolo et al, Small (2023) 2304585



High-entropy $(Mn_{0.2}Fe_{0.2}Co_{0.2}Ni_{0.2}Zn_{0.2})_3O_4$ oxide nanofibers

(i,l) Intensity-colorized maps,
(j,m) lattice rotation maps (°), and
(k,n) lattice strain maps (% of cell size).